Methodology for on-site assessment of the reuse potential of post-consumer tempered glass

Delft University of Technology

Pascal Mobailly

TU Delft

Eckersley O'Callaghan

Methodology for on-site assessment of the reuse potential of post-consumer tempered glass

by

Pascal Mobailly

to obtain the degree of Master of Science
at the Delft University of Technology
to be defended publicly on July 12, 2024 at 14:00

Thesis committee:

Chair:	Prof. dr. ir. P.C. Louter	TU Delft
Academic supervisors:	Ir. C. Noteboom	TU Delft
	Dr. ir. R. Hartwell	TU Delft
Daily supervisor:	Ir. M. Edwards	Eckersley O'Callaghan
Advisor:	Ir. G. Coult	Eckersley O'Callaghan
Place:	Faculty of Civil Engineering and Geoscience, Delft	
Project Duration:	February, 2024 - July, 2024	
Student number:	5836727	

An electronic version of this thesis is available at `http://repository.tudelft.nl/`.

Faculty of Civil Engineering and Geoscience · Delft University of Technology

Acknowledgements

This thesis, which marks the end of my Master in Civil Engineering at TU Delft, has been made possible thanks to several people and organisations.

I would like to express my sincere appreciation to the members of my committee. I am especially grateful to my chair supervisor Prof. Christian Louter for his guidance through all stages of this project and his time with my countless questions. I am grateful to him and to Ir. Chris Noteboom for their inspiring lectures and guests during the Glass Science and Engineering module and their support from the very first day of this project. Even when followed remotely, this has inspired and motivated me to delve deeper into this subject. Special thanks to Dr. Rebecca Hartwell for her support on sustainability assessment as well as very diverse topics through every step of the thesis, and for the great welcome in Delft to train on a SCALP-05 device. I would also like to thank Eckersley O'Callaghan for their financial and logistical support for my thesis. Special thanks to Ir. Mitsu Edwards for her regular insights and great support which were much appreciated. Thanks also to Ir. Graham Coult for his insights and references on glass structures.

I would also like to praise the entire Paris office of Eckersley O'Callaghan for their support and friendly exchanges. I have had a great time learning and discussing with them. Special thanks to Ir. Pierre Bourdier for his great and pragmatic insights on the methodology, Ir. Douraya Kessaria for her regular feedback on the sustainability assessment and research approach, and Ir. Audrey Aquaronne for her useful advice and knowledge on the case study.

External organisations also made this thesis possible. I would like to thank Innowep GmbH for their support, and especially Julian Schary and Paulo Bombonatti for the great welcome in their office and for the training session on Traceit®. I would also like to acknowledge GlasStress Ltd for their answers and support on the use of SCALP-05. Also great thanks to Ir. Irene Sofokleous for her answers regarding Traceit® and her inspiring thesis.

The support of Saint-Gobain Glass and their specialists was also very useful. Special thanks to Pierrick Florin and François Roux for their knowledge on the glass panes from the case study and the Heat-Soak Test research topics.

Finally, I would like to express my gratitude to my friends, my family and my girlfriend for their priceless support.

Abstract

Flat glass is a widely used material in the construction industry. However, its production has a relatively high carbon footprint due to the high melting temperature required, and most of it is still sent to landfill or down-cycled at end-of-life. The reuse of glass therefore has a great potential, given its lower carbon footprint and the number of existing buildings with glass panes that would be suitable for reuse.

This research project aims to propose a novel methodology for estimating the potential of tempered glass for adaptive reuse. It is illustrated with a case study of a historic building in Paris, built over 50 years ago with about 2500 fully toughened glass panes for potential reuse.

Firstly, a brief environmental impact assessment quantifies the impact of reuse compared to recycling and down-cycling to provide a more critical understanding of the benefits of reuse.

Secondly, a probabilistic equivalence of the Heat-Soak Test (HST) is justified for thermally toughened glass. Based on statistical analysis of spontaneous breakage due to nickel sulphide (NiS) inclusions over time, a safety level over time is estimated. This level of safety can already be considered quite high from 20 years after installation and is equivalent to an HST after 50 years.

Finally, the residual strength of aged tempered glass is estimated. This strength is based on the combination of the pre-stress level and Linear Elastic Fracture Mechanics (LEFM). The pre-stress level and the largest flaw depth are measured on-site using portable optical devices on a representative sample. A visual inspection procedure is then defined to speed up the evaluation of the flaw depth. Once trained, the observer should be able to qualify the glass panes relatively quickly following different 'Quality Levels' with associated characteristic strengths (95% confidence level).

This methodology was applied to the case study. Pre-stress and flaw depth measurements were carried out on 70 glass panes. Visual inspection was tested and the margins calibrated to reach a 95% confidence level. The glass panes have an average surface pre-stress level of 81.41 MPa with a standard deviation of 4.17 MPa, which is consistent with other values reported in the literature for fully toughened glass. The largest flaw depths ranged from 4 µm to 147 µm, also in agreement with other publications. All of the glass panes analysed are suitable for reuse as heat-strengthened glass, and potentially better for some of them.

The proposed methodology has been summarised to be generalised to other reuse projects. Typical fully toughened, heat-strengthened and annealed glass (average pre-stressing level and surface quality based on previous measurements) have a great potential for reuse at the same characteristic strength if the surface quality estimated by visual inspection has flaw depths smaller than 20-40 µm. Qualification for reuse of these three types of glass with a reduced strength is also proposed. This could allow reusing glass panes with flaw depths of up to 500 µm for several design scenarios.

Contents

Nomenclature

List of Abbreviations

2PW	Two-parameter Weibull
AFM	Atomic force microscopy
AI	Artificial Intelligence
AR	As Received glass
BLW	Bilinear Weibull
BMW	Bimodal Weibull
CDF	Cumulative Distribution Function
CDR	Coaxial Double Ring test
EoL	End-of-Life
EPD	Environmental Product Declaration
FEA	Finite Element Analysis
FEM	Finite Element Model
GHG	Greenhouse Gasses
GWP	Global Warming Potential
HST	Heat-Soak Test
IGU	Insulated Glass Unit
LEFM	Linear Elastic Fracture Mechanics
ML	Machine Learning
MLE	Maximum Likelihood Estimation
NA	Naturally Aged glass
NDT	Non-Destructive Test
PCR	Product Category Rules
RSL	Reference Service Life
SEM	Electron microscopy
WLR	Weighted Least Squares Regression

List of Symbols

β	Shape factor of the Weibull distribution
δ	displacement
$\gamma_{m;A}$	Glass material factor
$\gamma_{m;V}$	Glass prestress factor
λ	Fracture stress of a specimen at a probability of 63.2 %
ν	Poisson's ratio
σ	Stress rate
σ_f	Failure stress
θ	Scale parameter of the Weibull distribution
A	Surface area
c	Flaw depth
E	Young's modulus
F	Failure load
$f_{g;k}$	Characteristic strength
$f_{mt,u,d}$	Design strength
h	Thickness of the glass specimen
k_A	Size effect factor (area)
k_a, k_e	Factor for the edge quality of glass
K_I	Stress intensity factor for mode I crack propagation
K_{IC}	Critical stress intensity factor for mode I crack propagation
k_{mod}	Modification factor for the load duration
k_{sp}	Factor for the surface treatment of glass
P_f	Probability of failure
R_d	Design resistance
R_M	Consequence class
Y	Geometry or shape factor

List of Figures

List of Tables

1

Introduction

1.1. Motivation

The production of flat glass is associated with a substantial amount of energy and material. For every tonne of glass produced, more than 1.2 tonnes of CO_2 are emitted. In Europe, the building industry generates over 2 million tonnes of glass waste. While most of this glass goes to landfill or is crushed into aggregate, the global demand for flat glass is currently at an all-time high (European Commission, 2024 ; Debrincat & Babic, 2019).

The setting up of the recycling supply chain is more advanced than the setting up of the reuse supply chain, although both are only in their own premises in the glass industry. Even though recycling is a positive step, its benefits are limited due to the melting process of the old product. Reuse has therefore a great potential in this field.

Unlike most other construction materials, glass is very brittle and sensitive to surface defects, making stakeholders in construction projects often hesitant to reuse it. However, recent research has confirmed the viability of reusing aged glass, particularly tempered glass which is widely used and has the best post-aged strength (Datsiou & Overend, 2017). Therefore, its reuse has a great potential considering its lower carbon footprint and the number of existing buildings where it could be applied.

1.2. Problem statement

The aim of this research is to present a methodology for evaluating the reuse potential of tempered glass in practice. This methodology will be illustrated with a case study of an existing building in Paris containing about 2500 tempered glass panels built about 50 years ago. Various design options are considered, allowing the glass to be reused as fully toughened, heat-strengthened or eventually annealed glass. The goal for this case study is then to be able to evaluate the reuse potential for these three scenarios. While aiming to have an in-depth understanding of the phenomena involved in aged glass, it will keep the idea of applying these concepts in a pragmatic way on site.

In the first step, an initial assessment of the benefits of reuse compared to recycling and down-cycling will be carried out. This will allow understanding the order of magnitude of the impact of reuse, and if this choice is worth it.

Then, the risk of spontaneous breakage due to nickel sulphide inclusions in aged glass should be compared with that of the new glass with Heat-Soak Test. Indeed, nickel sulphide inclusions are rare and hard to detect, but inevitable in tempered glass. They can cause spontaneous breakage even a few years after installation. More recently, the Heat-Soak Test drastically reduces the incidence of spontaneous breakage and has been made mandatory in France. Probabilistic equivalence of the Heat-Soak Test must then be demonstrated for the aged glass panels.

Finally, the greatest challenge is to estimate of the strength of aged tempered glass. Much of the strength of tempered glass comes from the residual pre-stress level, which must be measured. The residual strength is then very sensitive to the surface, edge and volume defects of the element. The distribution of

these defects within the material is unknown, and tends to increase over time due to transport, natural weathering and occupant's behaviour during the use phase. This phenomenon has been well explained in the literature based on the theory of Linear Elastic Fracture Mechanics and experimentally, based on destructive testing. While this can be explained deterministically in theory, it has to be determined in a probabilistic way in practice. In the case of tempered glass, the combination of the residual pre-stress level and of the weathering measured in situ should provide the residual strength of the glass.

1.3. Research question

The main research question of this MSc thesis is :
How can we assess the reuse potential of tempered glass in practice?

The sub-questions are:

- How can we get a first estimate of the benefits of reusing glass compared to recycling and down-cycling?
- How can the risk of spontaneous breakage due to NiS inclusion in aged glass be compared to that of new glass with HST?
- How can the strength of tempered glass be measured on-site?
- What is the reuse potential for the aged glass of this case study, based on LEFM with appropriate margins?
- To which extents could this methodology be generalized?

1.4. Scope

While this study aims to gain a comprehensive understanding of the various phenomena involved (pre-stress level, weathering and HST probabilistic equivalence), the focus remains on the practical application of these concepts on-site. It will be applied to a specific case study and generalized with the following limitations:

- This study focuses solely on soda-lime silica tempered glass. It is chosen as the one of the most representative of the glass elements in recent buildings and has one of the best post-aged strength. Other types of glass such as laminated glass are not covered.
- The manufacturing process of the panes is not considered in the structural assessment. The panes in the case study are made of drawn sheet glass using the TWIN process, whereas most of the glass today was produced on a tin bath using the FLOAT process.
- This research should be applicable on a case study conducted on-site, which may have more constraints than in a laboratory setting. The measuring devices should be portable and compatible with the on-site configuration.
- The strength prediction of aged glass is not deterministic, but rather probabilistic with structural mechanics bases. It is unrealistic to predict the exact location and failure strength of each panel individually, particularly in relation to the size and shape of the critical surface flaw to find on large windows on-site. However, a more accurate estimation can be made for the average and characteristic strength of the entire testing batch.

1.5. Research outline

The thesis is made of ten chapters. In **Chapter 1**, the topic is introduced and the problem is defined. **Chapter 2** presents the theoretical background based on the state-of-the-art literature review. This review focuses on the production processes of flat glass, flaw characterization, the strength of glass, Non-Destructive Tests and design standards on tempered glass. A short comparative environmental assessment is done in **Chapter 4**, in order to get an idea of the benefits of reuse compared to recycling and down-cycling. **Chapter 5** presents the probabilistic equivalence of the Heat-Soak Test for aged glass. In **Chapter 6**, the experimental protocol and results are presented regarding the pre-stress and weathering

level. The reuse potential is then investigated in **Chapter 7**, based on the remaining strength of the glass and our ability to measure it efficiently. **Chapter 8** summarises the proposed methodology for broader applications to reuse tempered glass. Transversal discussions relative to all of the previous chapters are done in **Chapter 9**. Finally, the main conclusions are drawn in **Chapter 10** with recommendations for further research on this topic.

2

Theoretical background

2.1. Glass as a building material

2.1.1. Material properties

A glass is an inorganic product of fusion, which has been cooled to a rigid condition without crystallization (Haldimann, 2008). The most commonly used material in construction is soda-lime silica glass since the mid-20th century. It is mostly made of sand (SiO), soda ash (Na_2CO_3) and limestone ($CaCO_3$). Its composition is standardised in the European norm EN 572-1+A1, as shown in Table 2.1. The exact composition varies between the suppliers and depending on the required combination of associated properties.

Table 2.1: Magnitude of the proportions by mass of the constituents of soda-lime silicate glass (EN 572-1+A1, 2016). Oxygen represents the balance to 100 %.

Constituents		Proportion by mass of element
Silicon	(Si)	32 % - 35 %
Calcium	(Ca)	3.5 % - 10.1 %
Sodium	(Na)	7.4 % - 11.9 %
Magnesium	(Mg)	0 % - 3.7 %
Aluminium	(Al)	0 % - 1.6 %
Others		0 % - 5 %

Soda-lime silicate glass can be described by the values in Table 2.2. These are not precise requirements, but generally accepted figures for use in calculations where a high degree of accuracy is not required.

Table 2.2: General characteristic values of basic soda-lime silicate glass (EN 572-1+A1, 2016)

Characteristic	Symbol	Value and unit
Density	ρ	$2500kg/m^3$
Young's Modulus (modulus of elasticity)	E	$7 \times 10^{10}Pa$
Poisson's ratio	μ	0.2
Specific heat capacity	c_p	$0.72 \times 10^3 J/(kg \cdot K)$
Average coefficient of linear expansion between 20°C and 300°C	α	$9 \times 10^{-6}/K$
Thermal conductivity	λ	$1W/(m \cdot K)$
Transition temperature	T_g	$530°C$

Regarding stresses, glass has an almost perfectly linear elastic, isotropic behaviour at ambient temperature. It does not yield plastically. This prevents any stress redistribution, making the material very brittle and sensitive to stress concentration.

Regarding deflections, glass panes can also displace by more than their own thickness. This requires the use of large deflection theory for an appropriate design.

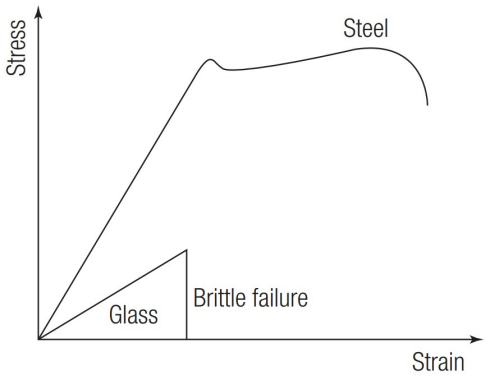

Figure 2.1: Qualitative comparison of the stress-strain graphs for glass and steel (O'Regan et al., 2014)

The glass material itself is extremely strong, with a tensile strength based on molecular forces reaching about 32 GPa. However, a further chapter will show that mechanical flaws systematically present in the glass panes reduce significantly this strength.

2.1.2. Production processes of flat glass

The oldest pieces of glass date from around 3500 BC in Egypt. It was coloured and typically used for jewellery or vessels. The Romans were the first to create clear glass in large enough quantities to use it as glazing. The glass was cast onto a table and pulled into shape while it was still relatively workable. This process was adopted by various countries throughout the following centuries (O'Regan et al., 2014).

The crown process was developed in the 14th century in France. The glassmakers would blew a large bubble of glass, which they then spun quickly while the glass was still soft, producing a disc of glass that was then cooled gently. It allowed providing panes of up to 0.5m $\times$0.75m of flat glass.

Figure 2.2: Crown glass manufacturing (O'Regan et al., 2014)

The Siemens-Martin firing method was invented in the 19th century and allowed recovering the heat from waste gases. This allowed reaching higher temperatures needed for a better quality glass.

At the same century, the cylinder process (or broad process) was developed. In this case, the bubble of glass was swang into a cylindrical shape. After cutting off the ends of the cylinder, it was slit, reheated and opened out into a flat sheet. This allowed producing panes of up to 1.0 $\times$1.3m.

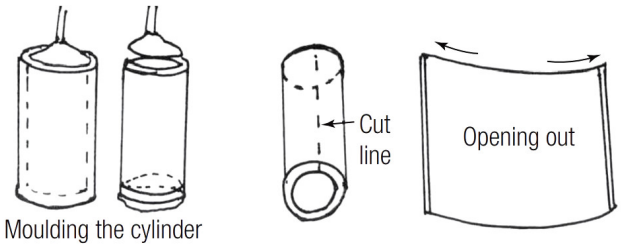

Figure 2.3: Cylinder process (Adapted from O'Regan et al., 2014)

From 1918, the rolled plate process (or Bicheroux process) included pressing molten glass with rollers to reach the desired thickness, casting, grinding and polishing. The polishing device can also be called a twin, hence the other name TWIN process. This provided glass of good quality but associated with relatively high costs and wastage.

The drawn flat sheet processes, notably the Belgian Fourcault and the American Colburn Processes, were also invented in the early 20th century. The Fourcault process is an example of 'vertical draw' process, where the glass is drawn in an upward direction. It provided good finish but greater limitations in size and wavy or stripped surface (Weeks, 1933).

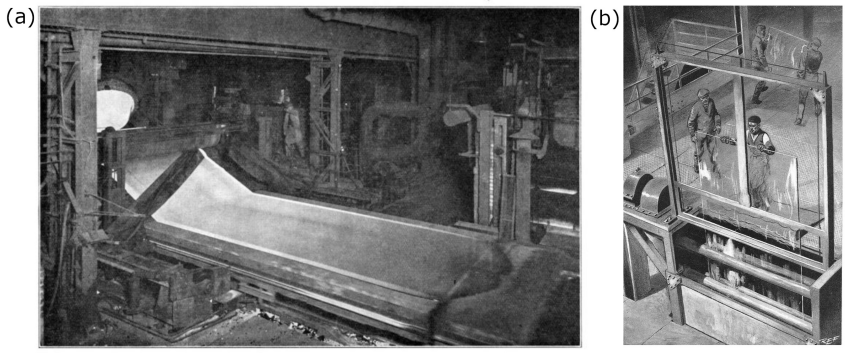

Figure 2.4: (a) Casting plate or Bicheroux process, (b) Fourcault process (Weeks, 1933)

The float glass process was patented by Pilkington in the mid-20th century. The glass is melt in a furnace at about 1500°C, and then fed onto the top of a molten tin bath. The glass ribbon is then cooled and fed into the annealing lehr. The speed at which the ribbon moves defines its thickness. The edges are then trimmed to obtain sheet cut into standard jumbo size of 6m $\times$3.21m before being stored (Haldimann, 2008). After quality inspection, any unwanted glass is collected and fed back into the furnace.

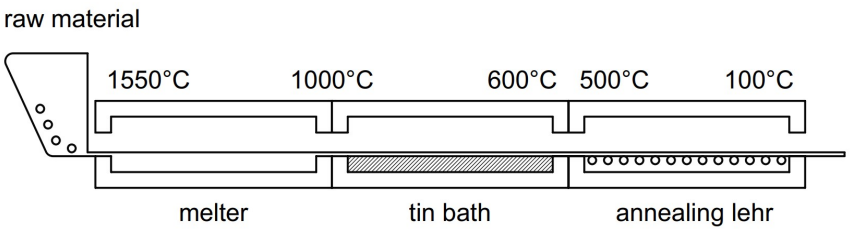

Figure 2.5: Float process (Haldimann, 2008)

Due to this production process, the mechanical strength of the surface on the tin side has been found to be slightly lower than on the air side. This tin side can be detected with ultraviolet radiation after production.

However, the float process still offers excellent quality of glass on both sides and large size of panes for a lower cost than the previous processes. This explains why it is still today the most common production process for flat glass.

2.1.3. Tempering of glass

In parallel, the phenomenon of thermally toughening a glass element was observed as far as 3000 BC in Syria (O'Regan et al., 2014). Various glass objects were produced with thermal toughening, but the first official patent was filed by the Austrian chemist Rudolph A. Seiden in 1900. This patent described the process of cooling the surface of the glass at a faster rate than the centre. This process pre-stresses the glass with compression at its surfaces, making it stronger than basic annealed glass.

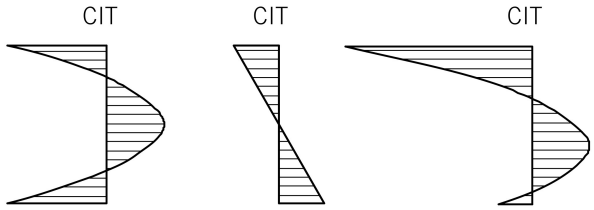

Figure 2.6: Superimposed diagrams for thermal pre-stress and bending stress (Adapated from Wurm, 2007)

We can distinguish four main types of glass in the building industry:

- **Annealed glass:** basic float glass that has been exposed to a slow cooling. Breaks into large pieces at failure.
- **Semi-tempered or heat-strenghened glass:** made of annealed glass that was re-heated and quenched by jets of cooled air (EN 1863-1, 2011). The surface pre-compression stress ranges typically from 24 MPa to 52 MPa. Breaks into medium pieces at failure.
- **Fully tempered or fully toughened glass:** made similarly than heat-strenghened glass but with a faster quenching (EN 12150-1, 2019). The surface pre-compression stress range is slightly different depending on the terms adopted: minimum 75 MPa for fully toughened glass in Europe (EN12150-1, 2019) and 69 MPa for fully tempered glass in the USA (ASTM C1048, 2012), with a typical maximum of 150 MPa. Breaks into small pieces at failure.
- **Chemically toughened:** made of annealed glass dipped into electrolysis baths in which the sodium ions on the surface of the glass are exchanged for potassium ions, which are 30% bigger. The surface pre-compression stress typically ranges between 150 MPa and 200 MPa, but is very variable depending on the process parameters. This allows toughening glass panes that are thinner, curved or that need cutting and drilling after toughening.

The pre-stress cross-sectional diagrams of the different types of tempering can be compared in Figure 2.7. When a surface flaw goes deeper than the compression zone, their tip reaches the tensile zone and subcritical crack growth occurs without external load. From these stress profiles, one can see that chemically toughened glass is more exposed to this phenomenon.

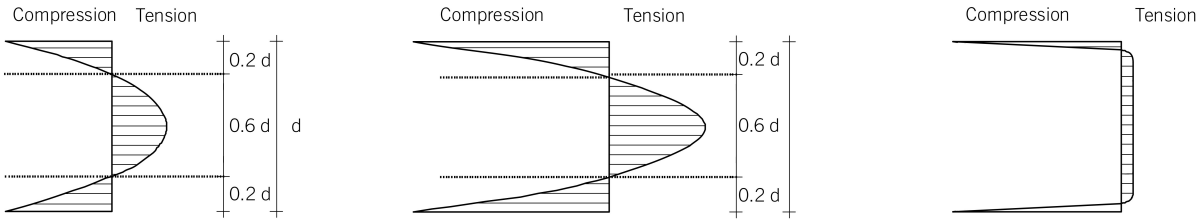

Figure 2.7: From left to right: heat-strenghened, fully toughened and chemically strenghened stress cross-sectional diagrams (Adapated from Wurm, 2007)

The following typical residual surface stress levels were reported by Achinta (2021):

Table 2.3: Reported surface compressive residual stress in different glass specimens (Mithilda, 2021)

Glass type	Surface residual stress (MPa)
Annealed	5
Heat-strengthened	30
Fully toughened	95

It is to note that even when manufacturers comply with the standards about tempered glass, there is still a relatively high variability of the pre-stress level - and then of the fracture strength - from one pane and batch to another (Haldimann, 2008), as shown in Figure 2.8.

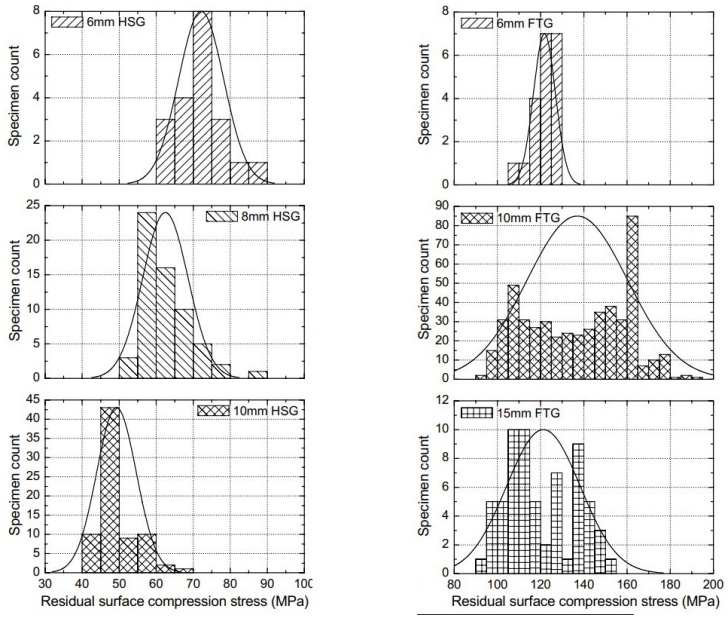

Figure 2.8: Residual stress data, pooled by glass thickness on histograms with fitted normal distributions (Haldimann, 2008)

Moreover, the surface pre-stress level is never completely uniform over the whole glass pane surface. Due to the non-uniform cooling process, there is usually a gradient from the borders to the central area of the glass pane, with a maximum pre-stress level at the center. In addition, some smaller asymmetrical deviations have also been measured (Iglesias et al., 2022). Fortunately, since most of the glass panes are supported with hinges on their four edges, this pre-stress gradient somehow corresponds to the mechanical strength requirements when the pane is subject to a uniform load.

The fracture pattern is a function of the energy stored in the glass. Thus, higher level of tempering is

usually associated with breakage in smaller pieces, as shown in Figure 2.9. At the opposite of annealed glass, fully toughened glass breaks into the small pieces of about 100 mm². These fragments are relatively harmless, which is why this type of glass is also called *'safety glass'*. However, smaller fragments are causing a lower post-failure performance.

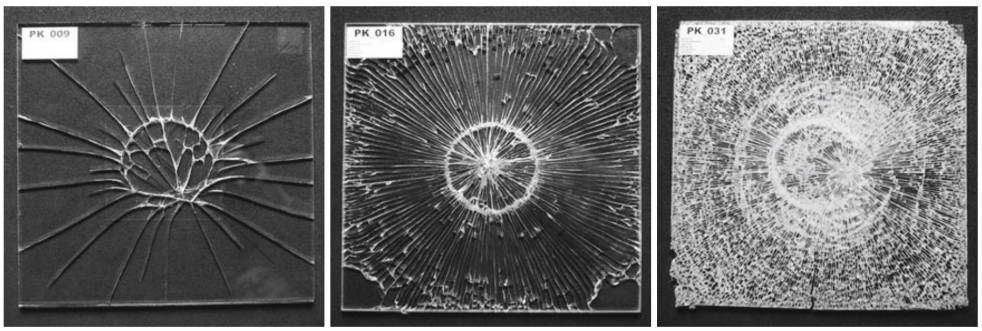

Figure 2.9: From left to right: annealed, heat-strenghened and fully toughened fracture patterns (Adapated from Belis et al., 2019)

2.2. Flaw characterization

2.2.1. Flaw origins

A glass pane is exposed to several types of phenomena after production, causing various types of flaws. The most important causes are the following:

- **Temperature:** because of its thermal conductivity coefficient smaller than 1 W/mK (compared to 50W/mK for steel), glass does not allow quick temperature equalisation. This can cause internal stresses and eventually breakage of the glass. This phenomenon is facilitated by existing cracks. For example, cracks of 0.02 to 0.08mm combined with temperature differences of 30 to 60°C can already lead to thermal glass breakage (Stuurstraat, 2023).
- **Acidity:** when exposed to alkaline liquids (with a pH higher than 7), a mechanism of congruent dissolution happens with silica (Si). The surface is gradually 'dissolved', forming craters and pits of different sizes observed on microscopes (Papadopoulos & Drosou, 2012).
- **Air pollution:** studies reported that environmental pollution with 5ppm SO_2 (sulphur dioxide) or 1ppm NO (nitrogen monoxide) does increase the rate at which glass corrodes by about a factor of 3, compared to glass exposed at the same temperature and humidity in an ambient laboratory air.
- **Humidity:** when exposed to water, the amorphous atomic structure of the glass is ordered to a crystalline structure. This phenomenon called re-crystallisation forms a pitting-like surface on the glass. According to previous research, this may have a greater effect than air pollution, and a quadratic relationship with the hydration rate. For example, if the hydration rate increases by a factor of 10, the speed of decay to reach a certain depth is increased by a factor of 100 (Papadopoulos & Drosou, 2012).
- **UV-radiation:** the formation of Si-ions is favored by UV-radiations. Their lower valence (ability to form bonds) can result in cracks in the glass. Moreover, UV radiations can form oxidation with organic contaminents combined with water on the glass surface (Stuurstraat, 2023).
- **Weather:** impacts on the glass surface depend on the amount of solid particles in the environment, wind intensity and pane exposure. This type of damage is instantaneous and physical only.
- **Production process:** geometric imperfections and impurities appear to some extent since the production process is never perfect. These flaws should be very limited due to quality control, but they can be a basis for larger flaws developing with other causes.
- **Handling and transportation:** the way the glass panes are handled, stored and moved can expose the panes to small physical impacts.

- **Use phase:** the handling during the service life of the glass panes is usually safer than during installation, but for a much longer period of time where small impacts can occur. Another type of damage also happens with cleaning. When sweeping a cloth over a glass pane, some particles may cause some small scratches.

The term 'weathering' will stand for the natural aging of the glass involving all these potential defect causes. It is not always possible to know and distinguish all of theses causes. Weathering is always a combination of several defect types from various origins. The interactions between these origins can also accelerate the weathering, for example by fostering other chemical reactions (Papadopoulos & Drosou, 2012).

2.2.2. Global surface quality level

On a large scale over the whole glass pane, a global surface quality level can be defined. Recent research showed two approaches to quantify it.

The first approach consist of using a scanner from a manufacturing IGU line to quantify the number and length of spot-like and scratch-like flaws. The scanner assesses the optical quality of the glass, and an algorithm can then analyse the pictures to quantify and classify the flaws (Rota, Zaccaria & Fiorito, 2023).

This methodology is ideal to have an overview of the damage level of the glass panes. Further research coupled with AI algorithm could be interesting to explore. However, it has a few limitations according to the authors. It is not possible to distinguish on which face a specific flaw is, and the depth is not measured. Therefore, the link between the measured data and the actual glass strength is rather indirect, and a glass pane with very few but deep flaws could be considered of good quality but still have a lower strength than new glass. Moreover, this involves dismantling part of the envelope to reuse and transportation to manufacturing lines, which could be costly and not always possible.

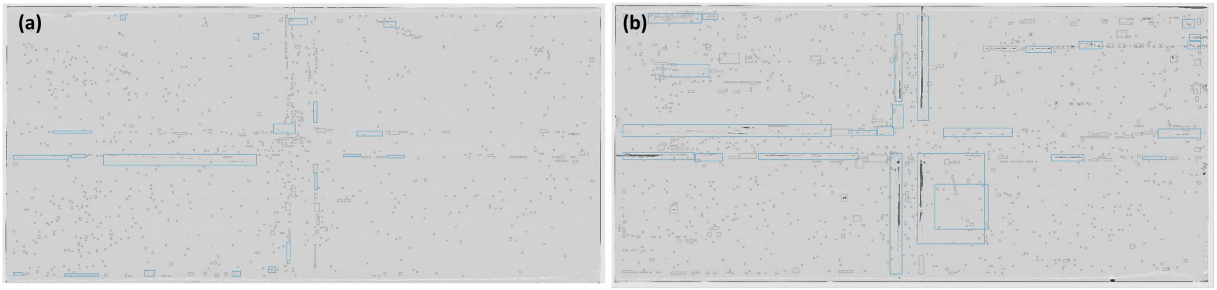

Figure 2.10: Scans showing the flaw density of the interior (a) and exterior (b) glass panels of an IGU (Adapated from Rota, Zaccaria & Fiorito, 2023)

The second approach consists in measuring the roughness of the glass pane surface and extend the measured samples to the whole pane using statistics to estimate the largest potential flaw. The surface qualities of various historical glasses were investigated by Carmona et al. (2010). Figure 2.11 shows the surface quality of an early 20th century glass pane using electron microscopy (SEM), and compares its topography to a 'model' glass with a similar chemical composition but an 'as-new' surface condition using atomic force microscopy (AFM). Both AFM images have the same scale, allowing to get an idea of the surface condition such glass can have over time.

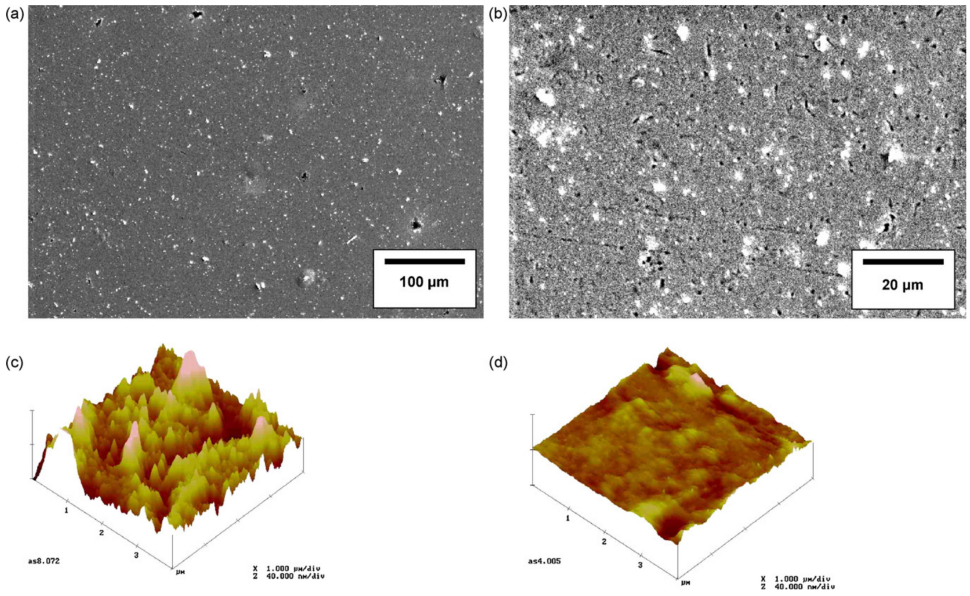

Figure 2.11: (a and b) SEM images from an early 20th century glass at different magnifications, (c) AFM image from the historical glass, (d) AFM image from an equivalent new glass (Carmona et al., 2010)

There are various ways to define a roughness value (ISO 4287, 2000). The chosen approach here is the quadratic mean, or root mean square (RMS) average of profile height deviations from the mean line:

$$R_q = \sqrt{\frac{1}{l_r}\int_0^{l_r} z(x)^2\,dx} \tag{2.1}$$

where
l_r is the evaluation length
$z(x)$ is the height of the assessed profile at any position x

The aged glass has a roughness value of 10.2nm (peaks of up to 80nm), compared to 2.0nm for the 'model' glass. According to the authors, the observed diffuse flaws are mostly due to various chemical reactions combined with surface defects from the original glass and dust deposits. In comparison, a research from Zammit & Overend (2009) also used AFM on annealed weathered glass and reported peaks of up to 240nm. This approach is more closely related to the structural mechanics phenomena involved, but requires statistical sampling with more uncertainties, which will be discussed in a further chapter.

2.2.3. Local flaw classification

When looking at localised flaws, we can distinguish 3 geometric flaw categories:

- **Spot:** One-off, single, localised surface flaws with length and width of similar dimensions.
- **Linear:** Scratches or equivalent surface flaws with one dimension much larger than the other.
- **Inclusions:** volume flaws included in the thickness of the glass.

Inclusions are *volume-distributed*.Spot and linear flaws are *surface-distributed*, where some flaws are even *edge-distributed* (Quinn, (2020). The two first categories correspond to the ones from existing norms (EN 572-8+A1, 2016) mentioning 'spot faults' and 'linear faults'. Moreover, these categories correspond to the two most common and distinct values for the shape coefficient Y to estimate the glass strength later on.

Table 2.4: Localised flaw types

Geometric category	Flaw type	Description
Spot	Pit	Small open flaws with an elliptical shape. Can be caused by bubbles very close to the surface, and/or various corrosion reactions.
Spot	Dig	One-off, irregular flaws. Due to contact damage from very diverse origins.
Spot	Chip	Localised part of an edge that was chipped off due to contact or impact damage. Can be seen like a dig on an edge of the glass.
Linear	Scratch	Marks with one dimensions much larger than the others, not necessarily linear. Can be extended by thinner, repeated arc-shaped cracks called chatter marks along the scratch. Can originate from very diverse causes during handling, polishing, transportation or due to stresses.
Linear	Crack	Breakage pattern of the glass, than can sometime be mistaken for a scratch but is much deeper and can eventually go through the whole thickness of the glass. Due to very diverse impact, contact, or thermal damage.
Inclusion	Knot and striae	Inclusions of glass of different composition. Knots are one-off flaws while striae are longer inclusions, often together.
Inclusion	Chill check	Small wavy crack included in the thickness of the glass. Due to localised thermal stress.
Inclusion	Bubble	Smooth pores usually filled with gas, or sometimes with small solids. Due to material decomposition and contamination.
Inclusion	Stone inclusion	About 50 different types of stone inclusions reported in glass, but most of them are harmless. Caused by devitrification of the glass, unreacted raw material or contamination with other materials.
Inclusion	NiS inclusion	Nickel sulphide inclusions, usually between 40µm and 450µm. Relatively rare but can cause spontaneous breakage at any time without warning.

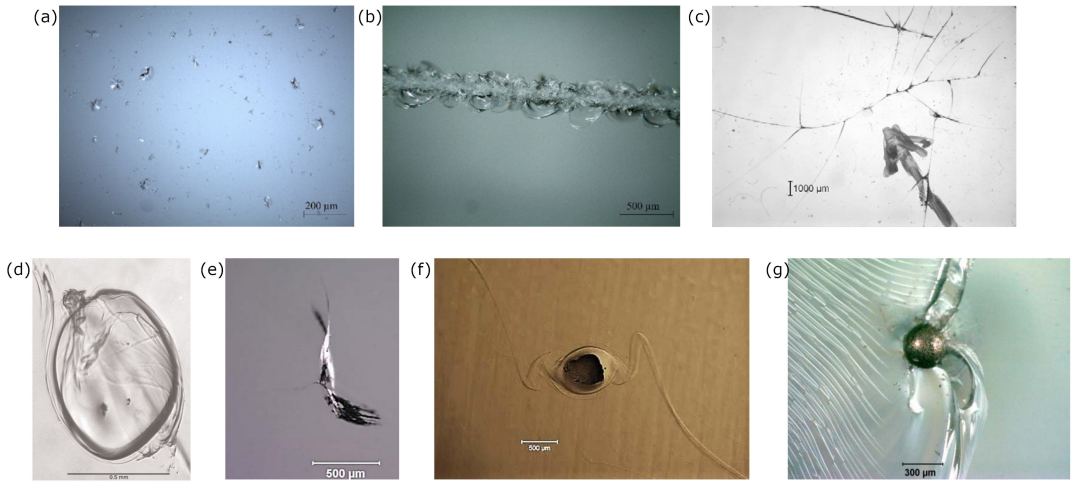

Figure 2.12: (a) digs from sand-abrasing (Datsiou & Overend, 2016), (b) scratch from a sharp indenter (Datsiou & Overend, 2016), (c) cracks (Quinn, 2020), (d) knot (Müller et al., 2001), (e) chill check (Quinn, 2020), (f) stone inclusion with striae (Quinn, 2020), (g) NiS inclusion (Quinn, 2020).

2.3. Strength of glass

2.3.1. Fracture mechanics

The theoretical tensile strength based on molecular forces of glass can reach 32 GPa (Orowan, 1934):

$$\sigma_m = \sqrt{\frac{E\gamma}{r_0}} \tag{2.2}$$

where
$E = 70GPa$ is the Young's modulus
$\gamma = 3Jm^{-2}$ is the fracture surface energy
$r_0 = 0.2 \times 10^{-9}m$ is the equilibrium spacing of the atoms

This value is extremely high: in comparison, a standard S355 steel has a yield strength f_y of 355 MPa and an ultimate strength f_u of 490 MPa. However, the mechanical flaws induced by the fabrication process, transportation and use phases reduce significantly this tensile strength of glass. According to the theory of minimum energy, an elastic solid deformed by a surface force finds its equilibrium state at the minimum potential energy. The reduction in potential energy being equal to the strain energy due to the formation of a crack, the following energy balance theory on fracture was derived (Griffith, 1921):

$$\sigma_G = \sqrt{\frac{2E\gamma}{\pi c}} \tag{2.3}$$

where
σ_G is the failure stress
E is the Young's modulus
γ is the fracture surface energy
c is the crack depth

This formula can be modified to introduce a term called *stress intensity factor* (SIF). As shown in Figure 2.13, this term quantifies the magnitude of the stress field at the crack tip.

The SIF being a function of the stress field, it has different values for each failure mode (K_I, K_{II}, K_{III}). However, it was shown that the SIF for mode I is always larger than that for mode II and III (Wang & Hadfield, 2004). Therefore, the *critical stress intensity factor* also called *fracture toughness* K_{IC} will always be considered equal to K_I in this study.

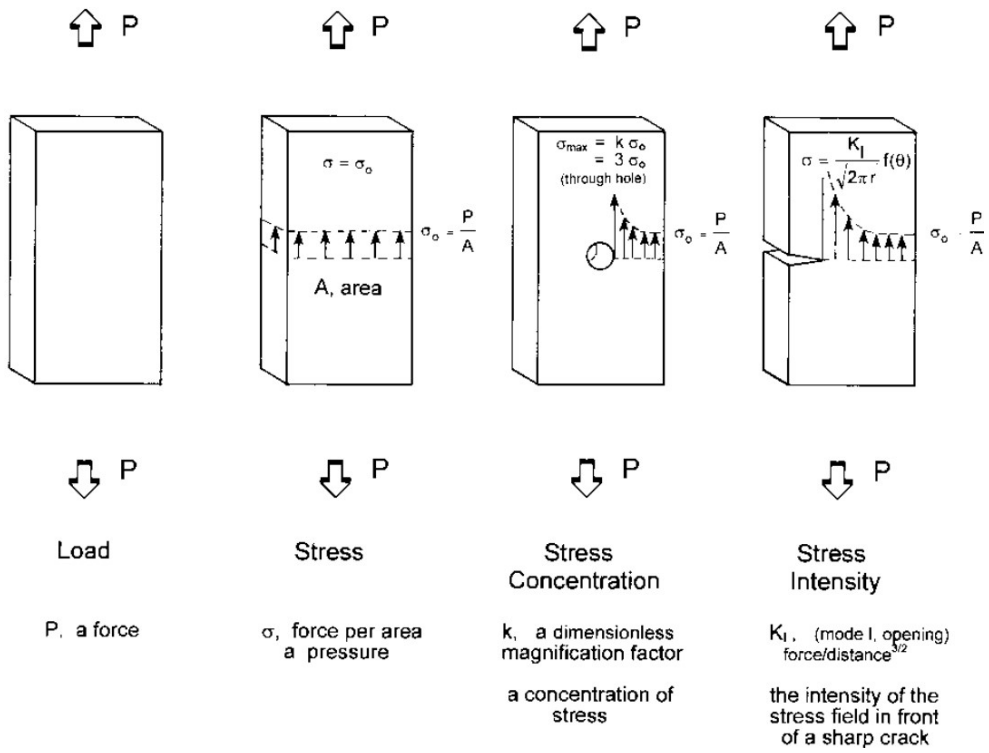

Figure 2.13: Stress concentration and stress intensity (Quinn, 2020).

There are three ways a surface crack can propagate to failure, as shown in Figure 2.14.

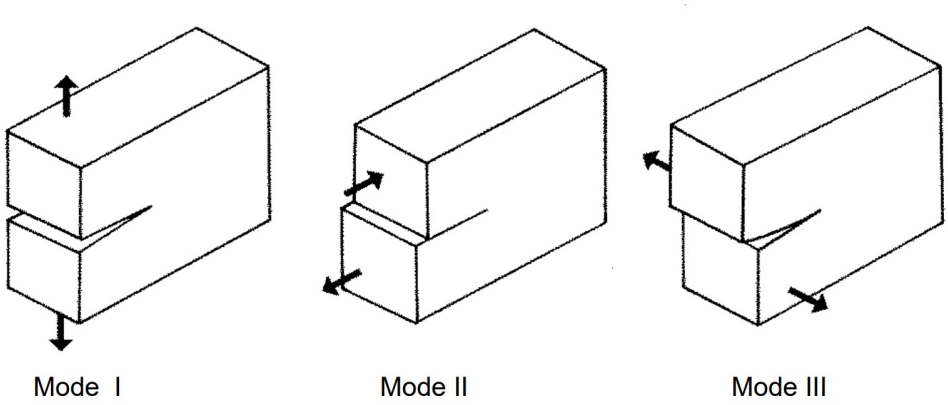

Figure 2.14: Failure modes of a surface crack, from left to right: mode I for opening, mode II for in-plane shear, mode III for out-of-plane shear (Quinn, 2020).

The SIF for mode I loading can be described as follow (Lawn, 1993):

$$K_I = \sigma Y \sqrt{\pi c} \tag{2.4}$$

where
K_I is the SIF for mode I loading
σ is the tensile stress normal to the crack's plane
Y is the shape factor of the flaw
c is the flaw size in meter

Once K_{IC} and Y have been defined, the strength can be estimated from the flaw depth:

$$\sigma_{max} = \frac{K_{IC}}{Y\sqrt{\pi c}} \tag{2.5}$$

This formula has been confirmed by various experiments (Overend & Zammit, 2009, 2012 ; Datsiou & Overend, 2017 ; Haldimann, 2008 ; Sofokleous, 2022).

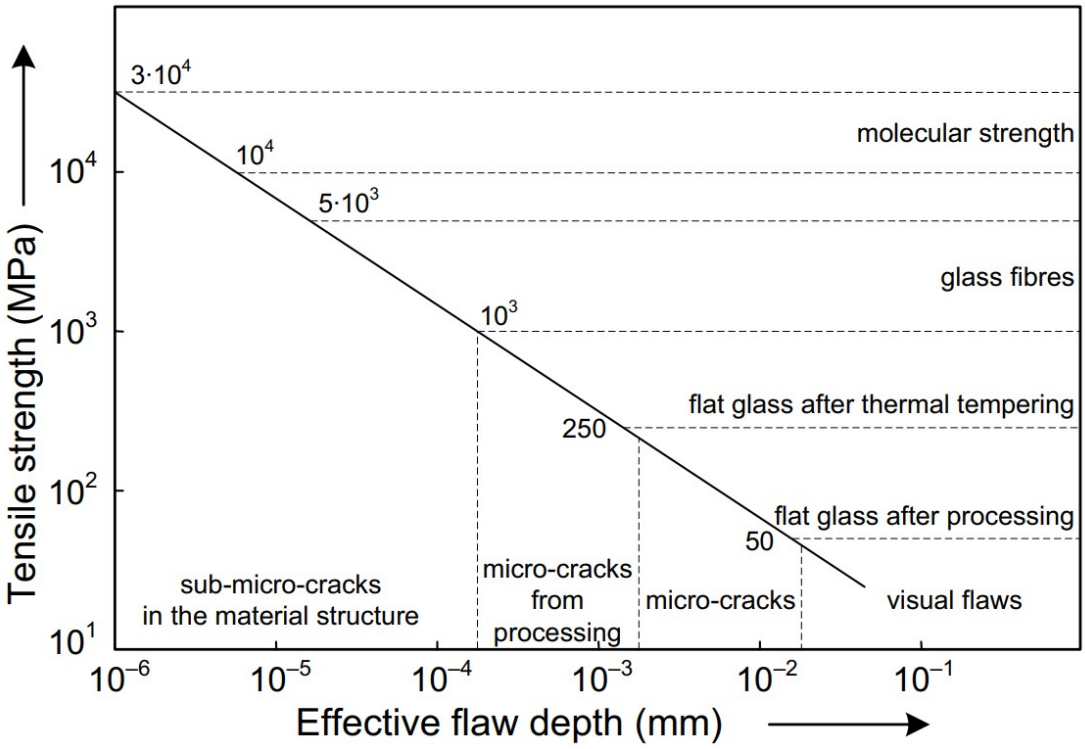

Figure 2.15: Typical strength as a function of the flaw depth (Haldimann, 2008)

The fracture strength of annealed glass can be very variable from one pane to another, with values mostly influenced by the flaw depths. Their characteristic strength is in the order of magnitude of 50 MPa for new glass and 30 MPa for aged glass, with high variability in both cases (Datsiou & Overend, 2017 ; Sofokleous, 2022).

Thermally and chemically tempered glass tends to have more stable results due to the pre-stress contribution to the tensile strength. The surface pre-compression tends to improve the resistance to abrasion of tempered glass to a certain extent. When exposed to the same sand-abrasion process than annealed glass, the measured average flaw depth was 127µm for fully toughened glass, compared to 472µm for annealed glass.

However, this benefit has its limitations. The more the flaw depth is increased, the more the pre-stress level is reduced at the flaw tip, following the stress profile across the glass thickness. If the flaw tip reaches the central tensile area, the pre-stress can even become detrimental to the glass strength and cause breakage without any other external load. Due to its stress profile, chemically tempered glass is more exposed to this risk (Datsiou & Overend, 2017).

2.3.2. Probability distribution functions

Weibull probability distribution

The two-parameters Weibull probability distribution is based on the Weakest-Link Theory, where a brittle material fails when one of its flaw is failing (Weibull, 1951 ; Schneider et al., 2012). It is appreciated

because of its physical background. When assuming that the flaw depths are following an inverse power law probability distribution, the glass strength can be derived to obtain a two parameter Weibull probability distribution (Quinn & Morrell, 1991 ; Ballarini, Pisano & Royer-Carfagni, 2016).

The two parameters Weibull probability distribution is defined according to the shape and scale parameters θ and β:

$$P_f = 1 - exp(-\beta A \sigma_f^{\theta}) \tag{2.6}$$

where
β is the shape parameter
A is the surface area
σ_f is the glass strength
θ is the scale parameter

Normal probability distribution

The normal distribution or Gaussian distribution is the most commonly used distribution to represent random variables whose distributions are not known, partly due to the central limit theorem. It corresponds to the statistical realization of the sum of several random variables (Weisstein, 2020).

The univariate normal probability distribution is defined according to its mean μ and variance σ^2:

$$P_f = \frac{1}{\sqrt{2\pi\sigma^2}} e^{-\frac{(x-\mu)^2}{2\sigma^2}} \tag{2.7}$$

where
μ is the mean parameter
σ is the standard deviation parameter (and σ^2 the variance)
x is the variable

Log-normal probability distribution

The log-normal distribution or Galton distribution is also a continuous probability distribution whose logarithm is normally distributed. It corresponds to the statistical realization of the product of several random variables (Weisstein, 2020).

The univariate log-normal probability distribution is defined according to its mean μ and variance σ^2:

$$P_f = \frac{1}{x\sigma\sqrt{2\pi}} e^{-\frac{(\ln x-\mu)^2}{2\sigma^2}} \tag{2.8}$$

where
μ is the mean parameter
σ is the standard deviation parameter (and σ^2 the variance)
x is the variable

2.4. Non-Destructive Tests

2.4.1. Pre-stress measurements

Pre-stress measurements principles

The purpose of pre-stress measurements is to obtain an estimate of the surface residual pre-stress level. This allows having more accurate information on the tempering contribution to the glass strength.

The most common and accurate way to measure residual pre-stress level on glass is to use the birefringence property of glass (Ramesh & Ramakrishnan, 2016). Like some other materials, the refractive index of glass depends on the polarization and propagation direction of light. When the material is subject to mechanical stresses, this phenomenon is amplified. The experimental method used to analyse stress distribution, called photoelasticity, is based on the same phenomenon.

In a general three-dimensional photoelastic material where the principal stress directions are assumed to remain constant or where the birefringence is weak, the optical information can be related to the stress distribution according to the integral Wertheim law:

$$\begin{aligned} \delta cos2\theta &= C \int (\sigma_x - \sigma_y) dz \\ \delta sin2\theta &= 2C \int \tau_{xy} dz \end{aligned} \tag{2.9}$$

where
δ is the optical retardation
θ is the isoclinic angle
C is the photoelastic constant
σ_x, σ_y and τ_{xy} are the components of the stress tensor

If the residual stress state is isotropic ($\sigma_x = \sigma_y$), a single measurement is sufficient and the residual stress is given by:

$$\sigma(h^{'}) = \frac{\delta_h^{'}}{Csin^2\alpha} \tag{2.10}$$

where
$h^{'}$ is the length of the light path
$\delta_h^{'} = \frac{d\delta(h^{'})}{dh^{'}}$ is the gradient of the optical retardation
C is the photoelastic constant

If the residual stress state is anisotropic, two orthogonal measurements must be done, given by:

$$\begin{aligned} \sigma_x &= \frac{\delta_2^{'} + \delta_1^{'} cos^2\alpha}{C(1 - cos^4\alpha)} \\ \sigma_y &= \frac{\delta_1^{'} + \delta_2^{'} cos^2\alpha}{C(1 - cos^4\alpha)} \end{aligned} \tag{2.11}$$

where
δ_i is the gradient of the optical retardation along axis i
C is the photoelastic constant

Chosen equipment

The most common equipments used to measure the residual pre-stress level of glass are scattered light polariscopes. Among these tools, the SCALP-05 is one of the few portable polariscopes available. In addition, it has been shown in various studies to be quite suitable and accurate for measuring the residual pre-stress level on glass panes (Aben et al., 2010 ; Ramesh & Ramakrishnan, 2016). Therefore, this device was selected for the pre-stress measurements and rented to GlasStress Ltd for this study.

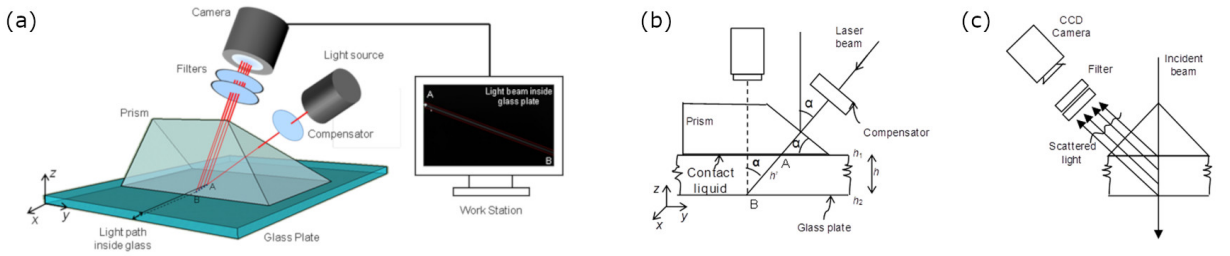

Figure 2.16: (a) Illustration of the scattered light polariscope, (b), (c) schematic optical arrangement of the portable scattered light polariscope (Adapted from Ramesh & Ramakrishnan, 2016)

SCALP-05 emits a polarised laser beam which passes through the glass pane at an angle α to the normal vector, as shown in Figure 2.16. The intensity of the scattered light is recorded by a CCD camera. The software includes a light path detection algorithm to track the laser beam inside the glass. Refraction of the light is prevented by the use of a glass prism and a contact liquid. From this data, the SCALP-05 software calculates the absolute optical retardation at each point along the laser beam, as well as the stress profile through the glass thickness, using the above equations (GlasStress Ltd, 2013).

Initial tests of the device with TU Delft researchers have shown that any bubbles in the liquid or external light source can alter the results and must be carefully avoided. According to them, the precision of SCALP-05 is approximately of 10-20 MPa with the 'very noisy' parameter, 5 MPa with the 'normal' parameter and 3 MPa with the 'good' parameter to qualify the background. The two indicators 'Excl. pixels' and 'Fit error' help to evaluate the quality of the stress profile measurements.

2.4.2. Weathering measurements

Weathering measurements principles

The purpose of the weathering measurements is to obtain an estimate of the global surface quality of the glass and of the largest flaw depths.

Visual inspection for flaw detection on large glass panes (such as windows) can be difficult. Tests using four different inspectors to assess the surface condition of different samples reported a threshold of depth detectability of 40µm (Haldimann, 2008). Considering that the previously reported flaw depths ranged from approximately 20µm to 1400µm (Datsiou & Overend, 2017 ; Sofokleous, 2022), this threshold seems acceptable. Since failure to find the largest flaw or underestimation of the flaw depth can lead to considerably overestimated predicted failure strength, a minimum flaw depth may have to be assumed for a safer design. Although systematically finding the largest flaw on each window does not seem realistic, obtaining an estimate of its size with appropriate statistical margin seems a more achievable goal.

Chosen equipment

A list of the NDTs and equipments used in research has already been made by Sofokleous (2022). The measuring methods used in research differ from those used in the production lines of glass. Various researchers have tried to detect flaws on the glass surface using equipment initially intended for material science or other fields. Although optical microscopes and AFM can provide accurate measurements, only portable device can be considered for on-site measurements.

Previous studies by Kwan and Sofokleous (2022) reported that the Traceit® optical profilometer, conceived by Innowep GmbH, provides accurate measurements within a few seconds. It is also one of the few devices that is portable and can be moved on-site. Therefore, this device was chosen for the weathering measurements in this study.

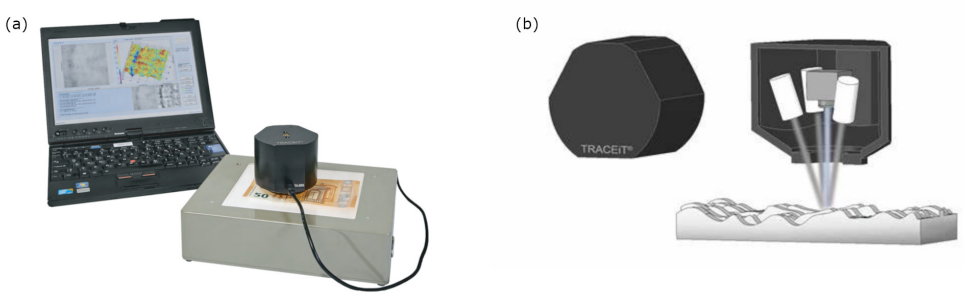

Figure 2.17: (a) Traceit® portable profilometer setup, (b) measurement principle: head with 3 white light optics for topography measurement and additional built-in camera for visual impression (Innowep GmbH, 2024)

The 2D measurement range is 5×5mm. The maximum number of collected data per measurement is 2000 and the accuracy is 2.5µm on the three axis. The surface roughness is defined by the parameters R_a, R_q and R_z which measure the vertical characteristics of the surface deviations (ISO 4287, 2000).

R_a is the average of all absolute roughness distances to the centreline of the roughness profile of the 3D map:

$$R_a = \frac{1}{l_r} \int_0^{l_r} |z(x)| \, dx \tag{2.12}$$

R_q or RMS is the standard deviation of all absolute roughness distances to the centreline of the roughness profile of the 3D map:

$$R_q = \sqrt{\frac{1}{l_r} \int_0^{l_r} z(x)^2 \, dx} \tag{2.13}$$

R_z is the difference between the mean height of the five highest peaks and the five deepest valleys of the 3D map:

$$R_z = \frac{1}{2l_r} (\sum_{i=1}^{n} z(p_i) + \sum_{i=1}^{n} z(v_i)) \tag{2.14}$$

where
l_r is the evaluation length
$z(x)$ is the height of the assessed profile at any position x
$z(p_i)$= Peaks or positive roughness values i
$z(v_i)$= Valleys or negative roughness values i

A Traceit® device was provided by Innowep GmbH for this project. After a training session provided by Innowep's specialists, it became possible to use the device on-site.

2.5. Design standards on glass

2.5.1. Characteristic strength

The characteristic strength of annealed, heat-strengthened and fully toughened glass are taken from the Eurocodes and summarised in the table below.

Table 2.5: Characteristic strength of annealed, heat-strengthened and fully toughened glass from the Eurocodes

Glass type	Characteristic strength	Standard
Annealed	45 MPa	EN 572-1+A1
Heat-strenghened	70 MPa	EN 1863-1
Fully toughened	120 MPa	EN 12150-1+A1

These values are consistent with the orders of magnitude from experimental results found in the literature. However, some publications showed higher characteristic strengths, probably linked with the safety margins taken by the manufacturers (Overend & Zammit, 2009, 2012 ; Haldimann, 2008).

2.5.2. Design strength

Design strength from the Dutch norms

The design strengths of annealed glass is defined as follow (NEN 2608, 2014):

$$f_{mt;u;d} = \frac{k_a \times k_e \times k_{mod} \times k_{sp} \times f_{g;k}}{\gamma_{m;A}} \tag{2.15}$$

where
$f_{mt;u;d}$ is the design value of the bending strength of annealed glass
k_e is the factor for the edge quality of the pane
k_a is the factor for the surface effect
k_{mod} is the modification factor for the load duration and reference period
k_{sp} is the factor for the surface structure of the pane
$f_{g;k}$ is the characteristic value of the bend-induced tensile strength of glass
$\gamma_{m;A}$ is the material factor for glass

The design strengths of pre-stressed glass is defined as follow (NEN 2608, 2014):

$$f_{mt;u;d} = \frac{k_a \times k_e \times k_{mod} \times k_{sp} \times f_{g;k}}{\gamma_{m;A}} + \frac{k_e \times k_z \times (f_{b;k} - k_{sp} \times f_{g;k})}{\gamma_{m;V}} \tag{2.16}$$

where
$f_{mt;u;d}$ is the design value of the bending strength of pre-stressed glass
k_e is the factor for the edge quality of the pane
k_a is the factor for the surface effect
k_{mod} is the modification factor for the load duration and reference period
k_{sp} is the factor for the surface structure of the pane
$f_{g;k}$ is the characteristic value of the bend-induced tensile strength of glass
$\gamma_{m;A}$ is the material factor for glass
k_z is the factor for the zone of the pane
$f_{b;k}$ is the characteristic value of the bend-induced tensile strength of pre-stressed glass
$\gamma_{m;V}$ is the material factor for the pre-stressing of pre-stressed glass

Design strength from the French norms

The design strengths of annealed and pre-stressed glass is defined as follow (FD CEN/TS 19100-1, 2022):

$$f_{g,d} = k_e \times k_{sp} \times \lambda_A \times \lambda_l \times k_{mod} \times \frac{f_{g,k}}{\gamma_M} + k_p \times k_{e,p} \times \frac{f_{b,k} - f_{g,k}}{\gamma_p} \tag{2.17}$$

where
$f_{g,d}$ is the design value of the bending strength of pre-stressed glass
k_e is the factor for the edge quality of the pane
k_{sp} is the factor for the surface structure of the pane
λ_A is the factor for the surface effect
λ_l is the factor for the dimension effect
k_{mod} is the modification factor for the load duration and reference period
$f_{g,k}$ is the characteristic value of the bend-induced tensile strength of glass
γ_M is the material factor for glass
k_p is the factor for the pre-stressing process
$k_{e,p}$ is the factor for the zone of the pane
$f_{b,k}$ is the characteristic value of the bend-induced tensile strength of pre-stressed glass
γ_p is the material factor for the pre-stressing of pre-stressed glass

The Dutch and French norms are very similar. Some coefficients are renamed and applied with slightly different values in some cases, but the global equations and calculated strengths provide the same results in most cases.

2.5.3. Heat-Soak Test

Nickel sulphide (NiS) inclusions are small compounds that cannot be completely avoided during production. These inclusions typically have an elliptical shape with a diameter in the order of 100µm. It exists in different phases at different temperatures. Below 379°C, NiS is stable in the β-phase form. Above this temperature, it is stable in the α-phase. The fast cooling process of thermally toughened glass does not allow enough time for the phase transition to complete. The inclusions are then 'trapped' in the glass in their α-phase.

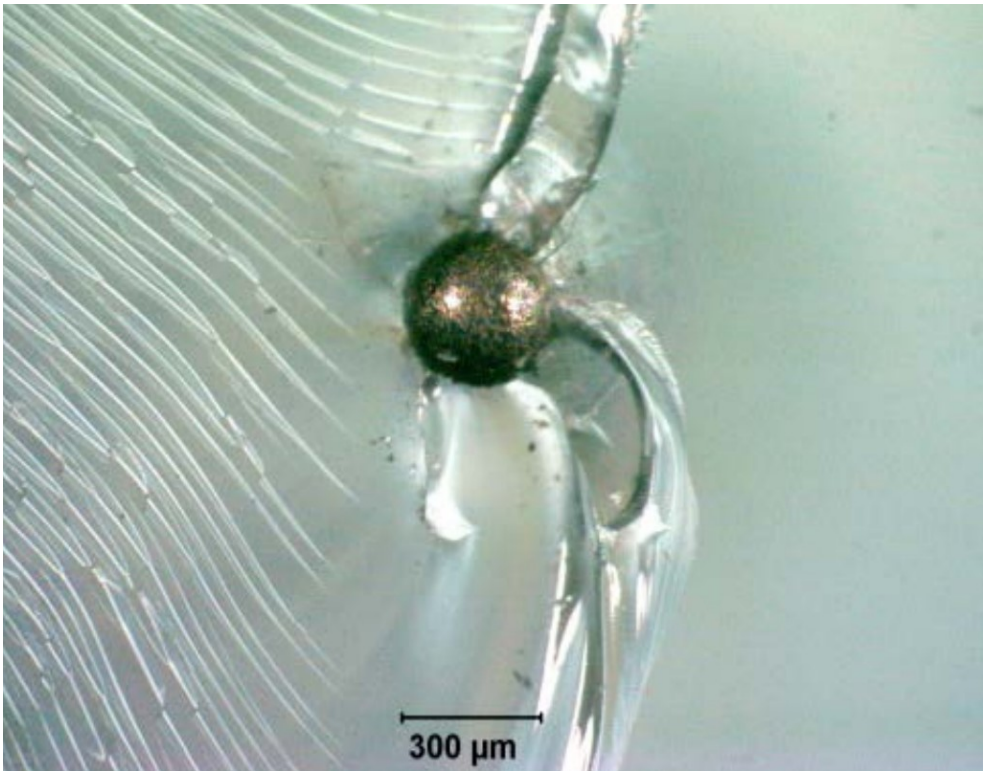

Figure 2.18: Example of a NiS inclusion in glass

Figure 2.19: Typical fracture pattern in tempered glass due to Nis inclusion (Belis et al., 2019)

When cooling down, these inclusions attempt to return to the β-phase, increasing their volume by about 4% (Jacob, 2001). If this inclusion is located in the core tension zone of the tempered glass, the additional tension due to the NiS expansion can cause glass breakage. This type of breakage, which can occur months or years after installation without any precursor sign, is called spontaneous breakage. They produce a typical fracture pattern often referred to as a 'double D' or 'butterfly' pattern.

To date, the only reliable, scalable and widely used method in the industry to prevent spontaneous breakage due to NiS inclusions is the Heat-Soak Test (HST), defined in EN 14179. It was first introduced in 1982. It basically consists of reheating the tempered glass at 290 $\pm$10°C for two hours to accelerate the phase transition and break the glass panes that were at risk.

The breakage frequency before and after HST (and then the HST efficiency) is still subject to discussions. Commonly estimated values are of one breakage every 6 tons of glass without HST, and every 400 tons of glass after HST, giving an HST efficiency of 98.5%.

This process still has some drawbacks. Firstly, the surface compression of tempered glass is slightly reduced in the process. Secondly, this reheating is still relatively costly compared to its benefits. Finally, there are still discussions about the correct temperature and time calibration for this test (Karlsson, 2017).

2.6. Environmental assessment of reuse

2.6.1. Life Cycle Assessment

General approach

Life Cycle Assessment (LCA) is a methodology used to quantify the environmental impacts associated with all the stages of the life-cycle of a commercial product, process or service. It involves a detailed inventory of the energy and materials that are required as inputs and emitted as outputs. In the context of the building industry, an LCA typically includes five life-cycle stages: production, transportation and installation on site, use, and end-of-life (Baker-Brown, 2021).

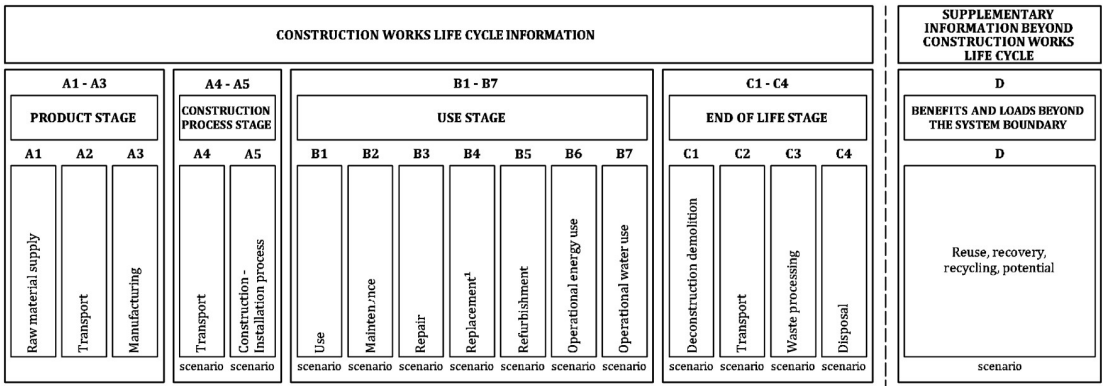

Figure 2.20: Life-cycle stages in an LCA (Adapted from EN 15804, 2019)

The LCA is defined in the international standards ISO 14040 (2006) regarding its 'principles and framework', and ISO 14044 (2006) regarding the 'requirements and guidelines'. Additionally, European standards EN 15804 (2019) and EN 15978 (2011) apply respectively at product level and building level (Baker-Brown, 2021). Modules A1-A3 are material-based, whereas the following modules are scenario-based.

Step A: product and construction process

Modules A1-A3 are related to product stage and includes:

- **Module A1:** raw material extraction and processing, processing of secondary material input (e.g. recycling processes).
- **Module A2:** transport to the manufacturing site including road, boat and/or train transportation of each raw material.
- **Module A3:** manufacturing of product and packaging.

Modules A4-A5 are related to construction process stage and include:

- **Module A4:** transport to the building site.
- **Module A5:** installation into the building.

Step B: use

Modules B1-B5 are related to use stage for building fabric and include:

- **Module B1:** use or application of the installed product.
- **Module B2:** maintenance.
- **Module B3:** repair.
- **Module B4:** replacement.

- **Module B5:** refurbishment.

Modules B6-B7 are related to use stage for building operations and include:

- **Module B6:** operational energy use (e.g. operation of heating system and other building related installed services).
- **Module B7:** operational water use.

Step C: end-of-life

Modules C1-C4 are related to end-of-life stage and include:

- **Module C1:** de-construction, demolition.
- **Module C2:** transport to waste processing.
- **Module C3:** waste processing for reuse, recovery and/or recycling.
- **Module C4:** disposal.

Environmental Product Declarations

In order to carry out the LCA of e.g. a building, data relative to each construction product or service should be taken from Environmental Product Declarations (EPDs).

According to EN 15804 (2019), an EPD *'provides quantified environmental information for a construction product or service on a harmonised and scientific basis. It also provides information on health related emissions to indoor air, soil and water during the use stage of the building'*. There are several databases of EPDs issued by manufacturers and professional associations available to the public.

Limitations

The LCA approach still has the following main limitations:

- Variations in terms of assumptions and information included in LCA studies (Matthews et al., 2014).
- Non-uniform Product Category Rules (PCRs). Although it should provide guidance to compare products of the same category, PCRs can be inconsistent among program operators (Ingwersen & Subramanian, 2014).
- Inconsistent databases due to lack of precise site-specific data and use of generic data instead (Modahl et al., 2013), or unavailability of EPDs and PCRs for a product which involves the previous products can lead to inaccurate declarations (Gelowitz & McArthur, 2016).
- Lack of satisfactory third-party critical review for EPDs. Reviewing of only generic aspects and not specific ones can lead to different interpretations of EPDs for similar products (Lasvaux et al., 2013).

Consequently, an LCA on the same product completed by 10 different stakeholders could lead to 10 different results. The aforementioned standards aim to normalise this, but are not overly restrictive and could still yield 10 different answers (Matthews et al., 2014). Therefore, the results should be interpreted with caution.

2.6.2. Reuse compared to recycling and down-cycling in the LCA

Global approach

Although the global warming indicator is the most widely used, it should be kept in mind that the LCA is a multi-criteria tool. The latest European standards include 13 impact indicators (such as global warming,

ozone depletion, acidification of soil and water, and abiotic resource depletion) and 17 flow indicators (such as consumption of primary energy, water, and waste). When comparing reuse with recycling and down-cycling, the following indicators can be considered:

- **Components for reuse (kg):** total quantity of elements intended for reuse in a second life-cycle.
- **Materials for recycling (kg):** total quantity of elements intended for recycling.
- **Global Warming Potential total (kg CO_2 eq.):** total quantity from all classified flows converted into kg CO_2 eq. respective to their related impact.

Recycling enables savings to be made in terms of extracting raw materials such as sand and limestone. However, it still requires a manufacturing step, such as melting down and reshaping into a glass pane. In contrast, reusing a product can avoid the impacts associated with both extracting raw materials and re-manufacturing.

Reusing a product changes the stages in the LCA of both the first and second product life-cycles. In the first life-cycle, the deconstruction stage may involve more labour and energy-consuming tools, technical performance checks and transportation for the reused products. On the other hand, waste disposal is reduced. During the second life-cycle, the production stage is significantly reduced due to less extraction and manufacturing.

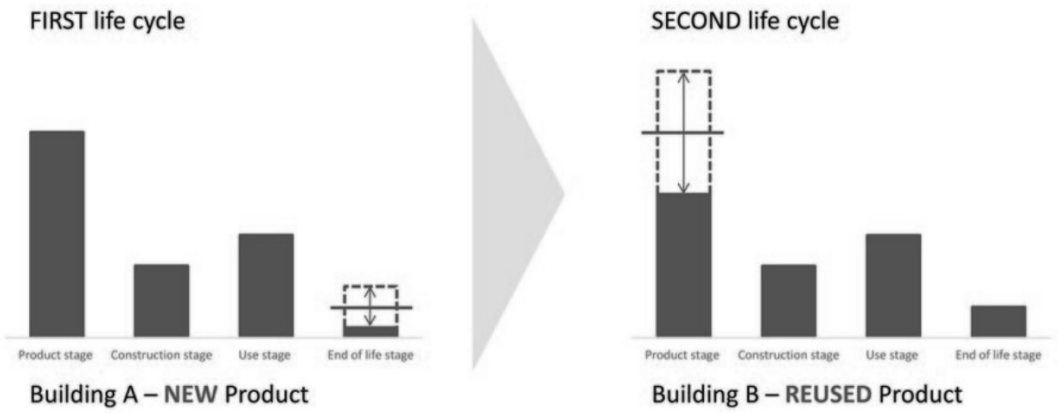

Figure 2.21: Installation of a new product in building A, then reuse of the product in building B (Baker-Brown, 2021)

In most cases, reuse allows substantial environmental benefits, although some additional impacts may also be generated. These benefits should be ensured by checking that additional, end-of-life impacts are not excessively significant and that the re-manufacturing process generates less of an impact than manufacturing a new product would (Baker-Brown, 2021).

Recycling and reuse can prevent the environmental impacts of different modules, as shown in Figure 2.22. In order to compare these different scenarios, these benefits must be included in module D.

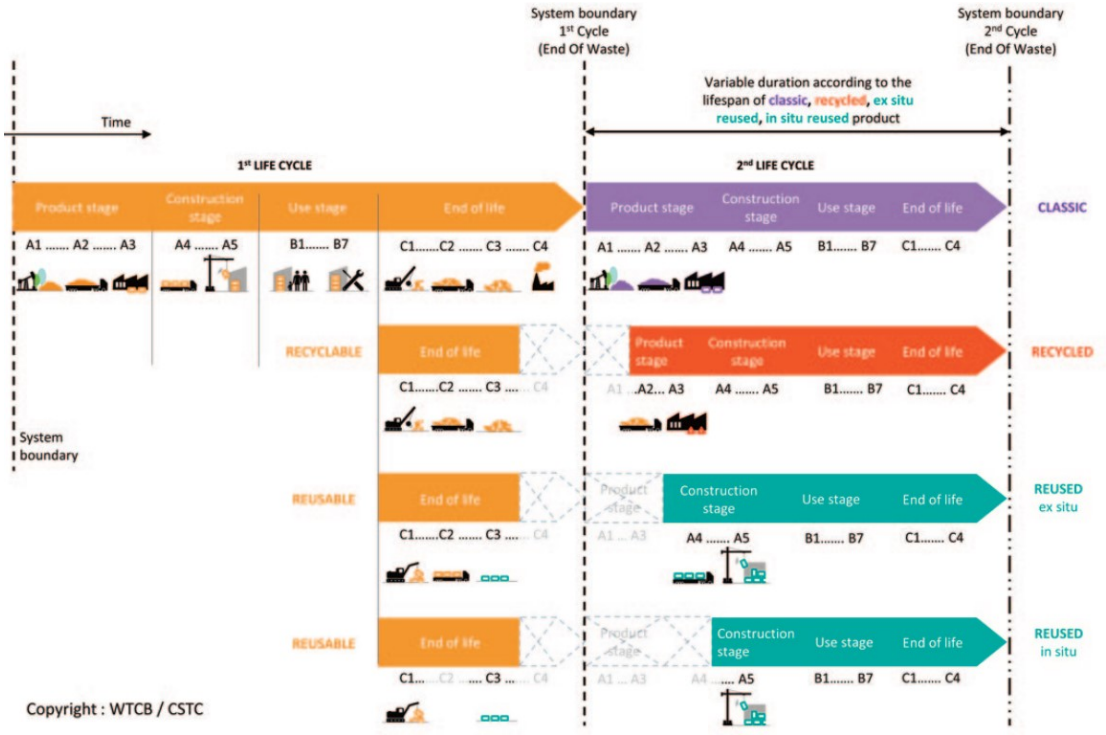

Figure 2.22: Impact of recycling and reuse on life-cycle modules (Baker-Brown, 2021)

Assessment of module D

Module D includes reuse, recovery and/or recycling potentials, expressed as net impacts and benefits. It is influenced by the following factors (Baker-Brown, 2021):

- **Reuse rate:** determines the proportion of product which can be used again.
- **End of waste state:** defines the boundary between the two life-cycles of the product, which may alter the allocation of certain environmental impacts between the first and second life-cycles.
- **Substituted primary materials:** clarifies which primary material has been replaced by secondary material.
- **Point of functional equivalence:** establishes whether the reused product can perform all the same functions as the new product.

Reference Service Life

Finally, the lifetime of new products is taken into account in the EN 15804 (2019) under the name of Reference Service Life (RSL). Environmental impact is calculated for a product's whole RSL, taking into account for potential replacements with the following equation:

$$T = I \times (1 + N) \tag{2.18}$$

where
T is the total impact of the product over the whole RSL
I is the impact of the product over its own service life
N is the number of replacements of the product

The RSL of a new product depends on criteria such as the product properties, design application parameters, assumed quality of work, environment, usage condition and maintenance. If the reused product can meet

the same standards, requirements and usage as a new product, the same RSL may be applicable. Otherwise, it must be evaluated to try justifying its own RSL (Baker-Brown, 2021).

3

Case study

3.1. Context

The case study is a confidential building in Paris with a double skin façade built about 50 years ago. As the building is relatively old and overheats in summer, a renovation project is being studied. While the outer skin cannot be reused due to various safety and regulatory requirements, the inner skin may be suitable for reuse.

The building is currently occupied by French public administrations, which makes it more difficult to organise site visits. Fortunately, some floors are currently unoccupied and more easily accessible. These floors are considered large and varied enough to provide representative glass samples for this study.

Eckersley O'Callaghan is involved as façade engineer in this project. The team is quite optimistic about the reuse potential of the glass panes in this case study. However, their safety has yet to be proven to the authorities, and the client has yet to be convinced.

The structural assessment must be carried out in accordance with the Eurocodes and the French National Annexes. The French regulations are known to be particularly stringent. As this subject is not yet fully addressed in the regulations, equivalent performance and safety levels must be rigorously demonstrated using structural mechanics principles and regulations.

Another requirement of the 'bureau de contrôle' is that the 50 year old reused panels without HST must be shown to have an equivalent level of safety to new glass panels with HST. As the equivalent risk of spontaneous breakage due to NiS inclusion is not fully covered by the regulations, it must be demonstrated based on the existing literature.

3.2. Glass panes

This case study focuses on the inner part of the double skin façade, which consists of approximately 2500 fully toughened glass panes. The façade follows a single repeating pattern, allowing the same window size to be repeated across almost the entire façade.

Figure 3.1: Inside view of a room with the repeated façade system

Figure 3.2: Inside view of the double skin façade

The inner skin is made of a single monolithic layer of tempered glass, measuring 2.2x1.4 metres and 10 mm thick. After a quick visual inspections during the first on-site visits, they appear to be in generally good condition with only a few small visible digs and scratches. The windows can be opened and are continuously supported at the top and bottom sides with dry connections. This type of connection is relatively easy to disassemble and quite suitable for reuse.

Figure 3.3: Opening of the inner skin

The glass panes have two different types of stamps, called either 'Pont à Mousson' or 'Securit'. After discussion with Saint-Gobain engineers and consultation of the project archives, these glass panes should all be of the same type (SECURIT tempered glass by Saint-Gobain), from the original 1970s construction. The sampling contains 39% of panes with 'Pont à Mousson' stamps and 61% with the 'Securit' stamp, so there are too many panes of both types to consider any replacement in the past. Furthermore, there is no known replacement campaign for the inner glass panes. According to Saint-Gobain specialists, the most likely explanation is that the glass panes were manufactured shortly after the purchase of the 'Pont à Mousson' factory, when all the stamps had not yet been updated. The absence of any significant difference between the two categories will be confirmed in the following chapters and annexes.

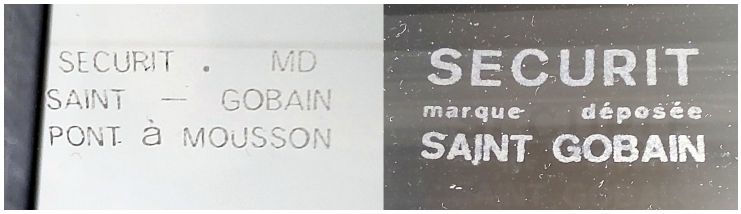

Figure 3.4: Stamps 'Pont à Mousson' (left) and 'Securit' (right) observed on the glass panes.

One point of interest is that the FLOAT process was still under Pilkington's patent approximately at that time. Therefore, the manufacturing process for these glass panes was the TWIN process instead. This process is closer to the Bicheroux or drawn sheet processes described in Subsection 2.1.2. This process is not expected to have a significant effect on the surface quality of the glass, but still should be noted.

Archives from Saint-Gobain indicate an average strength of 210 MPa. It would therefore be reasonable to expect a characteristic strength of glass above the design requirement of 120 MPa from the Eurocodes. If this margin proves to be true, it could help to demonstrate the reuse potential of these glass panes.

3.3. Objectives for the case study

Different design options are considered to allow the glass to be reused as fully toughened, heat-strengthened or annealed glass. The aim of this case study is then to be able to assess the reuse potential for these three scenarios. There is some flexibility in the type of qualification for the glass to be reused. Whenever the glass panes could not be safely demonstrated to have the strength of fully toughened glass, then a qualification for heat-strengthened or even annealed glass could still be useful for this project. The focus is more on the safety of the glass panes to reuse, with the following elements:

- Short impact study: understand and communicate about the global impact of reusing these glass panes.
- Probabilistic equivalence of the Heat-Soak Test: due to the French regulations, an equivalent safety level regarding spontaneous breakage due to NiS inclusions must be argumented.
- Breakage safety: breakage must produce only small pieces of glass. Measurements of a pre-stress level equivalent to fully toughened glass should be sufficient to prove it.
- Strength qualification: classification as fully toughened, heat-strengthened or annealed glass in a safe and efficient way.

4

Comparative environmental impact assessment

4.1. Scope of the study

This study will present the findings from an environmental assessment conducted on the internal glass panes of a confidential building in Paris. It aims a better highlight of the comparative environmental savings using an end-of-life (EoL) recycling approach, also known as avoided burden. This approaches operates under the assumption that environmental benefits are only granted for the fraction of material that is recovered and recycled after the use phase.

This comparative study will only focus on modules where noticeable differences apply between the different scenarios. The 'reuse in situ' scenario is the one involving the largest number of different modules, as previously shown in Figure 2.22. Modules A1 to A3 are considered as the raw material supply, transport and manufacturing can have a significant environmental impact and can be at least partially compensated in module D. Module A5 is not considered in this study as its impact is expected to be the same for all scenarios. Modules B1 to B7 are excluded as the Reference Service Life (RSL) of the reused and recycled products is expected to be the same as the one of a new product, leading to the same values for these modules. Module C1 is excluded because the relative difference between the different end-of-life scenarios under study is considered to be marginal (Quéheille et al., 2022). Module C2 is included to take into account the impact of transport at end-of-life stage. Modules C3 and C4 are included to take the reprocessing and disposal costs into account.

The included modules for this study are summarised in Figure 4.1:

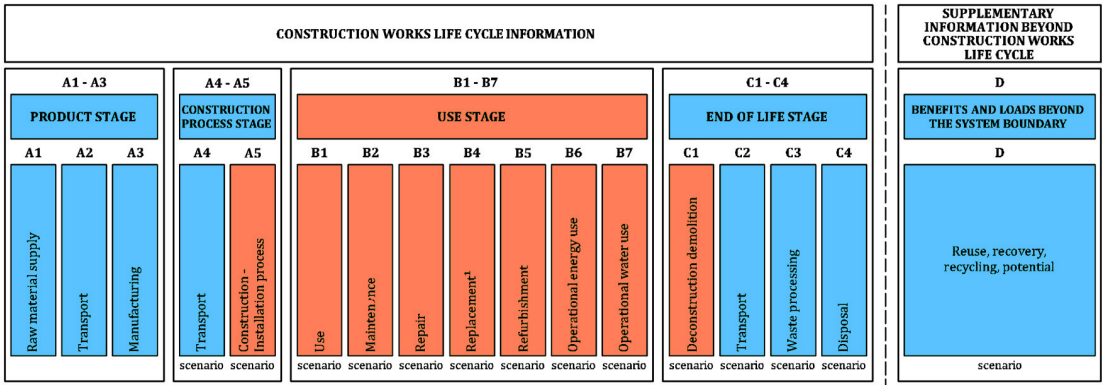

Figure 4.1: Modules in which this study will focus (Adapted from EN 15804, 2019 ; Hartwell & Overend, 2019)

The comparison will focus on four idealised EoL scenarios:

- **Reuse:** 100% glass panels are reused on-site on the same building without any transportation.
- **Recycling:** 100% glass cullets are recycled to be used for container glass.
- **Down-cycling:** 100% glass cullets are downcycled to be used for concrete rubbles or other inert materials.
- **Landfill:** 100% glass panels are sent to landfill.

The environmental indicators under study are the components for reuse (kg), materials for recycling (kg) and Global Warming Potential total (kg CO_2 eq.).

Firstly, the comparative study will focus solely on the glass panes to provide values for the GWP gains for the four scenarios. The mass of reused or recycled material and amount of avoided kg CO_2 eq. in each end-of-life scenario will be evaluated.

Secondly, the values for the studied glass panes will be compared to the façade system (frames, insulation, coverings, external skin). This will provide a complementary perspective on the relative impact of reuse and recycling.

4.2. Comparative LCA: absolute values

The existing glass panes are marked by Saint-Gobain and have been identified. The chosen functional unit (FU) is based on the EPD from Saint-Gobain: 1m² of 10mm SECURIT® SGG glass (=25kg). The total amount of glass in this study reaches 8280m² (=207 tonnes).

According to this EPD, the modules A1-A3 would have a GWP of 34.2 kg CO_2 eq. per FU. However, this value is too optimistic for this study as this EPD is based on the use of 12.5% of secondary material. Instead, the GWP for stages 1-3 of 1.29 kg CO_2/kg_{output} (32.25 kg CO_2 per FU) is taken as a basis for flat glass with 0% of secondary material and without toughening (Hartwell, Coult & Overend, 2023). The contribution of toughening in these modules A1-A3 can be estimated from the difference between the PLANICLEAR® and SECURIT® SGG glass EPDs, with a value of 7 kg CO_2 per FU. The sum of these two values is 39.25 kg CO_2 per FU.

The module A4 is calculated on the basis of a scenario with the parameters listed in Table 4.1, which is equivalent to a GWP of 0.61 kg CO_2 eq. per FU.

Table 4.1: Module A4 parameters

Parameter	Value/description
Fuel type, consumption of vehicle	Average truck trailer with a 27t payload Diesel consumption 38 liters for 100 km
Distance	650 km
Capacity utilisation	100% of the capacity in volume 30% of empty returns in mass
Bulk density of transported products	2500kg/m^3
Volume capacity utilisation factor	<1

Module C2 considers a 50km transport distance to landfill, resulting in 0.061 kg CO_2 eq. per FU. Module C3 includes the reprocessing costs. It is considered negligible in these end-of-life scenarios. Module C4 has a GWP of 0.35 kg CO_2 eq. per FU.

Module D for reuse in situ is based on the assumption that modules A1 to A4 are completely compensated. The value of 39.86 kg CO_2 eq. is obtained. This is consistent with the existing regulations made to encourage reuse, but slightly more optimistic than the reality.

Module D for recycling is based on the total for A1 to A3 of the new product produced with 100% of recycled content (RC). The emissions savings associated with the production of flat glass with 100% cullet are equal to 0.77 kg CO_2 eq./kg of glass output. This was extracted from the supplementary information

documents from Hartwell, Coult & Overend (2023). Considering a FU of 25kg, this value is multiplied by 25 and subtracted from A1-A3 to obtain $39.25 - 0.77 \times 25 = 20 kg CO_2 eq$.

Module D for down-cycling is based on the embodied carbon for stages 1-3 of aggregate products (Hammond & Jones, 2011), and the C module for glass. The reference value for stages 1-3 of aggregate products is 0.0052 kg CO_2 eq/kg, which is relatively low. This value becomes 0.13 kg CO_2 eq. per FU.

The Reference Service Life (RSL) of the new product reaches 30 years in the EPD. Since the recycled and reused products are assumed to comply with the same structural and optical requirements than that of new products, their RSL are also considered to reach 30 years.

The total avoided burden T is calculated based on the C and D modules as follows:

$$T = (C1 + C2 + C3 + C4 + D) \times mass \tag{4.1}$$

Table 4.2: Difference of kg CO_2 equivalent between reuse, recycling, down-cycling and landfill end-of-life scenarios

	A1-A3	A4	A5	B1-B7	C1	C2	C3	C4	D (estimate)	T (total avoided burden)
Reuse in situ	39.25	0.61	-	-	0	0.061	0	0.35	-39.86	-326 638
Recycling	39.25	0.61	-	-	0	0.061	0	0.35	-20	-162 197
Down-cycling	39.25	0.61	-	-	0	0.061	0	0.35	-0.13	2 327
Landfill	39.25	0.61	-	-	0	0.061	0	0.35	0	3 403

4.3. Comparative LCA: relative values

Comparison of the four scenarios about the avoided carbon emissions relative to the total emissions of the facades. The goal here is then to have an idea of the impact of the recovery strategies compared to the initial environmental impact of the façades. It will be done by evaluating the relative impact between the avoided burden of each recovery scenario for the internal glazing, and the production/transport stage A1 to A4 for the whole façade.

The unit taken here corresponds to one 'oriel', with two internal and external glass panes and the surrounding elements. Table 4.3 details the chosen EPDs for each element of the façade, the coefficients to apply in order to reach the right amounts for one 'oriel' and the associated masses.

Table 4.3: EPDs used for the different façade components for one module

Element	Chosen EPD	Functional Unit	Quantity	Mass per FU (kg)	Mass (kg)	RSL (years)
Aluminium plates	SOLID COIL COATED ALUMINIUM SHEET ELVAL ENF 1 mm	1 m²	6.59	2.7	17.79	50
Steel elements	Heavy Steel Plates ArcelorMittal Europe	1 ton	0.0437	1000	43.71	100
Separating glazing	Saint-Gobain PLANICLEAR 8mm	1 m²	1.84	20	36.80	30
External glazing	Saint-Gobain CLIMAPLUS/CLIMALIT PLUS 8t-16-6	1 m²	7.88	35	275.80	30
External plates	SOLID COIL COATED ALUMINIUM SHEET ELVAL ENF 2 mm	1 m²	2.7	5.4	14.58	50
Studied internal glazing	Saint-Gobain SECURIT 10mm	1 m²	6.44	25	161.00	30

The GWP is then calculated as the sum of the weighted scores for each façade element, as shown in Table 4.4. The 'studied internal glazing' corresponds to the glass panes available for recovery.

Table 4.4: GWP in kg CO_2 equivalent of the different façade components, for one module

Element	A1-A3	A4	Total A1-A4
Aluminium frames	71.57	0.00	71.57
Steel elements	34.09	0.00	34.09
Separating glazing	34.04	0.95	34.99
External glazing	432.61	6.82	439.44
External plates	55.57	0.00	55.57
Studied internal glazing	252.77	3.93	256.70
Total	880.65	11.70	892.35

The relative recycled and reused mass of the recovered glass panes are calculated as follow for one 'oriel' module:

$$\begin{aligned} R_{recycling} &= \frac{M_{recycling}}{M_{facade}} = \frac{161.00}{549.68} = 29\% \\ R_{reuse} &= \frac{M_{reuse}}{M_{facade}} = \frac{161.00}{549.68} = 29\% \end{aligned} \tag{4.2}$$

with
$R_{recycling}$ the relative recycled mass of the recovered glass panes in a module
R_{reuse} the relative reused mass of the recovered glass panes in a module
$M_{recycling}$ the recycled mass of the recovered glass panes in a module
M_{reuse} the reused mass of the recovered glass panes in a module
M_{facade} the total mass of the façade system in a module

The relative impact is calculated based on the avoided burden of each recovery scenario for the internal glazing, divided by the production/transport stage A1 to A4 for one 'oriel' module. The c coefficient scales the avoided burden from the whole building to one 'oriel' module.

$$\begin{aligned} I_{relative,reuse} &= \frac{T_{reuse} \times c}{I_{facade}} = -30\% \\ I_{relative,recycling} &= \frac{T_{recycling} \times c}{I_{facade}} = -15\% \\ I_{relative,downcycling} &= \frac{T_{downcycling} \times c}{I_{facade}} = 0\% \end{aligned} \tag{4.3}$$

with
$I_{relative,reuse}$ the relative avoided GWP with the reuse scenario
$I_{relative,recycling}$ the relative avoided GWP with the recycling scenario
$I_{relative,downcycling}$ the relative avoided GWP with the down-cycling scenario
T_{reuse} the avoided burden with the reuse scenario
$T_{recycling}$ the avoided burden with the recycling scenario
$T_{downcycling}$ the avoided burden with the recycling scenario
c the coefficient to scale the avoided burden from the whole building to one 'oriel' module
I_{facade} the total GWP of the façade system for one module

From theses results, the relative values of avoided GWP can be summarised in Table 4.5.

Table 4.5: Difference of kg CO_2 equivalent between reuse, recycling and down-cycling relative to the façade

	Relative reused mass	Relative recycled mass	Relative GWP difference
Reuse	29%	0%	-30%
Recycling	0%	29%	-15%
Down-cycling	0%	0%	0%

4.4. Discussions

The numbers taken from EPDs always have to be interpreted with caution, as explained in Subsection 2.6.1.6. Moreover, the four defined scenarios are idealised with 100% of the glass being reused, recycled, down-cycled or sent to landfill. The reality is most of the time a mix of these different scenarios.

The most common scenario in the glass industry currently is a mix of down-cycling, landfill and recycling. The current recycling rate of glass cullets in the UK as well as in Europe is still very low (Hartwell, Coult & Overend, 2023) and can be estimated at 1%, while the landfill rate is estimated at 20%.

The reuse and recycling rates increased regularly over the last years, and are expected to keep rising in the near future. These values will then have to be updated accordingly.

In the recycling and reuse scenarios, the rates are often below 100% as not all glass qualify. Especially for reuse, some panels may not comply with the structural and optical requirements, and some other may be damaged during handling or required for some destructive tests. Even in a favourable situation where all panels would qualify for reuse, a reuse rate of 95% is more realistic. This value of 95% corresponds to the recycling rate used in some EPDs for tempered glass.

All these mixed scenarios alter the benefits of a circular economy approach compared to a linear one, but result in a more realistic and nuanced comparison.

Table 4.6: Mixed scenario composition based on existing rates from EPDs and statistics from Saint-Gobain

Scenario	Mix
Mixed reuse	5% landfill, 95% reuse
Mixed recycling	5% landfill, 95% recycling
Mixed down-cycling	20% landfill, 79% down-cycling, 1% recycling

The ratios of these scenarios are very dependent on the project, time and companies involved. It may evolve relatively quickly and should be specific to each project.

Table 4.7: Difference of kg CO_2 equivalent between mixed scenarios

Scenario	Total difference (kg CO_2 eq.)
Mixed reuse	-310 306
Mixed recycling	-154 087
Mixed down-cycling	897

Table 4.8: Difference of kg CO_2 equivalent between mixed scenarios relative to the façade

	Relative reused mass	Relative recycled mass	Relative avoided GWP
Mixed reuse	28%	0%	-28%
Mixed recycling	0%	28%	-14%
Mixed down-cycling	0%	0%	0%

Therefore, the benefits of a mixed reuse scenario compared to a mixed down-cycling scenario are of 161 tons of reused material and 309 409 kg CO_2 eq. in total. Relative to the building façade, it provides 28% of reused mass and 28% of avoided GWP.

5

Probabilistic equivalence of the Heat-Soak Test

5.1. Initial probability of failure with and without Heat-Soak Test

A commonly accepted breakage rate due to NiS inclusions without HST is 1 breakage per 6 tonnes of glass, which becomes 1 breakage every 400 tonnes of glass after HST. Although the efficiency of the HST could even be higher in practice sometimes (Kasper, 2019), these values are chosen since these are the most commonly adopted and prognosticated.

Table 5.1: Chosen probabilities of failure

Tonnes of glass for one breakage, without HST	6
Tonnes of glass for one breakage, with HST	400
Efficiency of the HST	98.50%

5.2. Probability of failure without Heat-Soak Test over time: dataset 1

The first dataset regarding probability of failure due to NiS inclusions over time is based on data from a single major project (Jacob, 2001 ; Jacob & Calderone 2003) analyzed during 14 years.

Table 5.2: Failure data due to NiS inclusions over time, each year (dataset 1)

Year	1	2	3	4	5	6	7	8	9	10	11	12	13	14
Number of failure	15	13	16	14	9	5	4	2	6	2	2	4	2	2
Cumulated number of failure	15	28	44	58	67	72	76	78	84	86	88	92	94	96

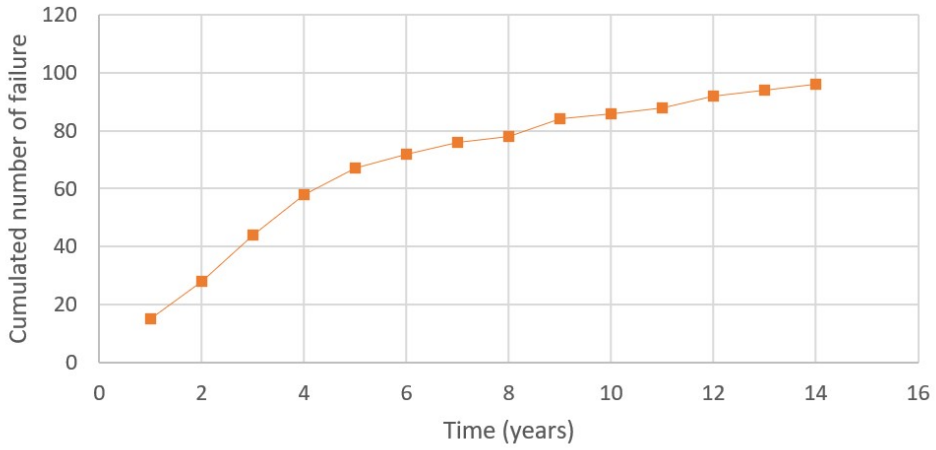

Figure 5.1: Cumulated failure data due to NiS inclusions over time (dataset 1)

The cumulative probability of failure over time can be represented by various functions, among which the log-normal distribution is considered to be the most appropriate (Jacob & Calderone, 2003). This function is fitted by the Least Square Method.

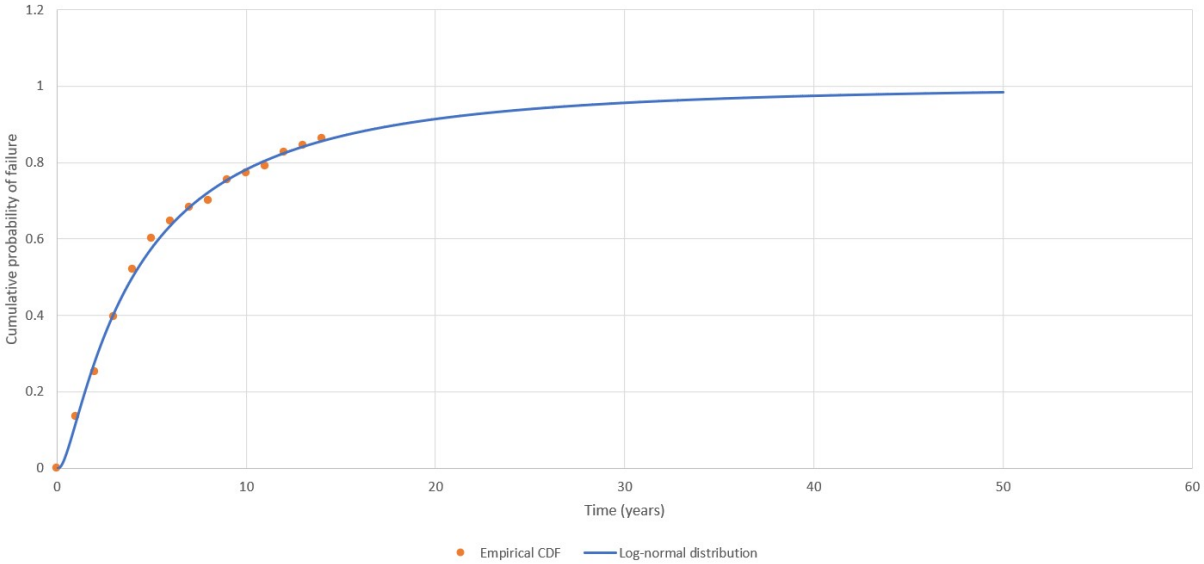

Figure 5.2: Cumulative probability of failure caused by NiS inclusions over time (dataset 1). Log-normal distribution with μ = 1.3816, σ= 1.1834 and a maximal number of breakage of 111.

Values from the distribution function are taken every 10 years to be compared to the efficiency of the HST. Given these values, a probabilistic equivalence of the HST can be defined at 50 years where an efficiency of 98.38% $\approx$ 98.5% is reached.

Table 5.3: Probabilistic equivalence of the HST over time

Year	Probabilistic equivalence (Log-normal)
0	0%
10	78.18%
20	91.37%
30	95.60%
40	97.44%
50	98.38%
60	98.91%
70	99.23%
80	99.44%
90	99.58%
100	99.68%

5.3. Probability of failure without Heat-Soak Test over time: dataset 2

The second dataset of this kind is related to HS glass instead of FT glass, but can still be of some interest for this study. It was measured graphically from the publication by Kasper, Colvin, Rubbert & Serruys (2023).

The breakage rate reaches here a peak approximately 4 years after installation, depending on the exposure of the pane to temperature variation. These temperature variations would mostly act as a catalyst for transitions from α-NiS to β-Nis (Kasper, Colvin, Rubbert & Serruys, 2023).

Table 5.4: Failure data due to NiS inclusions over time, each year (dataset 2)

Year	0.50	1.87	2.41	2.44	2.83	3.44	3.50	3.57	3.65	4	4.29	4.35	4.42	4.48	5.42	5.66	6.45	6.57	6.64
Number of failure	0	1	1	1	1	1	1	1	1	1	1	1	1	1	1	1	1	1	1
Cumulated number of failure	0	1	2	3	4	5	6	7	8	9	10	11	12	13	14	15	16	17	18

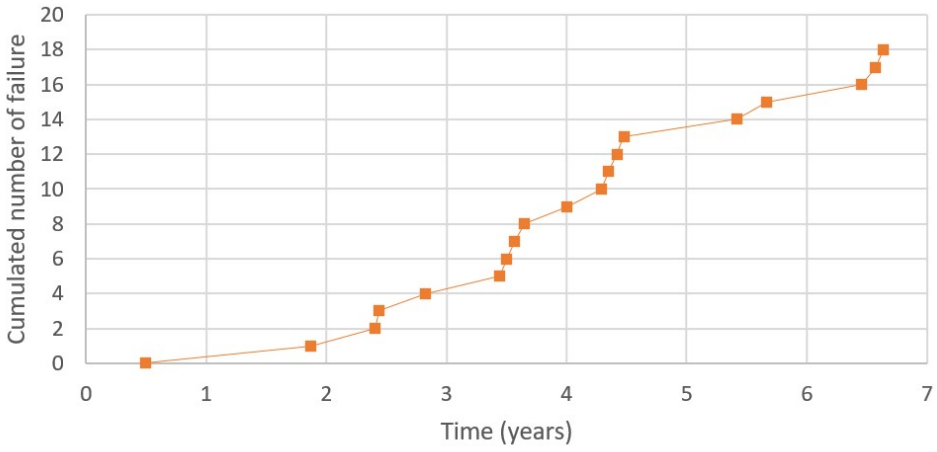

Figure 5.3: Cumulated failure data due to NiS inclusions over time (dataset 2)

The cumulative probability of failure over time was calculated using a Weibull distribution in the study by Kasper, Colvin, Rubbert & Serruys (2023) , with a maximum number of failures estimated at 20. This led to a CDF increasing relatively quickly, with a probabilistic equivalence to the HST reaching 98.5% before 9 years. This parameter was then modified to be more conservative and relatable to the first dataset. If we

make the simplified assumption that the percentage of breakage at 6.5 years compared to the maximum number of breakage is the same as in the first dataset (67%), the maximum number of breakage for this dataset is then equal to 27.

The Weibull distribution with this more conservative parameter is plotted in Figure 5.4. To provide comparable results to the first dataset and to obtain a more conservative distribution, a log-normal distribution is fitted in the same figure. Both functions are fitted using the Least Square Method.

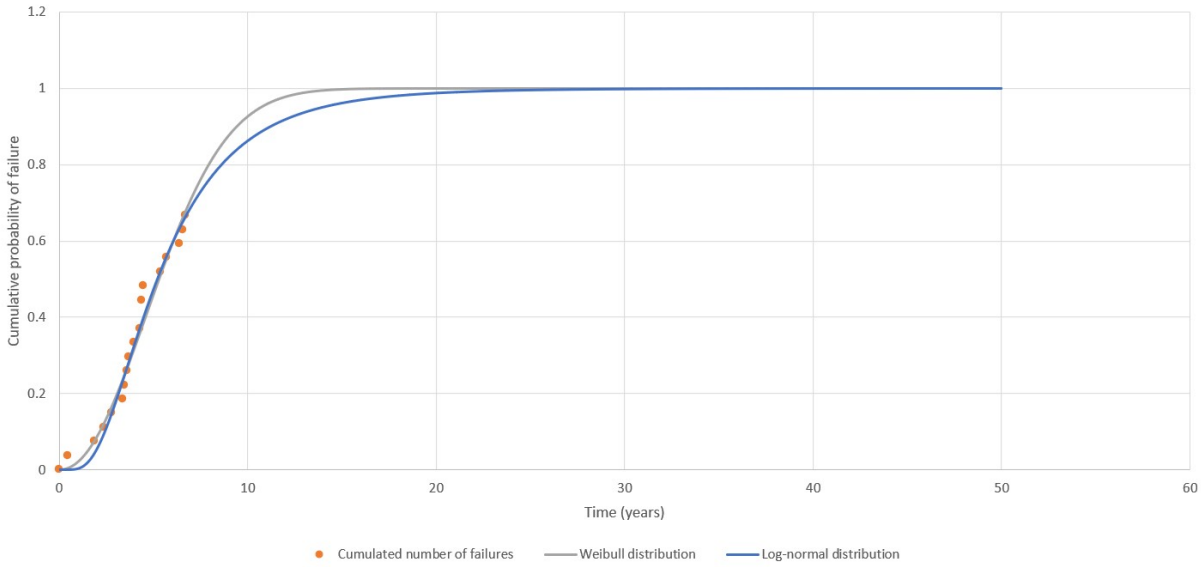

Figure 5.4: Cumulative probability of failure caused by NiS inclusions over time (dataset 2). Weibull distribution with λ= 6.3049 and k = 2.0826. Log-normal distribution with μ = 1.6479, σ= 0.5993 and a maximal number of breakage of 27.

Values from the distribution functions are taken every 10 years to be compared to the efficiency of the HST. Given these values, the probabilistic equivalence of the HST is reached at approximately 20 years according to the Weibull distribution and 30 years according to the Log-normal distribution.

Table 5.5: Probabilistic equivalence of the HST over time

Year	Probabilistic equivalence (Weibull)	Probabilistic equivalence (Log-normal)
0	0%	0%
10	92.67%	86.27%
20	99.99%	98.69%
30	~100%	99.83%
40	~100%	99.96%
50	~100%	99.99%
60	~100%	~100%
70	~100%	~100%
80	~100%	~100%
90	~100%	~100%
100	~100%	~100%

5.4. Discussion

Data on the number of failures due to NiS inclusion over time is very scarce. Only the two datasets presented in this chapter were found for this study. As these datasets are not very diverse and contain only a limited number of failures over time, they must be treated carefully. However, a good understanding of the phenomena with statistical analysis using conservative assumptions could let us assume safely that a probabilistic equivalence of the HST can be reached approximately after 30 years, and even more safely after 50 years.

More data on spontaneous breakage due to NiS inclusions over time would be very useful to make more accurate predictions. However, the difficulty of assessing glass panes over several years, distinguishing NiS inclusions from other possible causes of breakage and the reduced interest in the industry since this issue was solved with the HST make it difficult to obtain more data of this type.

Some studies have attempted to define statistical models to predict this type of failure based on the inclusion size distribution, location distribution and material properties (Bonati, Pisano & Royer Carfagni, 2019), but according to their authors, their inputs still need calibration to provide accurate results.

Although we may not be able to find much more accurate models in the near future, this probabilistic equivalence should be sufficient to defend the safety of post-consumer glass, which is usually produced decades ago.

6

Experimental measurements

6.1. Tests protocols

6.1.1. Sample size

Theoretical sample size

The sample size can be theoretically defined based on a given confidence interval (standard of 95% usually chosen), population proportion (0.50 for continuous variables) and margin of error.

The margin of error can be defined to be consistent with the precision of the measuring devices. According to the reliability study of Traceit® in Annex B, the lowest margin of error could be taken from the standard deviation between two measurements (14µm) of the largest flaw (147µm), leading to a margin of 11.8% to reach.

The sample size for an unlimited population is calculated based on the following formula:

$$n = \frac{z^2 \times \hat{p}(1-\hat{p})}{\epsilon^2} = 48.59 \tag{6.1}$$

where
n is the sample size for an unlimited population
$z = 1.645$ is the z-score for a 95% confidence interval on one side (90% if both sides are considered)
$\hat{p} = 0.50$ is the population proportion
$\epsilon = 11.8$% is the margin of error estimated for the Traceit® device

For a limited population, which is made of 2464 panels to potentially reuse, the formula is:

$$n' = \frac{n}{1 + \frac{z^2 \times \hat{p}(1-\hat{p})}{\epsilon^2 \times N}} = 47.65 \tag{6.2}$$

where
n is the sample size for an unlimited population
n' is the sample size for a limited population
$z = 1.645$ is the z score for a 95% confidence interval on one side (90% if both sides are considered)
$\hat{p} = 0.50$ is the population proportion
$\epsilon = 11.8$% is the margin of error estimated for the SCALP-05 device
$N = 2464$ is the population size (number of glass panes to reuse)

According to this formula, at least 48 measurements are needed to have a confidence level of 95% that the real value is within $\pm$11.8% of the measured value on one side, assuming a normal distribution.

It should be noted that this margin of error does not necessarily has to correspond to the device precision level. This margin is still conservative. If a larger margin such as 20% had been chosen, Equation (6.1) and Equation (6.2) would result in only 17 samples. In contrast, reducing this margin to 5% for example could drastically increase the sample size to 244 samples, which becomes more time-consuming. Ultimately, the margin of error depends on the trade-off between the maximum measurement precision and the minimum sample size desired for the study.

Practical sample size

The practical sample size should be greater or equal to the theoretical sample size. However, it must take into account the available samples and practical measurement constraints on-site.

The case study building has 18 floors with the panels to be potentially reused. These floors are all almost identical and are divided into 3 parts called wings. These parts can have different tenants. As the glass panes are on the inner side of the façade, the sampling should be representative of the variety of tenants (different wings) and situations within these wings (different rooms, close to a partition wall, close to a door, etc.).

As the building is still occupied during the thesis, the access is limited to 7 unoccupied wings. These wings contain a total of about 330 glass panes distributed in very diverse configurations. They are therefore considered to provide a sufficiently large and varied sample to be representative of the whole building.

The selected glass samples are evenly distributed along the available wings. This distribution is also shifted between the different wings and floors in order to include more diverse samples. However, as some of the glass panes were difficult to open during the first site visit, this sampling has to be somewhat flexible. Whenever a glass pane is too difficult to open safely without equipment, or is inaccessible for some reason, a neighbouring pane could be selected instead.

The number of samples is chosen to be a multiple of 7, which is the number wings available. In total 70 different glass panes (2.8% of the total) are sampled for this estimation of the pre-stress and weathering levels.

From this practical number of samples, the Equation (6.1) and Equation (6.2) can be reversed to find the associated margin of error $\epsilon = 9.7\%$.

6.1.2. Pre-stress measurement protocol

Measurement protocol with SCALP-05

Firstly, the following verification tests are carried out:

- Local measurements: 5x9 points following a grid on the inner side of 7 panels
- Precision measurements: 1 point measured 10 times on 7 panels to verify the precision of SCALP-05 in ‘normal’ mode
- Sides measurements: 5x2 points on 7 panels to verify the pre-stress difference between both sides
- Isotropy measurements: 5 points on 7 panels measured at 0° (vertical) and 90° (horizontal) to verify the pre-stress isotropy

The measurement locations for the precision, sides and isotropy tests are taken from the grid of the local measurement, at the center and the four corners.

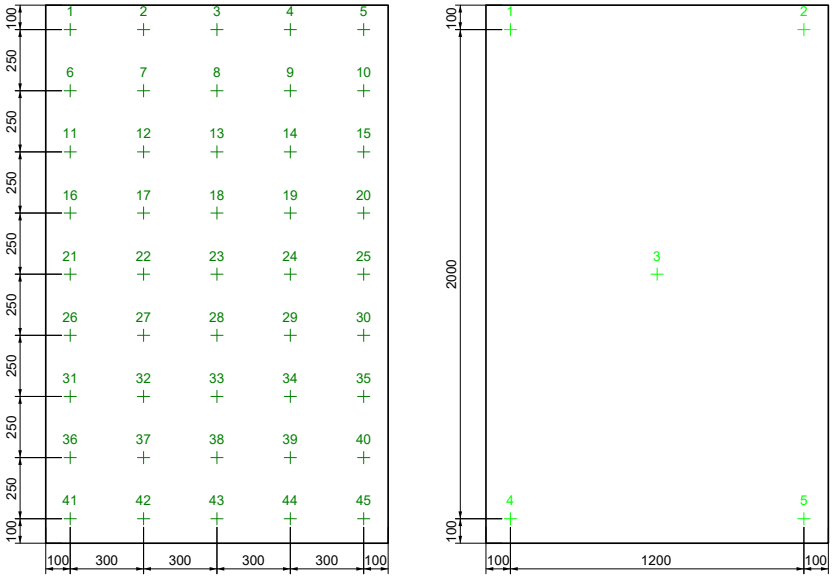

Figure 6.1: Measurement locations for the verification tests

Then, these results are quickly analysed to define the measurement locations for the global measurements, aiming at measuring a maximum number of panes with a minimal number of relevant points.

The measurement locations are be marked using a pre-perforated tracing paper for greater efficiency. A cross mark is traced 2cm below the measurement location. The SCALP-05 device is then simply placed above this mark.

The glass pane is covered on both sides with a black cloth, allowing the measurement with SCALP-05 would to be done almost in darkness. The suction cup is placed below or above the measurement location. A drop of mineral oil is put on the window of the SCALP-05, aiming at the point where the laser goes through it. The device is then positioned on the suction cup support, against the glass pane. Once in place, it is moved a few millimetres vertically and horizontally to spread the mineral oil over the contact surface.

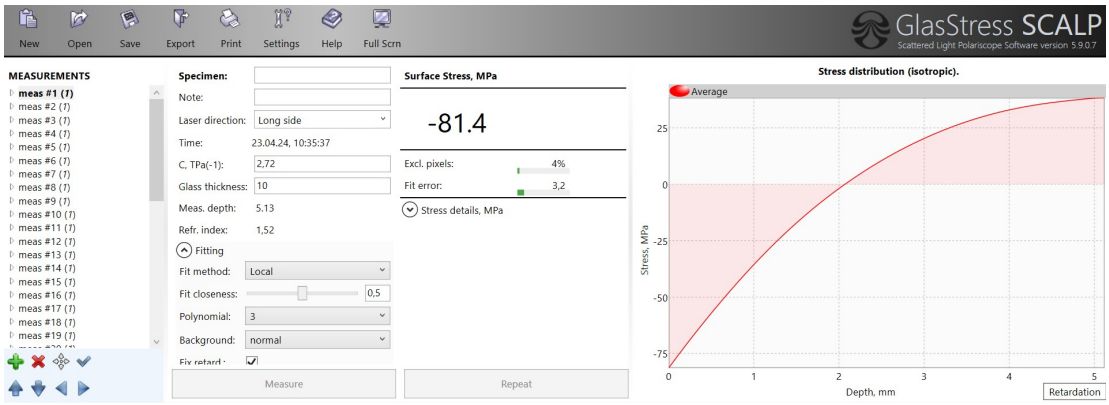

Figure 6.2: Example of a pre-stress measurement using the SCALP-05 software tool

Validity criteria

The measurement will only be considered valid if the following conditions are fulfilled:

- The live camera view should show a nearly dark background.
- The stress profile has a global shape consistent with what is expected for a thermally toughened glass, with compression on $20 \pm 5\%$ of the outer thickness of the section, and tension inside. The maximal tension value should reach approximately half of the maximal compression value. These criteria are not strict, but only there to quickly exclude unrealistic stress profiles.
- The excluded pixels rate should be smaller than 20%.
- The fit error RMS score should be smaller than 10.

After the measurement, the equipment is removed and the glass pane is cleaned. This protocol should be applied as carefully and consistently on the different measurements to improve the quality of the results. Particular attention should be paid to the lighting conditions. No direct light should reach the SCALP-05 window, and ambient light passing through the glass pane or from the sides should be limited. When measuring tinted glass and/or in a relatively dark environment (very cloudy day or at night for example), the black screen could even be removed. However, the results should be treated even more carefully to ensure that they are not altered by any external light source.

6.1.3. Weathering measurement protocol

Initial approaches

Initially, two approaches were considered for evaluating the maximum flaw depth per panel given a defined probability:

- **Systematic approach:** systematic measurements following a grid. These locations can be considered to provide samples with low flaw depths. The greyscale pictures from Traceit® are analyzed to estimate the flaw depths distributions. From this data, a Pareto distribution is fitted to estimate the largest flaw per panel.
- **Localised approach:** use of the global measurement, corresponding to the largest flaw found on each panel after careful visual inspection. Although it is not realistic to find the largest, critical flaw each time, it can provide a reasonable idea of their statistical distribution.

Both approaches have their advantages and drawbacks. The localised approach appears to be more relevant, but relies on the ability to find reasonably good defects. The systematic approach relies on a Pareto distribution, which has not been shown to be very accurate for aged glass, but could provide complementary results.

However, after a first trial session with Traceit® , it became clear that the systematic approach was not possible given the precision of the device. This is not worrying as the localised approach seems much more relevant in the case of aged glass.

Multi-scale observation approach

A multi-scale approach is defined to estimate the largest flaws on each glass pane:

- **Pane overview:** the glass pane is observed globally at a distance of approximately 1.5 metres in conditions approximating to diffuse daylight and open blinds. If some flaws or more damaged areas are already noticeable, the observer can directly focus on these flaws or restricted areas. Otherwise, it moves on to the next stage for the whole pane.
- **Close observation:** the glass is examined at a distance of about 30 centimetres, from left to right following 'strips' of approximately 30 centimetres high from bottom to top. The largest visible flaw on the first 'strip' is marked. Then, only flaws looking larger than the previous one(s) are marked. Finally, only the largest flaw is selected. If the largest flaw is a spot flaw, the largest linear flaw is also selected.

- **Depth measurement:** the largest flaw depth is measured with Traceit®. A lign is drawn in the software to show the height profile, and can be moved several times if necessary. The lowest point should be as low as possible in the height map. The highest point should be to the 'normal' height of the pane surface. This should be the highest point measured, excluding any errors or residue (e.g. remaining glue).

(a) (b) (c)

Figure 6.3: (a) Pane overview, (b) close observation, (c) depth measurement with Traceit®

It was found that the flaws were easier to detect in a diffuse daylight condition with the blinds open. The observer first attempted to inspect glass panes with a dark cloth behind them. Although this provides a homogeneous background, the flaws were not easier to find and required the use of a light with different viewing angles. It turned out that it was not so much a homogeneous dark background that made it easier to find flaws, but the reflections of the flaws when viewed from different angles. Therefore, the glass panes are observed in a diffuse daylight condition with the blinds open, and the process of close observation going from left to right increases the occurrence of flaw reflections to the observer's eyes. This process is also more efficient as it does not require any specific installation.

Measurement protocol with Traceit®

The following measurements are carried out:

- Precision measurements: 1 point measured 5 times at 0° (vertical) and 5 times at 90° (horizontal) on 3 panels to verify the precision of Traceit®.
- Global measurements: at least 1 point on 70 panels.

The Traceit® device provides a 'visual impression' of the 5 $\times$5mm examined area, and the associated height map. The measurements are relatively simple to carry out and take only a few seconds. However, the result quality (especially for the height map) can be influenced by external parameters such as the background, lighting and in-plane device angle. These parameters were investigated on-site:

- **Background:** it was initially assumed that a homogeneous background would help, done with a grey textureless PVC sheet placed behind the measurement location. However, it turned out that the height map quality was usually much better without any background, in a 'natural light' condition.
- **Light:** in order to have good quality measurements, this natural light condition should provide a relatively diffuse daylight an any direct sunlight should be avoided.
- **Angle:** since the three lights of the device are at 120° from each other, an in-plane rotation of the device of e.g. 90° can change the lighting and reflections of the flaw. This changes the visual impression and can improve the quality of the height map.

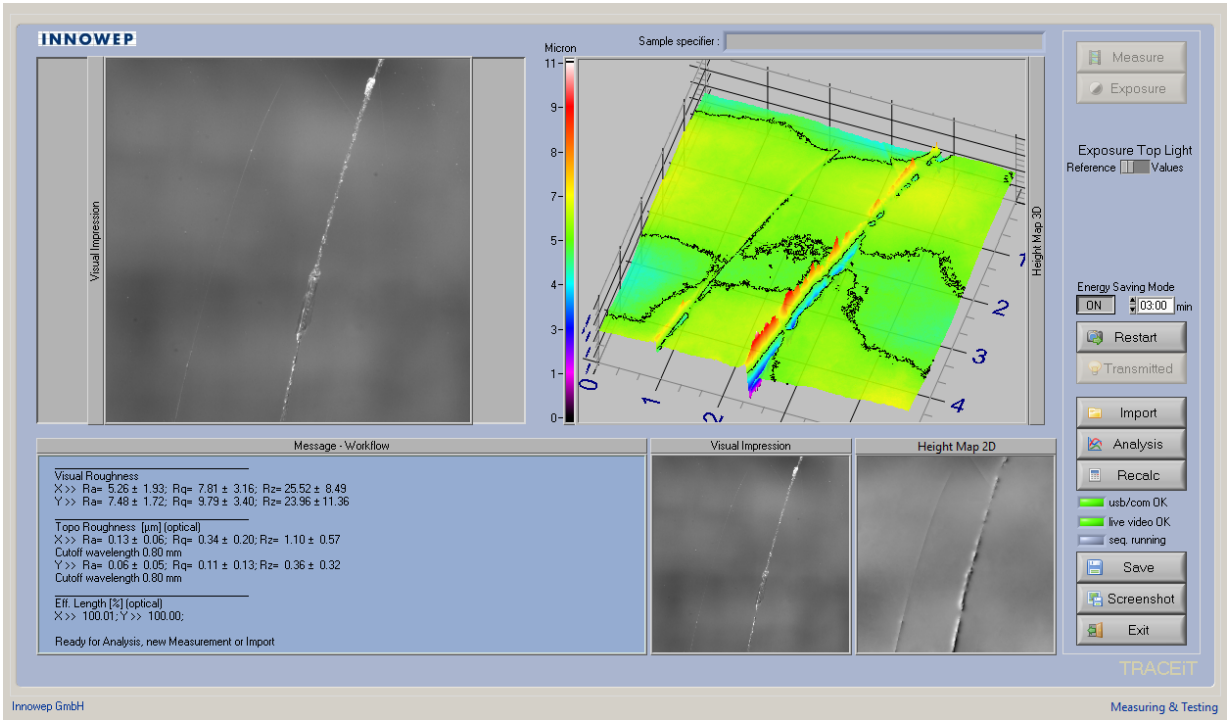

Figure 6.4: Example of a measurement overview with visual impression and height map using Traceit® software tool

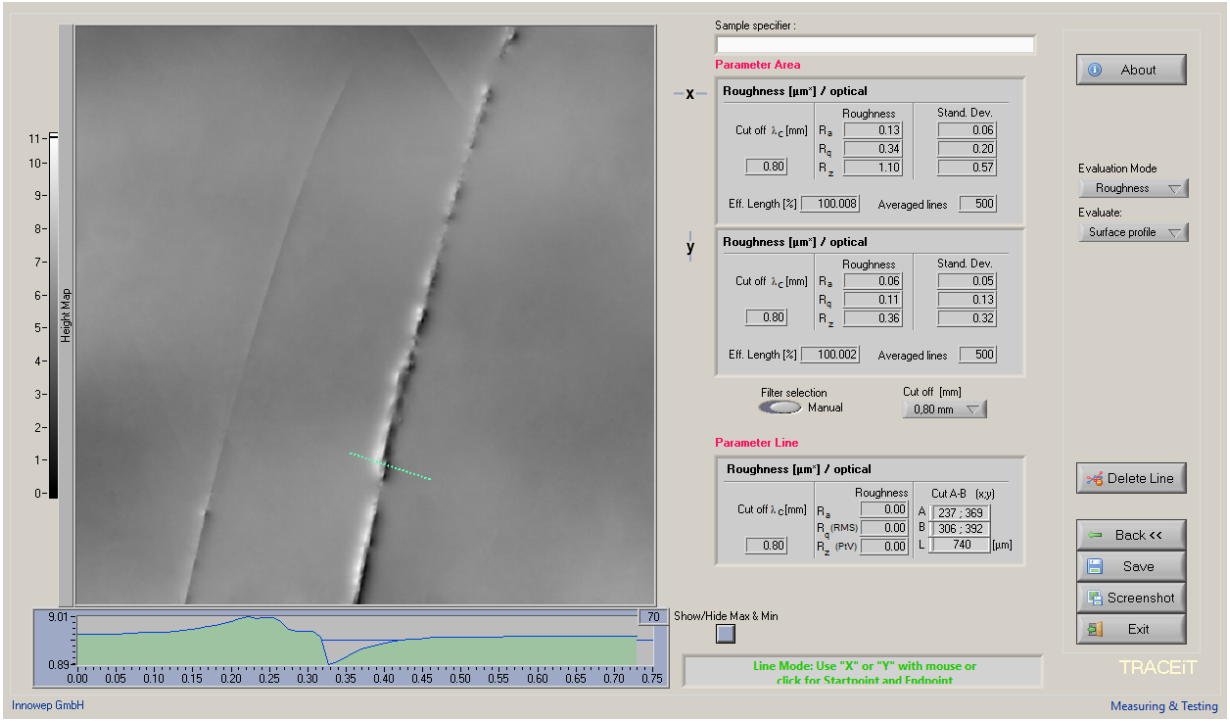

Figure 6.5: Example of height map with roughness values and choice of line to measure the flaw depth on the Traceit® software tool

After ensuring that the flaw location is in conditions approximating to diffuse daylight with the blinds open, the flaw is measured with Traceit® at least twice with an in-plane rotation of 90°. The flaw depth is measured by drawing a line on the height map in the associated software. The height profile along the line is displayed, with the highest and lowest values. The highest value should be the height of the glass surface without any flaw, as close as possible to the examined flaw. The lowest value should be the darkest visible point in the observation area.

Validity criteria

The measurement will only be considered valid if the following conditions are fulfilled:

- The visual impression and height map give consistent results, the same flaw is recognisable.
- The measurement location is of good enough quality to see and measure the flaw depth. Some noise and background colour variations can appear on the height map. These alterations are tolerated as long as the measurement location is preserved.
- The measured flaw depth should be within a realistic range from 4µm to 1000µm, and consistent with the flaw appearance to the naked eye. After a few measurement, the observer can have a notion of this flaw depth. Flaws with a depth smaller than 10µm are usually barely visible at a distance of 30 centimetres, while flaws with a depth of more than 40µm are usually visible even at a distance of 1.5 meters.
- The two measurements of the same flaw taken with a 90° rotation should show consistent flaw depths along the selected line with a difference of less than approximately 30µm for flaws smaller than 100µm, or 30% for flaws greater than 100µm. Noise and background colour variations may occur and differ between both height maps, as long as the measurement location is preserved. Otherwise, more measurements should be carried out until having at least two consistent results.

The flaw depth measurement obviously has a higher level of uncertainty, especially as it has to be done in a limited amount of time on site. The results should be analysed and interpreted even more carefully than those from SCALP-05. However, it has already been shown to provide sufficiently accurate information on the flaw depth to estimate the remaining strength of the glass. Moreover, the approach of this study is not so much to find the exact remaining strength rather than proving it is above a certain threshold.

6.2. Tests results

6.2.1. Pre-stress measurements

The local measurements confirmed a relatively homogeneous pre-stress level across the glass pane surface. Interestingly, some glass panes showed a slight gradient from about 80 MPa to 90 MPa along the long side. This could be explained by a vertical tempering process used at that time, as described in Chapter 2. These variations are not observed on all the seven measured panes. These variations should be treated with caution, since many of them are still within the SCALP-05's uncertainty level of $\pm$5 MPa in 'normal' mode. However, the observed gradient looks like a global trend and varies above this uncertainty level. The pre-stress measurements are detailed in Annex C.

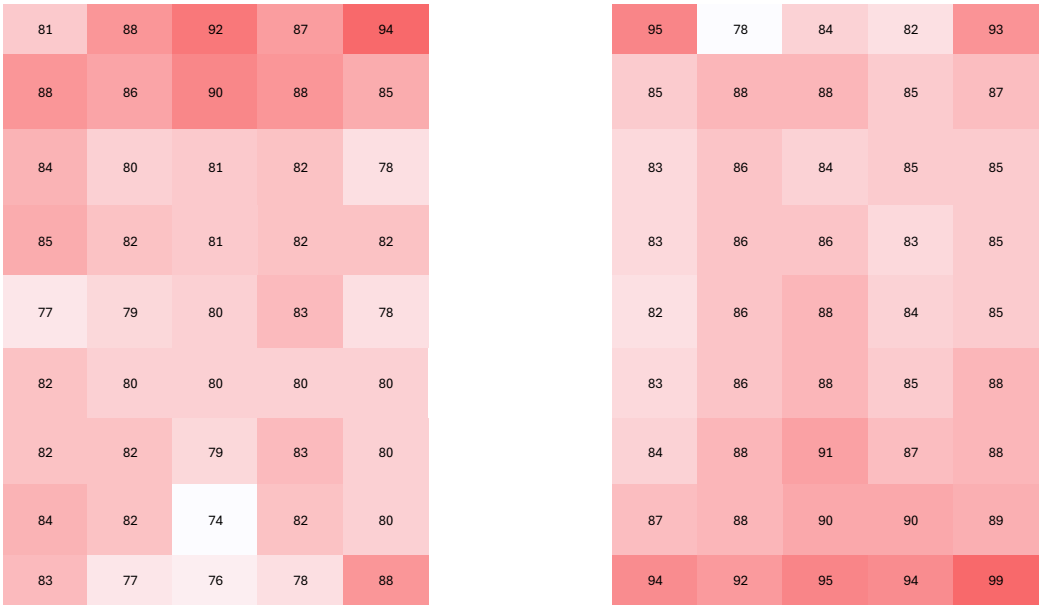

Figure 6.6: Examples of local measurements on glass panes with a slight tempering gradient, rounded to 1 MPa

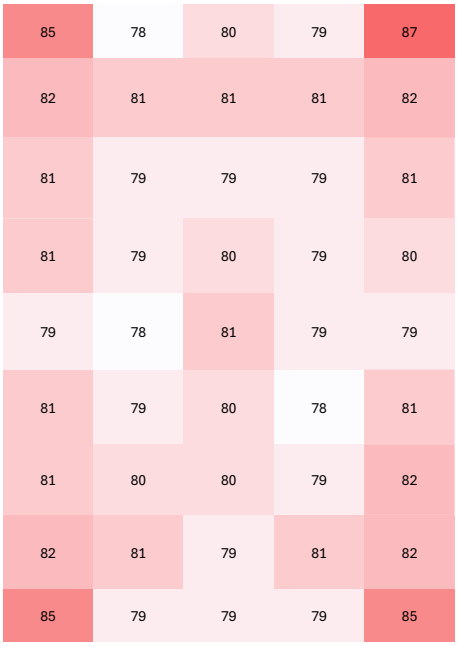

Figure 6.7: Average of the local measurements from the 7 glass panes, rounded to 1 MPa

Figure 6.7 shows the averaged local measurements. The pre-stress level is relatively homogeneous across the glass pane surface at about 80 MPa, with an increase in the corners going up to about 90 MPa.

The local measurement are made systematically following a grid, as described in Chapter 7. Since most of the variations are still within the device's uncertainty, they must be interpreted with caution.

The 2 face measurements verify the equality of the pre-stress level between the two surfaces of the glass pane. With the exception of one difference measurement (-13.23 MPa), the validity of which is doubtful, all the results confirm the equality between the two faces, with differences within the device's uncertainty.

The isotropy measurements verify the equality of the pre-stress level between vertical (0°) and horizontal (90°) directions. Most of the values are within the device's uncertainty, indicating little or no anisotropic stress. As expected, the central point shows particularly close values while the corners can show slight differences.

From these results, the global measurements are taken with only five points on all the other glass panes, as shown in Figure 6.8.

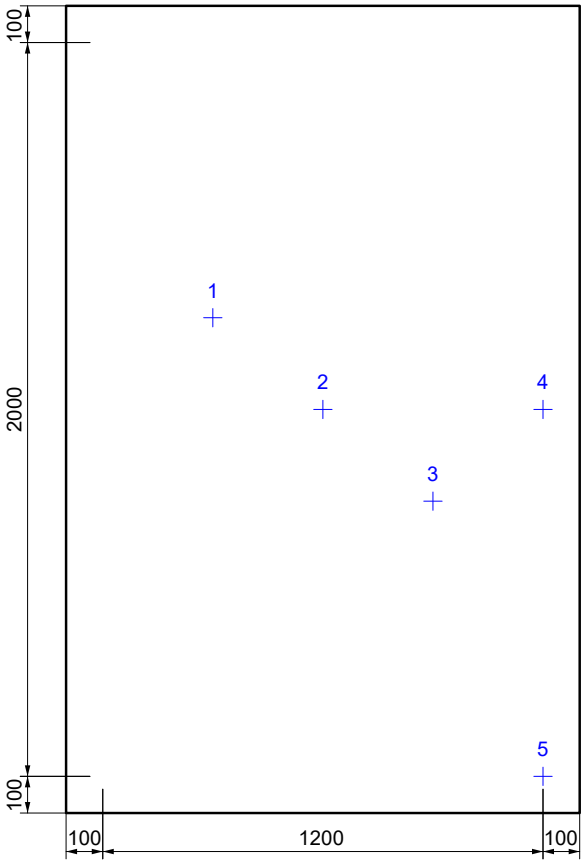

Global measurements: 5 points

Figure 6.8: Measurement locations for the global tests

Points 1 to 4 from the global measurements show consistent variations with those from the local measurements, as detailed in Annex C. Since the pre-stress variations between the average of these points is below the SCALP-05 uncertainty level and the glass pane has the highest stress at its centre under uniform loads, the central point could define the pre-stress level of each pane.

Only point 5 shows higher values of about 5.5 MPa most of the time. The consistency of this difference and the fact that it is slightly higher than the SCALP-05 uncertainty level indicates a tendency for the corners to have a slightly higher level of pre-stress. This can be explained by a faster cooling of the corners at the end of the tempering process, due to their position close to two boundaries. This phenomenon, although interesting to observe, is on the conservative side and does not significantly affect the overall strength of the pane.

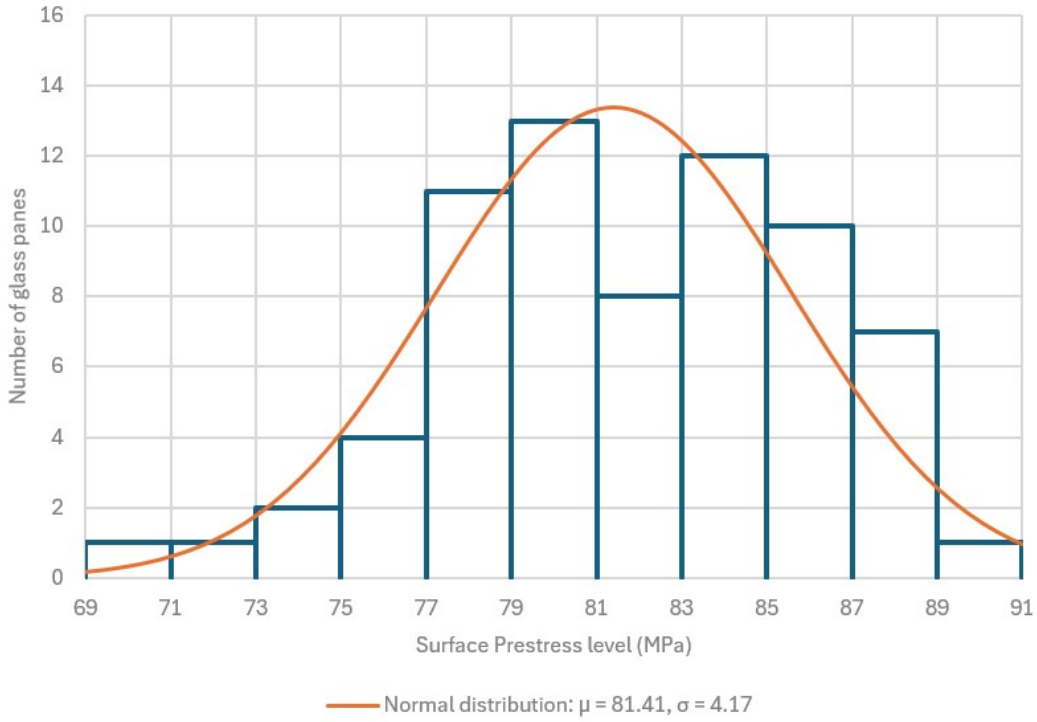

Figure 6.9: Histogram of the surface pre-stress level on the 70 measured glass panes, with a fitted normal distribution

The statistical distribution of the measured surface pre-stress level at the central point is presented in Figure 6.9, with a range from 69 MPa to 91 MPa.

The average of 81.41 MPa is relatively low for fully toughened glass, and its standard deviation is consistent with other datasets grouped by Haldimann in Figure 6.10:

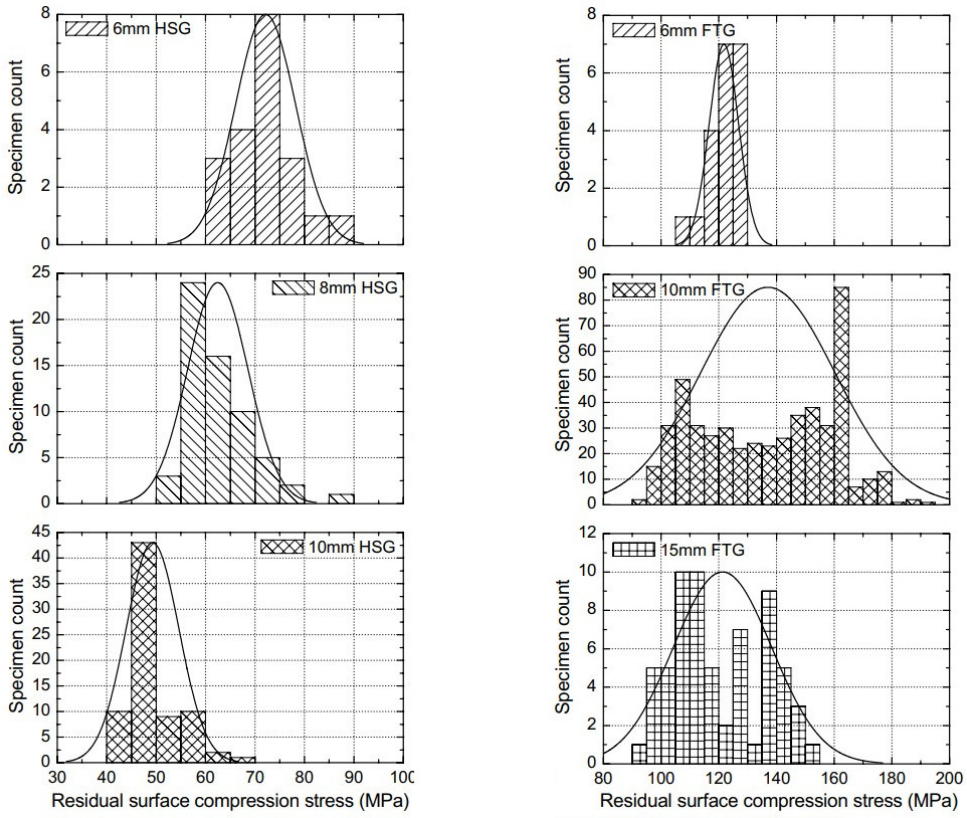

Figure 6.10: Residual stress data for comparison (Haldimann, 2008)

This dataset can also be compared to measured experimental failure strength and surface pre-stress levels done by Bos (2009) from his tests with a speed of 1mm/min, as shown in Table 6.1:

Table 6.1: Reliability study results for 10 measurements on 3 samples

Glass type	Average failure stress (MPa)	Average surface pre-stress (MPa)
Annealed (tested by Freek Bos)	64.5	(0)
Heat-strengthened (tested by Freek Bos)	132.5	44.2
Fully toughened (tested by Freek Bos)	230.6	103.2
SECURIT from Saint-Gobain (tested on-site)	210	81.4

The average failure stress for the SECURIT glass is taken from the Saint-Gobain brochure from that time (Saint-Gobain, 1970). Assuming this average failure strength is correct and the measured surface pre-stress stayed constant, the surface would be of similar quality (similar largest flaw depth) than the other tested samples. It may even be of better quality if the size effect is taken into account. The comparison between strengths is not investigated further here. The results are consistent between the different samples tested, and suggest that the SECURIT glass panes are of similar quality, but lower pre-stress level than these other tempered glass samples.

The average surface pre-stress level is 82.10 MPa for the ’Pont à Mousson’ stamped panes, and 80.97 MPa for the ’Securit’ stamped panes. The difference being way below the SCALP-05 precision level, both categories can be considered equivalent.

6.2.2. Weathering measurements

Minimum flaw depth

The minimum flaw depth can be estimated from two approaches: calculations based on the initial performance of the glass and the visibility threshold.

Firstly, very small flaw depths could lead to an even faster increase of the estimated glass strength (as shown in Figure 2.15), which could easily be overestimated. Based the average failure strength for this type of SECURIT glass of 210 MPa according to Saint-Gobain and the average surface pre-stress of 81.41 MPa measured on-site, Equation (7.3) can be reversed to find flaw depths of 9 µm for linear flaws and 20 µm for spot flaws. This would mean that based on these previous assumptions, this type of glass panes had scratches smaller than 9 µm and digs smaller than 20 µm on average when it was tested immediately after production. These values are of course only estimates based on several assumptions, but they give an idea of what the initial surface quality of the glass might have been. The largest flaw depths per pane should not be below this threshold as they probably never were, and smaller values would lead to an overestimation of the strength of the glass.

Secondly, a visibility threshold must be considered. The glass panes were generally in good condition. Some of them were in such a good condition that the observer could not spot any flaw to the naked eye. Although the observer could find flaws as small as 4 µm, these were barely visible and it would not be a safe assumption to ensure that a pane did not have any flaw of this size. Therefore, the observer considered a minimum thresholds of 10 µm for linear flaws and 30 µm for spot flaws at a 30 cm distance. This corresponds to the minimum flaw depth that the observer could see with a confidence level above 95%. Any value below this threshold is replaced in the adjusted depth list.

Flaw depths distribution

The flaw depth measurements are detailed in Annex D. These measurements were carried out on the same sample of 70 glass panes, with the results synthesized in Table 6.2:

Table 6.2: Statistics on the flaw depth measurements

Type	Value
Minimum measured depth	4 µm
Maximum measured depth	147 µm
Average measured depth	36 µm
Average adjusted depth	39 µm
5% largest adjusted depth	124 µm
Spot flaws	17%
Linear flaws	83%
Outer side (cavity)	13%
Inner side	87%
”Pont à Mousson” stamp	39%
”Securit” stamp	61%

The size and variation of the flaw depths are consistent with values from other experiments. Although 83% of the largest flaws measured were scratches, this does not mean smaller flaws followed the same ratio. Most of the flaws were observed on the inner side of the panes, directly exposed to the occupants. This was expected, but there were still 13% of the largest flaws measured on the outer side of the panes (in the cavity).

The average flaw depth is 42.9 µm for the ’Pont à Mousson’ stamped panes, and 43.9 µm for the ’Securit’

stamped panes. As the difference is well below the level of precision of Traceit®, both categories can be considered equivalent.

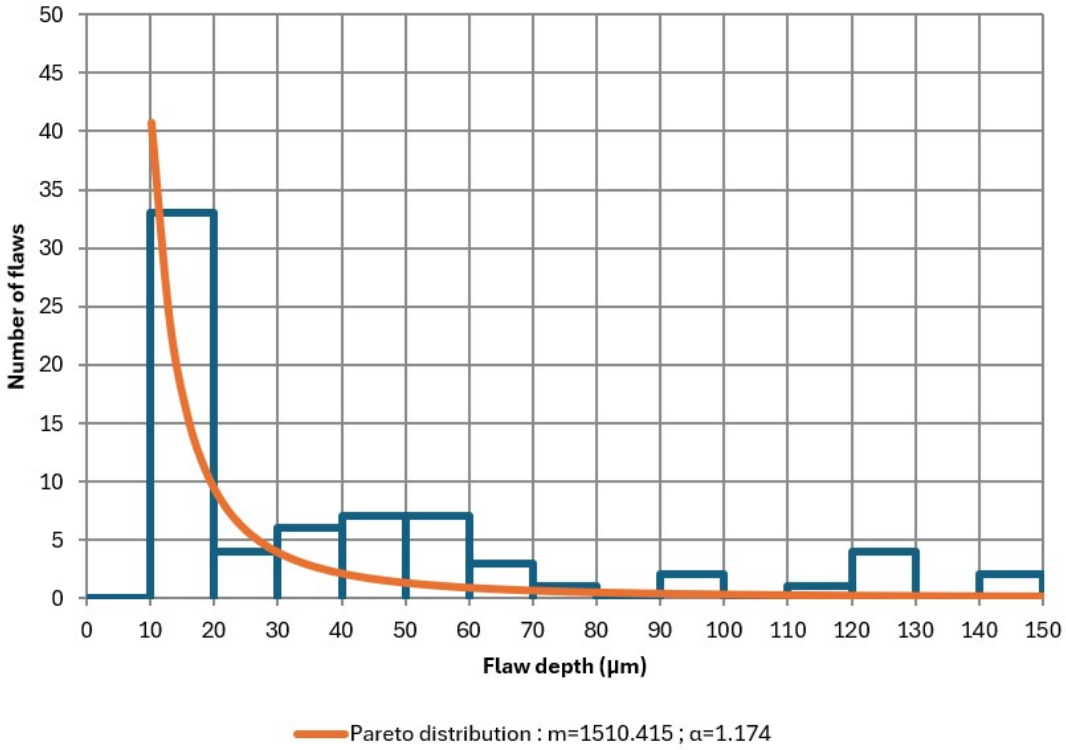

Figure 6.11: Flaw depths distribution with a fitted Pareto distribution (after minimum depth adjustment)

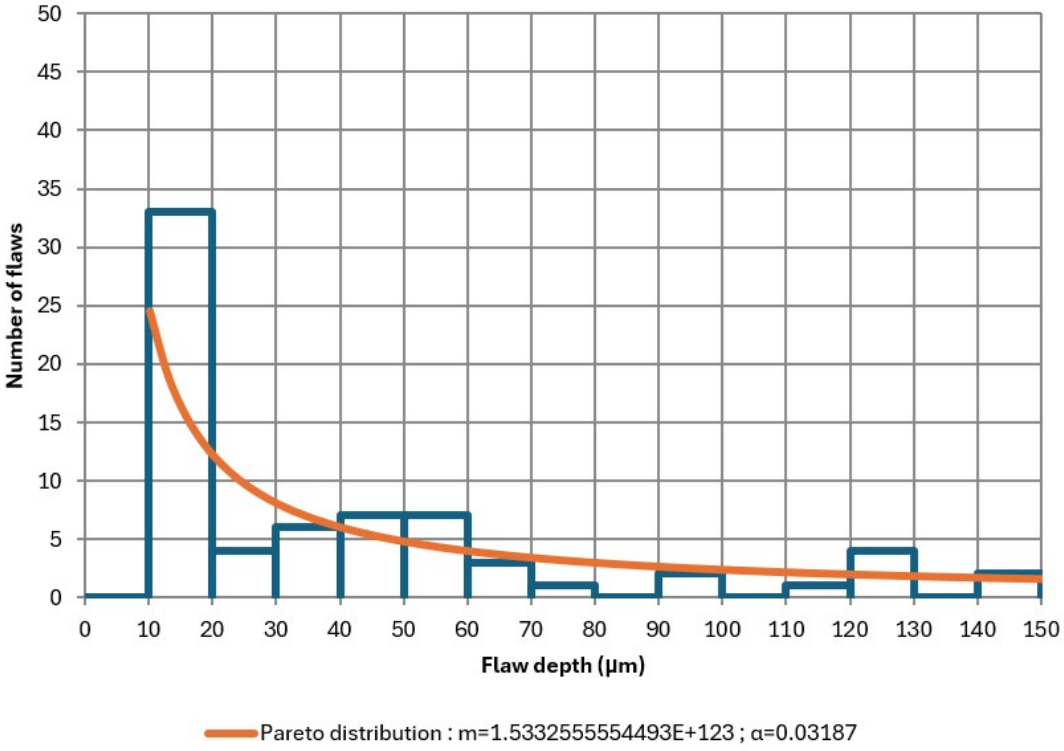

Figure 6.12: Flaw depths distribution with a fitted Pareto distribution excluding 20µm points (after minimum depth adjustment)

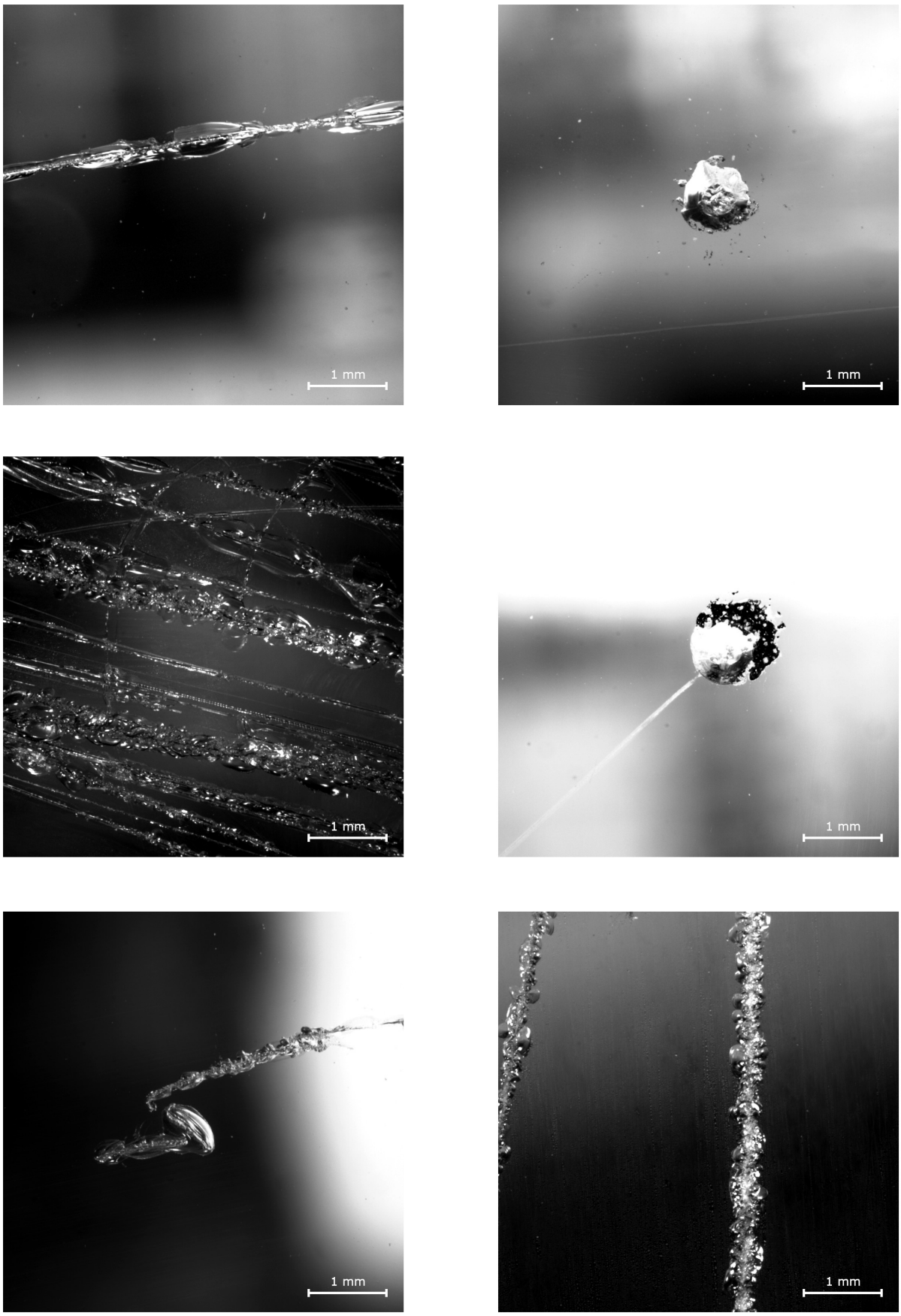

Figure 6.13: Examples of measured flaws

6.3. Discussion

The pre-stress measurements are consistent with results from other publications, although the pre-stress level appears to be slightly below average for FT glass. Many of the variations observed in the local, isotropy and side measurements are small and must be interpreted with caution. The global pre-stress level can vary significantly between different panes, but these variations are also consistent with previous research.

The weathering measurements show consistent values when compared with other research. The glass panes condition was generally relatively good, with most of the times only a few noticeable flaws per panes, with a depth often below 100 µm. The range [4 µm ; 147 µm] of largest flaw depth is very similar to the one from Sofokleous (2022) of [19 µm ; 161 µm] measured on annealed glass samples exposed to outdoor weathering for 50 years. It is also similar to the depths of 'edge machining flaws' measured experimentally by Lindqvist (2013) in the range [43 µm ; 170 µm]. For approximately the same exposure time, both samples seem to have similar ranges, although they were exposed to different phenomena (indoor vs outdoor 'weathering'). Compared to the measurements from Sofokleous, there appears to be a higher proportion of linear flaws and a smaller density of flaws in general. Exposure from the inside of the building may cause some noticeable damage less often than outside (lower density of flaws), but these events could cause more damage (impact from the tenants causing larger flaws than impacts from particles outside for example). These assumptions should still be investigated further.

However, the Traceit® device used on site involved more safety margins for the different reasons explained above.

It became even clearer during the on-site measurements that the challenge of reusing glass was sometimes not so much the strength of glass itself rather than our ability to prove it. The quality and precision of the measurements can be critical in ensuring a certain strength level. On the other side, a qualification protocol with relatively low strength requirements can allow an even faster and simpler measurement process.

7

Technical reuse potential assessment

7.1. Design requirements

The estimated characteristic strength will be compared with the characteristic strength of fully toughened, heat-strengthened and annealed glass from the Eurocodes.

If the characteristic value (5%-fractile of the normal distribution) of σ_s is greater than the Eurocode requirement of 120 MPa, 70 MPa or 45 MPa, the set of glass panes should be suitable for reuse as fully toughened, heat-strengthened or annealed glass respectively.

7.2. Pre-stress assessment

7.2.1. Pre-stress measurement location

The averaged local measurements showed relatively homogeneous results except in the four corners, as explained in Subsection 6.2.1. Most of the variations were still within the SCALP-05 uncertainty, and larger variations such as the observed vertical gradient led to higher values which are on the conservative side. This resulted in the 5 points defined for the global measurements from Figure 6.8.

Points 1 to 4 from the global measurements show very similar average and standard deviations. As their differences are very small and below the SCALP-05 uncertainty level, they can be considered equal. Point 5 tends to have slightly higher values, but is on the conservative side.

Based on these observations and given that the glass pane has the highest stress at its centre under uniform loading, the central point is chosen to represent the pre-stress level of the glass pane.

7.2.2. Pre-stress value

The characteristic value (5%-fractile) of the central point is taken as the general pre-stress level to comply with the Eurocodes.

This value can be taken from the fitted normal distribution, or the measured distribution. Based on the fitted normal distribution with $\mu_g = 81.41MPa$ and $\sigma_g = 4.17MPa$, the corresponding characteristic value is $\sigma_{char,function} = 74.55MPa$. In comparison, the characteristic value of the measured distribution is $\sigma_{char} = 74.46MPa$.

Although the fitted normal distribution can help generalise the histogram, it has been shown for these and other samples (Haldimann, 2008) that it is not a very good fit. As the characteristic value of the measured distribution is also slightly more conservative, it was chosen for this study.

7.3. Strength prediction based on LEFM

7.3.1. Predicted strength

The predicted glass strength is based on two parts. The first part is based on LEFM and mostly depends on the maximum flaw depth c_{max}. It is defined as follows:

$$\sigma_a(c_{max}) = \frac{K_{IC}}{Y\sqrt{\pi c_{max}}} \tag{7.1}$$

with
$K_{IC} = 0.75$ is the material 'constant' value established in other research (Haldimann, 2008 ; Sofokleous, 2022)
$Y = 0.713$ or 1.12 is the shape coefficient respectively for digs (spot flaws) or scratches (linear flaws)
c_{max} is the maximum flaw depth

The second part corresponds to the pre-stress contribution, with a pre-stress profile following a parabolic equation. This part depends mainly on the surface pre-stress level, but also on the flaw depth, which reduces this pre-stress at the flaw tip:

$$\sigma_r(\sigma_{r,srf}, c_{max}) = \sigma_{r,srf} \times (1 - 3 \times \frac{c_{max}}{d} + \frac{3}{2} \times (\frac{c_{max}}{d})^2) \tag{7.2}$$

with
σ_r is the surface pre-stress level
c_{max} is the maximum flaw depth
$d = 5mm$ is the half of the pane thickness

The final strength is defined as the sum of both parts:

$$\begin{aligned} \sigma_f(\sigma_{r,srf}, c_{max}) &= \sigma_a(c_{max}) + \sigma_r(\sigma_{r,srf}, c_{max}) \\ \sigma_f(\sigma_{r,srf}, c_{max}) &= \frac{K_{IC}}{Y\sqrt{\pi c_{max}}} + \sigma_{r,srf} \times (1 - 3 \times \frac{c_{max}}{d} + \frac{3}{2} \times (\frac{c_{max}}{d})^2) \end{aligned} \tag{7.3}$$

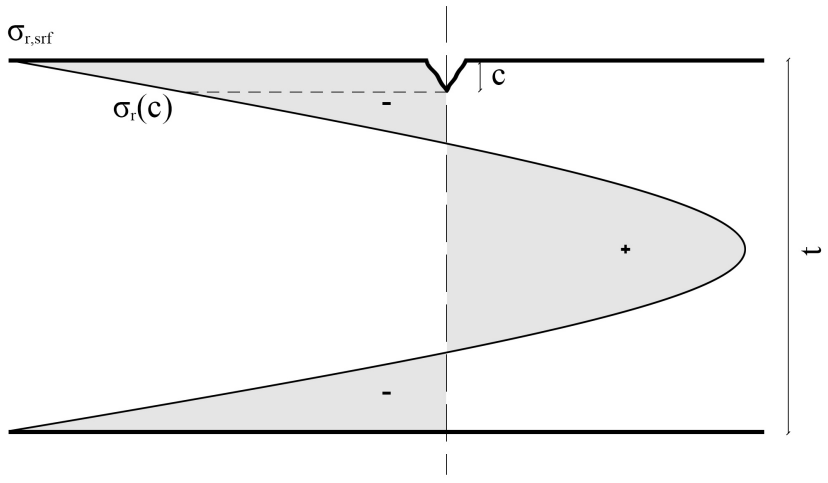

Figure 7.1: Pre-stress reduction at the flaw tip in thermally tempered glass

Since all of the 70 panes had their surface pre-stress and largest flaw depth measured, their strength could be estimated, and their distribution shown in Figure 7.2. These results must be interpreted with caution for two main reasons. Firstly, they are quite sensitive to a number of parameters such as the surface pre-stress level, the shape coefficient and the flaw depth. Other research has already shown that

it is difficult to predict the strength of each pane individually in a very accurate way, but that the global distribution of a sample may be more reliable. Secondly, this figure shows the results without any safety margins. It gives an idea of what could be the global distribution of glass strength if they were tested destructively, but it does not safely ensure a design strength.

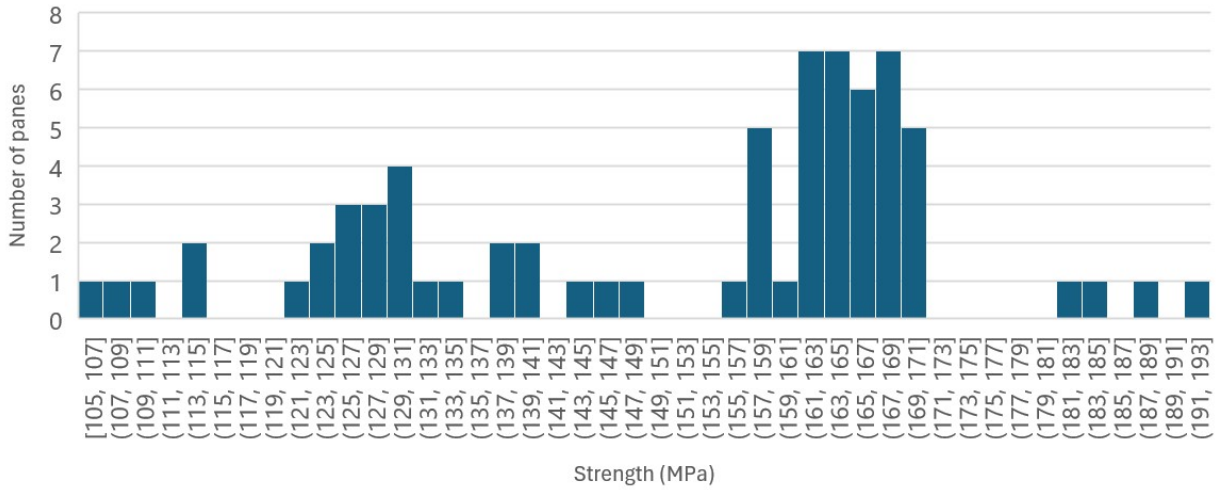

Figure 7.2: Estimated strength distribution without margin

7.3.2. Approach 1: lower bound safety margins

This first approach consists in defining the lower bound strength from the different parameters separately. Each parameter is either reduced (pre-stress level precision from SCALP-05) or increased (flaw depth precision from Traceit®, visual inspection) to include the measurements with the largest differences from the reliability studies.

According to Annex A, the largest difference between two pre-stress measurements at the same location was 4.98 MPa (6% for an average level of 81 MPa). In parallel, the manufacturer indicates a precision of 5% for the SCALP-05. Therefore, the margin due to the precision of the SCALP-05 is taken as M_{SCALP} = 6% of the measured surface pre-stress level.

According to Annex B, the largest difference between two measurements of the same flaw was 41 µm. This difference also tends to increase with the flaw size. Therefore, the margin due to the precision of Traceit® is taken as the minimum between M_T = 20 µm and M_T = 40% of the flaw depth. This margin includes the precision of the device, the precision in the selection of the top and bottom points and the noise. It defines an affine function that is constant in the range [0;50µm] and then linearly increasing. This margin is in line with the Traceit® reliability study of this study, as well as with that of Sofokleous (2022). Indeed, the precision can be improved by making 2 measurements of the flaw at 0° and 90° and choosing the highest value of the 2 measurements.

The margin regarding the visual inspection precision M_V will be defined in a later section, depending on the precision of the visual inspection compared to Traceit® measurements.

The margins related to the flaw depth may seem quite large, but are necessary as this protocol has to be carried out on-site and in an efficient way. In addition, the glass strength is not affected to the same extent. The pre-stress related part $\sigma_r(c)$ is hardly affected, and the LEFM part σ_a is inversely proportional to the square root of the flaw depth. For example, at a pre-stress level of 80 MPa, if the flaw depth increases from 40µm to 56µm (+40% margin), the glass strength decreases from 138 MPa to 128 MPa (-7%).

7.3.3. Approach 2: combined safety margins

From one characteristic strength to two variables

Another approach consists in combining the different safety margins to obtain a characteristic value with a confidence level above 95%. The final uncertainty must be less than 5%, but this does not mean that each margin taken separately must have such a high confidence level. Indeed, it is very unlikely to have the largest SCALP-05 measurement deviation, the largest Traceit® measurement deviation and the largest sampling deviation at the same time.

The objective of defining a characteristic value $\sigma_{f,0.05}$ can be defined as:

$$P(\sigma_f \leq \sigma_{min}) \leq 5\% \tag{7.4}$$

This equation depends on the two variables c_{max} and σ_r, considered independent from each other. It is satisfied with different combinations:

- $c \leq c_{max}$ and $\sigma_r \geq \sigma_{r,min}$ always leading to $\sigma_f \geq \sigma_{min}$
- $c \leq c_{max}$ and $\sigma_r \leq \sigma_{r,min}$ only if the combination leads to $\sigma_f \geq \sigma_{min}$
- $c \geq c_{max}$ and $\sigma_r \geq \sigma_{r,min}$ only if the combination leads to $\sigma_f \geq \sigma_{min}$

If these two variables were in the same unit, linearly combined and following normal distributions, the accepted uncertainty for these two variables individually could be calculated to reach a final uncertainty level of 5%, which is to say the X value from Equation (7.5) could be calculated:

$$P(\sigma_f \leq \sigma_{min}) \leq 5\% = P(c \geq c_{max}) \leq X\% \cap P(\sigma_r \leq \sigma_{r,min}) \leq X\% \tag{7.5}$$

However, since these two parameters are non-linearly combined and in different units in Equation (7.3), this X value cannot be calculated easily. A conservative and simple assumption could be to consider that X = 5% for each of these variables, which is to say:

$$P(\sigma_f \leq \sigma_{min}) \leq 5\% \approx P(c \geq c_{max}) \leq 5\% \cap P(\sigma_r \leq \sigma_{r,min}) \leq 5\% \tag{7.6}$$

Another approach consists in evaluating X based on a Monte Carlo simulation. The statistical distributions of the pre-stress level and the flaw depth are defined from previous measurements, and 100 000 samples are generated according to these distributions, as shown in Figure 7.3 and Figure 7.4.

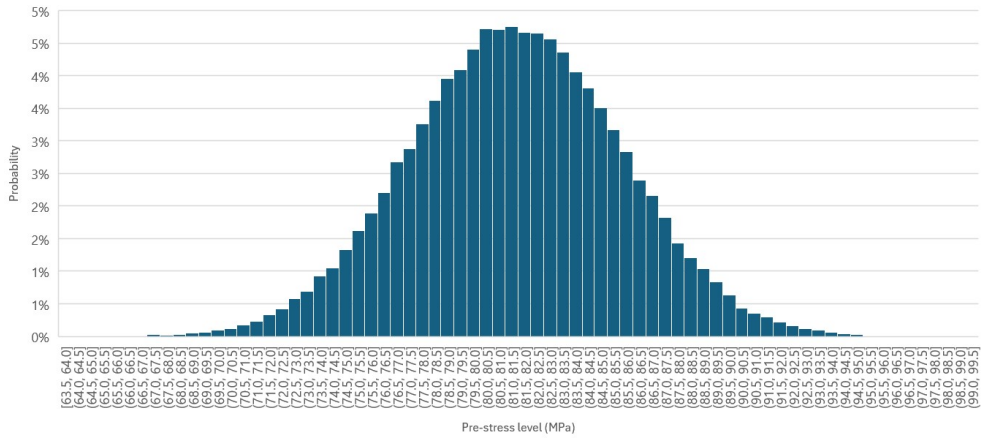

Figure 7.3: Monte Carlo simulation of the surface pre-stress level distribution. Average $\mu = 81.41MPa$ and $\sigma = 4.17MPa$.

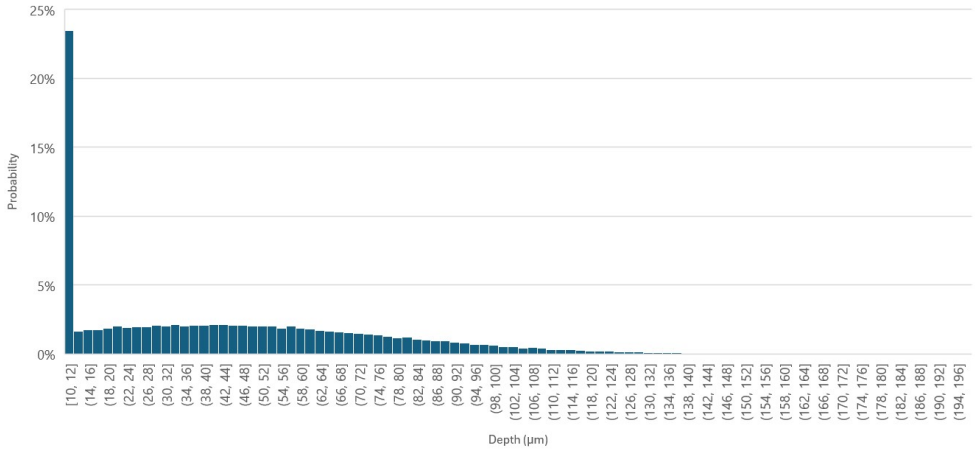

Figure 7.4: Monte Carlo simulation of the flaw depth distribution. Average $\mu = 39.27\mu m$ and $\sigma = 37.63\mu m$ with a minimum threshold of $10\mu m$.

These values are then combined according to Equation (7.3) to obtain 100 000 values for the glass strength. These values follow a more complex distribution which can be better understood with this Monte Carlo simulation, shown in Figure 7.5.

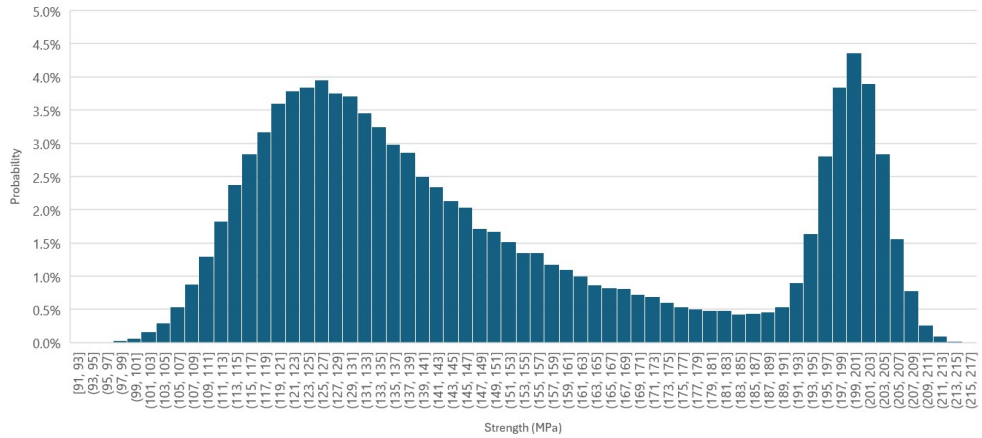

Figure 7.5: Monte Carlo simulation of the strength distribution. Based on c and σ_r from Figure 7.3 and Figure 7.4, with $Y = 1.12$ (more conservative), $K_{IC} = 0.75$ and a glass half-thickness $d = 5mm$.

The 5%-fractile of the pre-stress values σ_r and the 95%-fractile of the flaw depths c are taken from the empirical distributions. If these values are combined in Equation (7.3), a strength of 107.71 MPa is obtained, which corresponds approximately to the 1.5%-fractile of the strength distribution. This confirms that a risk level below 5% for both variables at the same time may be slightly too conservative.

This safety level is then gradually increased up to 10.5% for both variables, to arrive at a strength of 112.97 MPa based on these values. This strength is almost as high as the 5%-fractile of the strength distribution. In other words, based on this Monte Carlo simulation, the final strength can still have a risk level of less than 5% if the pre-stress and flaw depth values are combined with a risk level of 10.5% each. This value is rounded to 10% for safety.

This will help accepting slightly less favourable combinations of pre-stress levels and flaw depths, increasing the reuse potential of the glass panes.

Table 7.1: Results from the Monte Carlo simulation for the case study

Type	Value
Empirical 5%-fractile $\sigma_{r,0.05}$	74.45 MPa
Empirical 5%-fractile $c_{0.05}$	101 µm
Calculated $\sigma_{calc,0.05}$ from 5%-fractile inputs	107.71 MPa
Empirical 5%-fractile $\sigma_{f,0.05}$	113.08 MPa
Empirical 10.5%-fractile $\sigma_{r,e}$	76.18 MPa
Empirical 10.5%-fractile c_e	86 µm
Calculated $\sigma_{calc,e}$ from 10.5%-fractile inputs	112.97 MPa

In a more general setting, this Monte Carlo simulation was also tested with the most restrictive combination of parameters, in the following realistic bounds:

- $\sigma_{r,average} = 140MPa[5MPa : 140MPa]$
- $\sigma_{r,std} = 3MPa[3MPa : 8MPa]$
- $c_{average} = 10\mu m[10\mu m : 500\mu m]$
- $c_{std} = 60\mu m[20\mu m : 100\mu m]$
- $Y = 0.713[0.713; 1.12]$
- $d = 2mm[2mm : 8mm]$

The statistical distributions of the pre-stress level and the flaw depth are defined from these parameters, and 100 000 samples are generated following these distributions, as shown in Figure 7.6 and Figure 7.7:

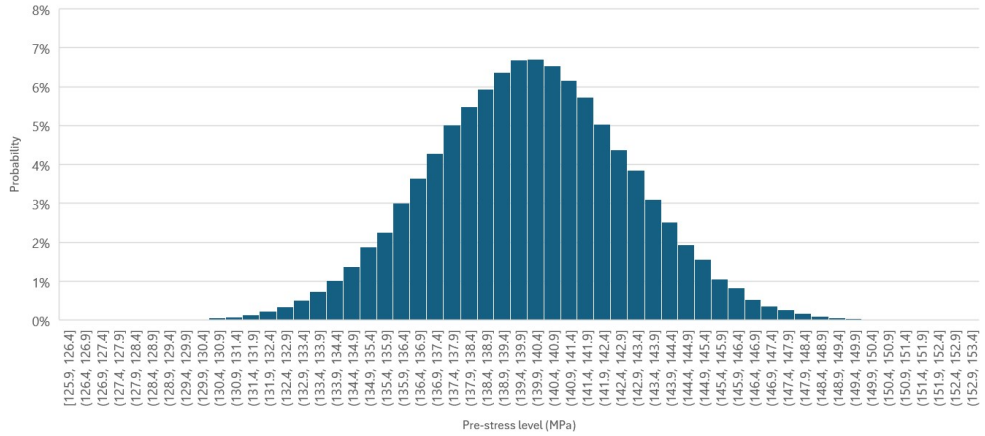

Figure 7.6: Monte Carlo simulation of the surface pre-stress level distribution. Average $\mu = 140MPa$ and $\sigma = 3MPa$.

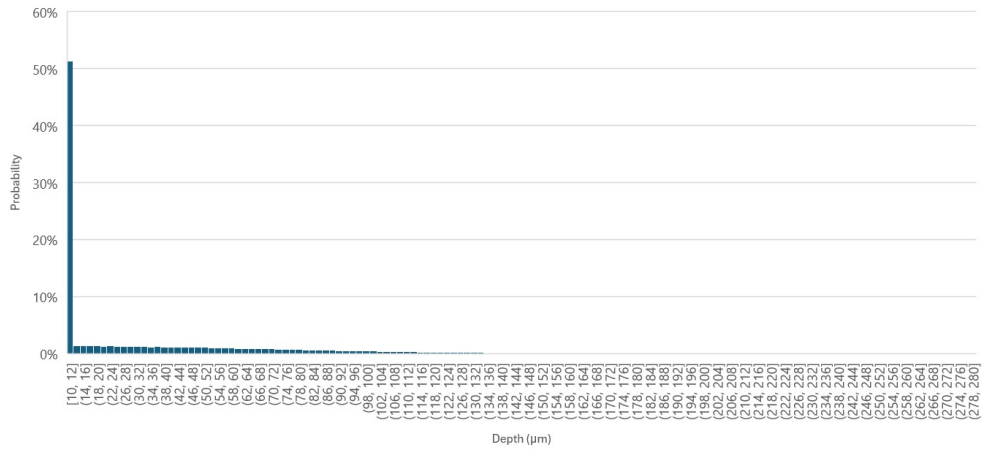

Figure 7.7: Monte Carlo simulation of the flaw depth distribution. Average $\mu = 10\mu m$ and $\sigma = 60\mu m$ with a minimum threshold of $10\mu m$.

These values are then combined following Equation (7.3) to obtain 100 000 values as well for the glass strength:

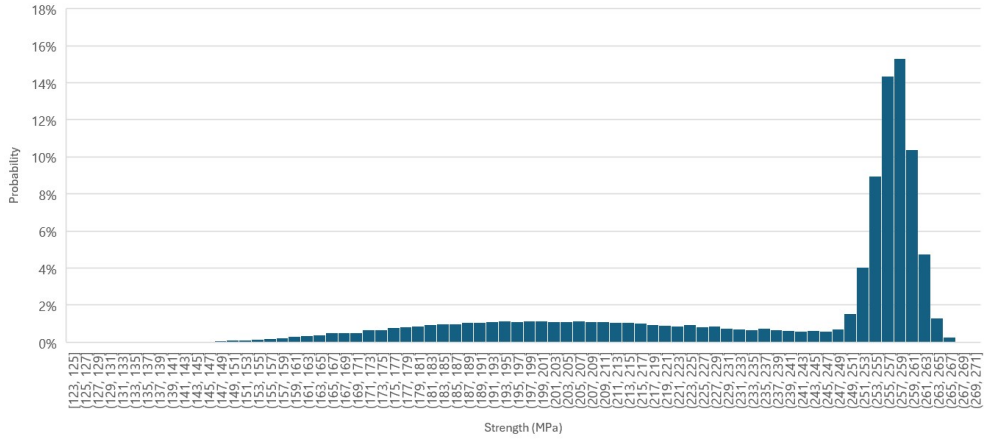

Figure 7.8: Monte Carlo simulation of the strength distribution. Based on c and σ_r from Figure 7.6 and Figure 7.7, with $Y = 0.713$, $K_{IC} = 0.75$ and a glass half-thickness $d = 5mm$.

In this worst-case scenario, the risk level for each variable can only be increased up to 6% to keep the overall risk level for strength below 5%. This change can be explained due to the non-linear combination of the variables. Therefore, an increased acceptable risk level of 6% can be chosen in a first time for heat-strengthened or fully toughened glass in general. This approach is of little interest for annealed glass, where a risk level of 5% can be maintained. For any new project with heat-strengthened or fully toughened glass, the bottom value of 6% can be used directly or a new Monte Carlo simulation must be performed.

Table 7.2: Results from the Monte Carlo simulation for the worst general case

Type	Value
Empirical 5%-fractile $\sigma_{r,0.05}$	135.06 MPa
Empirical 5%-fractile $c_{0.05}$	109 µm
Calculated $\sigma_{calc,0.05}$ from 5%-fractile inputs	170.60 MPa
Empirical 5%-fractile $\sigma_{f,0.05}$	174.56 MPa
Empirical 6%-fractile $\sigma_{r,e}$	135.33 MPa
Empirical 6%-fractile c_e	103 µm
Calculated $\sigma_{calc,e}$ from 6%-fractile inputs	173.36 MPa

The following calculations for the case study will be carried out using this 10% acceptable risk level for the pre-stress and flaw depth values.

Flaw depth safety margin

The flaw depth c has a safety margin M_T based on the the reliability study from Annex B. This reliability study is made of 10 measurements done each time on 3 different flaws. For each of these 10 measurements, the average and standard deviation are extracted. The 90%-fractile is also deduced assuming a normal distribution (this value can then be slightly larger than the largest of the 10 measurements). The measurements can take random values with an average µ. The difference $\delta = c_{0.90} - \mu$ quantifies the gap between the mean measured flaw depth and the 90%-fractile.

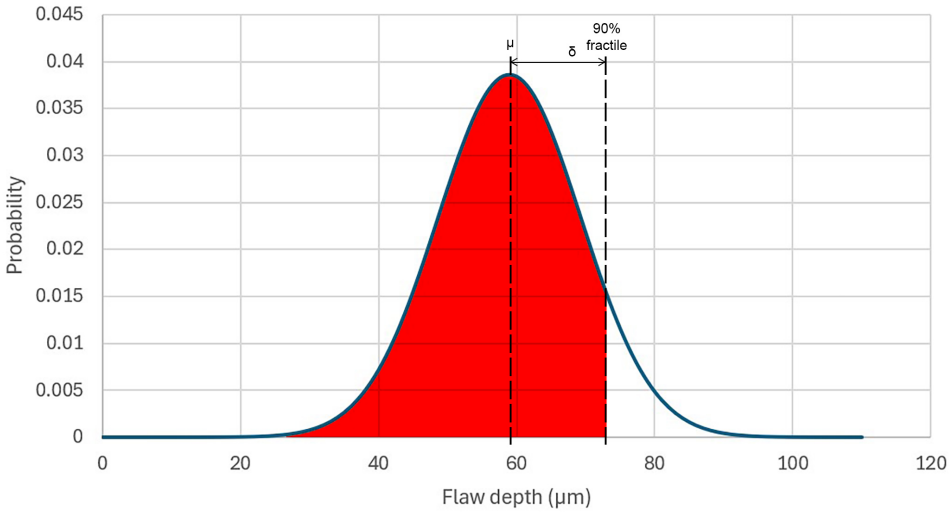

Figure 7.9: Safety margin δ based on the difference between the average measured flaw depth and the 90%-fractile.

Based on the averaged measurements, $\delta = 13\mu m$ and $M_T = \delta/\mu = 22.5\%$. The margin M_T is then rounded up to the maximum value between 20µm and 23%:

$$M_T = MAX(20\mu m; 23\%) \tag{7.7}$$

$$c_{margin} = MAX(c_{measured} + 20\mu m; c_{measured} \times 1.23) \tag{7.8}$$

The value c_{margin} now has a 90% confidence level to be above the real flaw depth c_{real}.

Pre-stress level safety margins

The pre-stress level $\sigma_{r,srf}$ has two uncertainties M_{SCALP} and $M_{sampling}$ related to the SCALP-05 precision level and sampling respectively. These two margins will be summed.

We know that the sum of two normally distributed variables $X \sim N(\mu_x, \sigma_X^2)$ and $Y \sim N(\mu_Y, \sigma_Y^2)$ can be described by $Z = X + Y$ and is also normally distributed as follows:

$$Z \sim N(\mu_X + \mu_Y, \sigma_X^2 + \sigma_Y^2) \tag{7.9}$$

Therefore, the standard deviation of Z is:

$$\sigma_Z = \sqrt{\sigma_X^2 + \sigma_Y^2} \tag{7.10}$$

As the standard deviation σ is directly proportional to the confidence interval:

$$M_{SCALP+sampling} = \sqrt{M_{SCALP}^2 + M_{sampling}^2} \tag{7.11}$$

The margin M_{SCALP} is defined similarly as M_T, based on the reliability study from Annex A. This reliability study is also made of 10 pre-stress measurements done each time on 3 different locations. For each of these 10 measurements, the average and standard deviation are extracted. The 90%-fractile is also deduced assuming a normal distribution. The measurements can take random values with an average μ. The difference $\delta = \sigma_{0.90} - \mu$ quantifies the gap between the mean measured pre-stress level and the 90%-fractile.

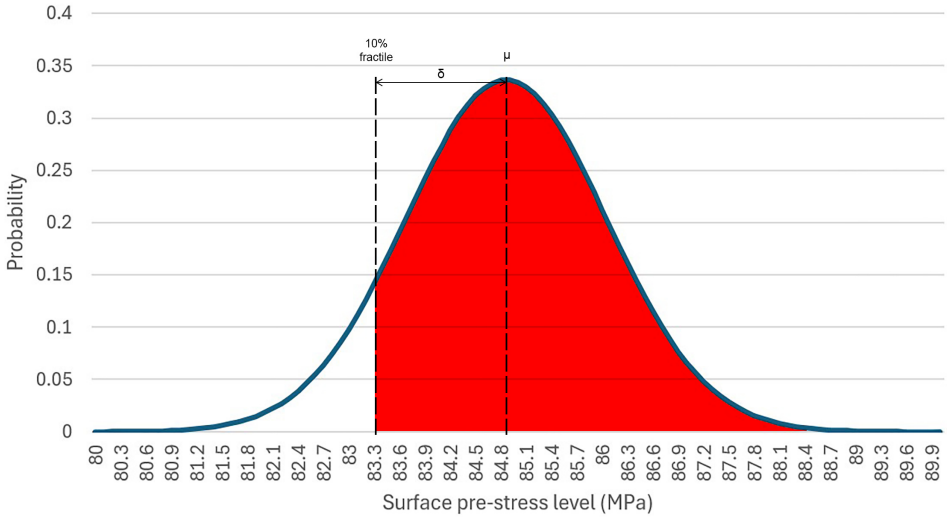

Figure 7.10: Safety margin δ based on the difference between the average measured pre-stress level and the 90%-fractile.

Based on the averaged measurements, $\delta = 1.52MPa$ and $M_T = \delta/\mu = 1.79\%$. Whenever the pre-stress level becomes very low, the margin should still be at least 1 MPa (minimum margin according to the SCALP-05 manufacturer). The margin M_{SCALP} is then rounded up to:

$$M_{SCALP} = MAX(1MPa; 1.80\%) \tag{7.12}$$

$$\begin{aligned} \sigma_{margin,SCALP} &= MIN(\sigma_{measured} - 1MPa; \sigma_{measured} \times (1 - 0.018)) \\ \sigma_{margin,SCALP} &= 0.982 \times \sigma_{measured} \end{aligned} \tag{7.13}$$

The margin $M_{sampling}$ corresponds to the potential difference between the 70 samples and the rest of the 2464 glass panes. From Equation (6.1) and Equation (6.2), the margin ϵ is now the only unknown and can be found as follows:

$$(\frac{z^2\hat{p}(1-\hat{p})}{\epsilon^2 n'} - 1)\frac{\epsilon^2 N}{\hat{p}(1-\hat{p})} = z^2 \tag{7.14}$$

Multiply by $n'\hat{p}(1-\hat{p})$:

$$-N\hat{p}^2z^2 - n'\epsilon^2 N + N\hat{p}z^2 = -n'\hat{p}^2z^2 + n'\hat{p}z^2 \tag{7.15}$$

Add $N\hat{p}^2z^2$:

$$-n'\epsilon^2 N + N\hat{p}z^2 = -n'\hat{p}^2z^2 + n'\hat{p}z^2 + N\hat{p}^2z^2 \tag{7.16}$$

Subtract $N\hat{p}z^2$:

$$-n'\epsilon^2 N = -n'\hat{p}^2z^2 + n'\hat{p}z^2 + n\hat{p}^2z^2 - N\hat{p}z^2 \tag{7.17}$$

Divide by $-n'N$:

$$\epsilon^2 = \frac{n'\hat{p}^2z^2 - n'\hat{p}z^2 - n\hat{p}^2z^2 + N\hat{p}z^2}{n'N} \tag{7.18}$$

As we only consider positive values for ϵ here, we obtain:

$$\epsilon = \sqrt{\frac{n'\hat{p}^2z^2 - n'\hat{p}z^2 - n\hat{p}^2z^2 + N\hat{p}z^2}{n'N}} \simeq 7.55\% \tag{7.19}$$

where
$n' = 70$ is the sample size (number of measured glass panes)
$z = 1.282$ is the z score for a (100% - (10 $\times$2)%) = 80% confidence interval
$\hat{p} = 0.50$ is the population proportion (0.50 for continuous variables)
$N = 2464$ is the population size (number of glass panes to reuse)

The margin for sampling is then:

$$M_{sampling} = 7.55\% \tag{7.20}$$

$$\sigma_{margin,sampling} = 0.9245 \times \sigma_{measured} \tag{7.21}$$

Both M_{SCALP} and $M_{sampling}$ are then combined:

$$\begin{aligned} M_{SCALP+sampling} &= \sqrt{M_{SCALP}^2 + M_{sampling}^2} = \sqrt{0.018^2 + 0.0755^2} \\ M_{SCALP+sampling} &= 7.76\% \end{aligned} \tag{7.22}$$

$$\begin{aligned} \sigma_{margins} &= (1 - \sqrt{M_{SCALP}^2 + M_{sampling}^2}) \times \sigma_{measured} \\ \sigma_{margins} &= 0.9224 \times \sigma_{measured} \end{aligned} \tag{7.23}$$

The value $\sigma_{margins}$ now has a 90% confidence level to be above the real surface pre-stress level σ_{real}.

Visual inspection safety margins

After doing several measurements with Traceit®, the observer could already have an idea the flaw depth value visually. For example, a barely visible scratch was expected to have a maximum depth of less than 20 µm, which was always confirmed with the Traceit® measurements afterwards.

This ability to evaluate the surface quality of the glass was tested, and compared to the Traceit® measurements. To do this, the observer came on-site on a different day. The same 70 glass panes were observed using the same observation procedure as before. However, in order to be scalable the process was made faster (less than one minute per pane).

This test was carried out after the measurements with Traceit®, but before processing the data. The observer had the experience of seeing flaws and measuring their depths with Traceit®, but this data had not been yet processed to define the exact location of the top and bottom points and see the exact flaw depth distribution. In addition, as the observer carried out this test on a different day, he did not necessarily find and estimate the same largest flaw on each pane, compared to the one that was measured with Traceit®. This uncertainty in the choice of the largest flaw is then built into the process. This allowed the observer to test his visual inspection ability by using the experience with Traceit®, without knowing too precisely what to expect.

The results of the visual inspection and their difference compared to the Traceit® measurements are detailed in Annex D. This visual inspection obviously involves a greater safety margin, with some flaws being underestimated or overestimated. However, it was interesting to see that these gaps could be relatively limited. Indeed, 93% of the estimated flaw depths were less than 50µm different than the Traceit® measurements, for flaws reaching up to 150 µm. These differences are both small for absolute values, and large for relative values. A classification system with appropriate margins could then allow ensuring minimum strength levels, depending on the surface quality of the pane.

The margins for visual inspection should have both absolute and relative values. The minimum absolute values correspond to the largest flaws that could be missed at a 95% confidence interval, while the relative values correspond to the observation errors at a 95% confidence interval as well.

Based on the visual inspection on site, spot flaws of up to 60 µm and linear flaws of up to 40 µm could have been missed in these conditions on site. These values can be used as absolute values for margins.

The 95%-fractile of the relative difference (absolute values) between the estimated flaw depth from visual inspection and the Traceit® measurement reaches 159%. This calibration process is described in detail in the next chapter.

Table 7.3: Visual inspection margins M_V

	Spot flaw	Linear flaw
Minimal margins	60 µm	40 µm
Relative margin	159%	159%

Although this relative margin may seem quite large, it is still very low in terms of absolute values. Moreover, the glass strength is not directly proportional to this margin: for a glass pane with the same characteristic pre-stress level and margins, this margin of 159% applied an average linear flaw depth of 40µm reduces the glass strength by only 17%. For the same values applied to annealed glass (no pre-stress contribution), this reduction reaches 34%.

This shows that even with a quick visual inspection, after an appropriate training with Traceit®, the observer can define a reasonable margin with a 95% confidence level.

7.4. Qualification process of the glass panes

7.4.1. Definition of the glass panes quality levels

Depending on the estimated flaw depth, the panes could be classified according to a defined 'quality level'. This quality level could be linked to a minimum strength level, with appropriate margins.

Rota, Zaccaria & Fiorito (2023) defined a classification system based on the size and density of the surface flaws, measured with scanners from float glass production lines and compared with destructive tests. This approach is particularly interesting because of its automation process and scalability. However, it cannot be carried out on-site, needs transportation and is dependent on the manufacturer's equipment. In addition, the link established between the optical quality level and the glass strength is not strictly physics-based, but rather indirect as the scanners do not measure the flaw depth.

This study does not pretend to replace the process proposed by Rota, Zaccaria & Fiorito (2023), but to propose another approach that could be used directly on-site. This study can be an alternative way to qualify glass for reuse, but it could also be a complementary step to estimate the reuse potential on-site before scanning the glass panes on the float production lines. Attempts could also be made to relate the two quality level classification systems.

The quality level classification for this study is proposed in Table 7.4. These quality levels have a fixed characteristic strength corresponding to the existing glass strength from the Eurocodes (QL1, QL3 and QL5) or to an intermediate strength level (QL2, QL4 and QL6).

Table 7.4: Quality levels classification with associated strengths

	QL1	QL2	QL3	QL4	QL5	QL6
Characteristic strength	120 MPa	100 MPa	70 MPa	60 MPa	45 MPa	35 MPa
Qualification	FT	FT-	HS	HS-	AN	AN-

7.4.2. Classification process

Overview

Based on the measured pre-stress level $\sigma_{r,srf}$, glass half-thickness d and required characteristic strength σ_{QL}, the margins associated with the sampling $M_{sampling}$, SCALP-05 measurements M_{SCALP}, Traceit® measurements M_T and visual inspection M_V are combined to obtain the maximum flaw depth with margins c_{class} associated with each 'quality level' class.

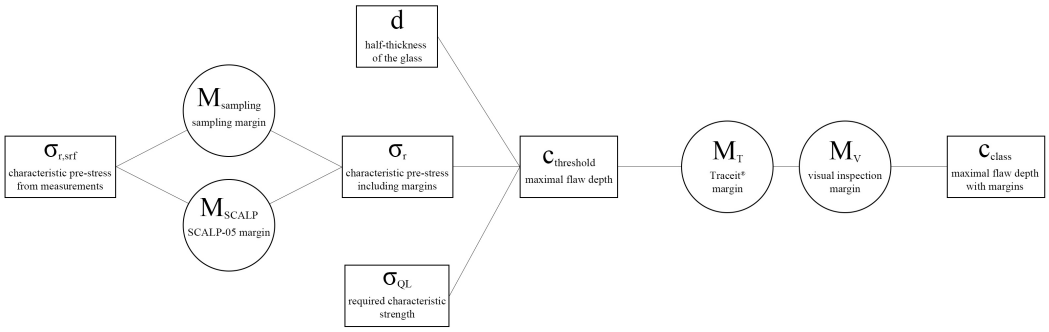

Figure 7.11: Summary of the classification value c_{class} links with the different measurements and margins, associated with a QL class.

This final value can be used to classify the glass panes. For example, if a glass pane is estimated to have a flaw depth smaller or equal to $c_{estimate} = 200m$ and if for QL2 $c_{class,QL2} = 72m$ and QL2 $c_{class,QL3} = 213m$, this glass pane is classified in QL3.

Definition of $c_{threshold}$

Using the characteristic measured pre-stress reduced by the combined margins $\sigma_{red} = 68.68MPa$, the maximum linear and spot flaw depths are calculated using Equation (7.3). These values $c_{l,threshold}$ and $c_{s,threshold}$ correspond to the maximum flaw depths used to calculate the glass strength for each glass. For example, using $c_{l,threshold}$ = 93 µm with the shape coefficient for linear scratches Y = 1.12 in Equation (7.3) will give a characteristic strength of 100 MPa.

Table 7.5: Quality levels with associated maximum flaw depths

	QL1	QL2	QL3	QL4	QL5	QL6
Characteristic strength	120 MPa	100 MPa	70 MPa	60 MPa	45 MPa	35 MPa
Maximum linear flaw depth $c_{l,threshold}$	31 µm	93 µm	398 µm	586 µm	959 µm	1227 µm
Maximum spot flaw depth $c_{s,threshold}$	94 µm	187 µm	551 µm	742 µm	1127 µm	1394 µm

Definition of c_{class} and M_V

The maximum linear and spot flaw depth estimates $c_{l,class}$ and $c_{s,class}$ correspond to the upper bound used to classify the glass panes. These values are based on $c_{l,threshold}$ and $c_{s,threshold}$ reduced with the visual inspection margins M_V following this principle:

$$c_{class} = c_{threshold} - M_V \tag{7.24}$$

The visual inspection margins M_V directly influence the classification. Larger margins will lead to smaller values for $c_{l,class}$ and $c_{s,class}$, affecting the classification. For example, a glass pane with a scratch estimated at $c_{estimate}$ = 150 µm will be classified in QL3 according to Table 7.7, as it is smaller than $c_{l,class,QL4}$ = 154 µm. However, if the relative visual inspection margin is increased from 159% to 170%, $c_{l,class,QL3}$ is reduced to 147 µm. The same scratch becomes then classified in QL4.

The opposite is also true. Smaller margins will lead to larger values for $c_{l,class}$ and $c_{s,class}$, which will also affect the classification. The point then is to find the most appropriate margins M_V. These values should be as small as possible to optimise the reuse potential, while maintaining a sufficiently high safety level.

As explained in Subsection 7.3.3.4, M_V is composed of absolute values (largest flaws that could be missed during visual inspection) and relative values (observation errors) with a 95% confidence level. The minimum absolute values were found to be 40 µm for linear flaws and 60 µm for spot flaws. The relative margin has to be calibrated according to the observation errors.

To do this, the relative error between the estimated flaw depth $c_{estimate}$ and the adjusted Traceit® measurement c is calculated for the 70 glass panes as follows:

$$\epsilon_{estimate} = |\frac{c - c_{estimate}}{c_{estimate}}| \tag{7.25}$$

Only the errors with $c_{l,estimate} \leq$40 µm or $c_{s,estimate} \leq$60 µm are kept. The 95%-fractile of these errors is then calculated, using for example the Excel function PERCENTILE.INC(). Using this dataset, a relative margin of 159% is found.

Applying this margin to the classified dataset gives a 'success rate' of 98.6%. This means that for 69 of the 70 glass panes, the following requirement is met:

$$c + M_T \leq c_{threshold} \tag{7.26}$$

Whenever this rate were smaller than 95% due to the limited sample size and fit error, the relative margin would be increased until reaching at least a 95% rate.

Table 7.6: Visual inspection margins M_V applied

	Spot flaw	Linear flaw
Minimal margins	60 µm	40 µm
Relative margin	159%	159%

The maximum flaw depth estimates $c_{l,class}$ and $c_{s,class}$ are then calculated as follows:

$$\begin{aligned} c_{l,class} &= MIN(c_{l,threshold} - 40\mu m; \frac{c_{l,threshold}}{1+1.59}) \\ c_{s,class} &= MIN(c_{s,threshold} - 60\mu m; \frac{c_{l,threshold}}{1+1.59}) \end{aligned} \tag{7.27}$$

Classification summary

The classification for this dataset can be summarised in Table 7.7:

Table 7.7: Final classification

	QL1	QL2	QL3	QL4	QL5	QL6
Characteristic strength	120 MPa	100 MPa	70 MPa	60 MPa	45 MPa	35 MPa
Maximum linear flaw threshold $c_{l,threshold}$	31 µm	93 µm	398 µm	586 µm	959 µm	1227 µm
Maximum spot flaw threshold $c_{s,threshold}$	94 µm	187 µm	551 µm	742 µm	1127 µm	1394 µm
Maximum linear flaw depth estimate $c_{l,class}$	-	36 µm	154 µm	226 µm	370 µm	474 µm
Maximum spot flaw depth estimate $c_{s,class}$	-	72 µm	213 µm	286 µm	435 µm	538 µm
Number of glass panes	0	53	17	0	0	0

From this sample, 53 glass panes are classified as QL2 and 17 as QL3. In other words, based on this pre-stress level, flaw depths and safety margins, all the panes could be reused as heat-strengthened glass or slightly better.

7.4.3. Global qualification process

Adaptation of the case study objectives

The goal here is to qualify the glass panes strength as fully toughened, heat-strengthened or eventually annealed glass. Given the low pre-stress level and minimal safety margins, the qualification as fully toughened (QL1) seems quite difficult and time consuming for this particular case study. Intermediate strength levels of QL2, QL4 and QL6 are not currently implemented in the norms. Therefore, these options are discarded for this specific case study. However, the qualification of these glass panes as heat-strengthened (QL3) or annealed (QL5) glass is still relevant and feasible.

Global qualification process of the 2464 glass panes

The other glass panes can be qualified using the same process as described in Section 7.4. For each glass pane, the maximum flaw depth is estimated according to the classification previously described. If no major flaw is found ($c_{l,class} \leq$370 µm or $c_{s,class} \leq$435 µm), the pane should easily qualify as annealed glass. If no large flaw is found ($c_{l,class} \leq$154 µm or $c_{s,class} \leq$213 µm), the pane should be qualified as heat-strengthened glass.

The qualification of the other 2464 glass panes is not done during the thesis, but may be done later. As all of the 70 panes tested were able to qualify as heat-strengthened glass, it is expected that most of the other panes will also qualify as heat-strengthened glass.

7.5. Protocol resilience

7.5.1. Influence of the residual stress level

The residual stress level has a direct impact on the reuse potential. A lower pre-stress level will make it more difficult to qualify the glass panes: to achieve the same strength level, the largest flaw depths must be smaller. Conversely, a higher residual stress level will make the glass panes easier to reuse.

As seen in the literature (Haldimann, 2008) and with the measurements from Chapter 6, there can be significant variations between glass panes of the same type, even if they are from the same manufacturer and batch.

As an example, if the 70 glass panes from the case study had a characteristic pre-stress level of σ_r = 100 MPa with similar flaw depths and safety margins, 50 of them could be reused as fully toughened glass (QL1) and the rest as heat-strengthened glass (QL2 and QL3).

7.5.2. Influence of the measuring margins

The safety margins obviously influence the final classification, but with different levels of importance depending on the pre-stress level and the flaw depth. As the equation is non-linear, an annealed glass pane with large flaws will be affected differently than a fully toughened glass pane with small flaws by these different margins.

The margin for SCALP-05 precision M_{SCALP} directly affects the pre-stress value, which is critical, but in a limited way. In the case study, it reduces the strength of all the samples by approximately 2 MPa. This value is quite reasonable and there is not much room for improvement there. The greater the pre-stress, the more important this margin becomes.

The margin from sampling $M_{sampling}$ only affects the pre-stress value, and is expected to be more significant. In the case study, it reduces the strength of all the samples by about 9 MPa. It is influenced by the confidence level of 95% and the sample size of 70 out of 2464 glass panes. The greater the pre-stress, the more important this margin becomes.

The margin related to Traceit® M_T is expected to be relatively high, but its effect on the final strength is usually more limited. For example, a 30% increase in flaw depth (with the same pre-stress level and margins as in the case study) will reduce the strength by 9.5%. If there were no pre-stress contribution, such as with annealed glass, this reduction would reach 18%. This margin can become significant when the flaw depths are very small ($\leq$40 µm) and the pre-stress contribution is low ($\approx$0 MPa with annealed glass).

The margin from visual inspection M_V is expected to be much higher than the rest, but like the previous one, its impact on the final strength is more limited. For example, an increase of 159% in the flaw depth (with the same pre-stress level and margins as in the case study) will reduce the strength by 17%. If there were no pre-stress contribution, such as with annealed glass, this reduction would be 34%. This margin also becomes significant when the flaw depths are very small ($\leq$40 µm) and the pre-stress contribution is low ($\approx$0 MPa for annealed glass).

7.5.3. Influence of the sampling size

The sampling size affects the sampling margin $M_{sampling}$. With 70 samples out of 2464 glass panes and the chosen confidence level, a margin of 7.55% was obtained. If the sampling had been reduced to 30 elements, this margin would reach 11.63%. Conversely, a sample of 100 elements would give a margin of 6.28%. The relationship between sample size and $M_{sampling}$ is not linear.

Based on Equation (6.1) for an unlimited population size, the sampling margin $M_{sampling}$ can be plotted as a function of the sample size. The results for a limited population size are expected to be quite similar, as long as the population size is large enough ($\geq$100).

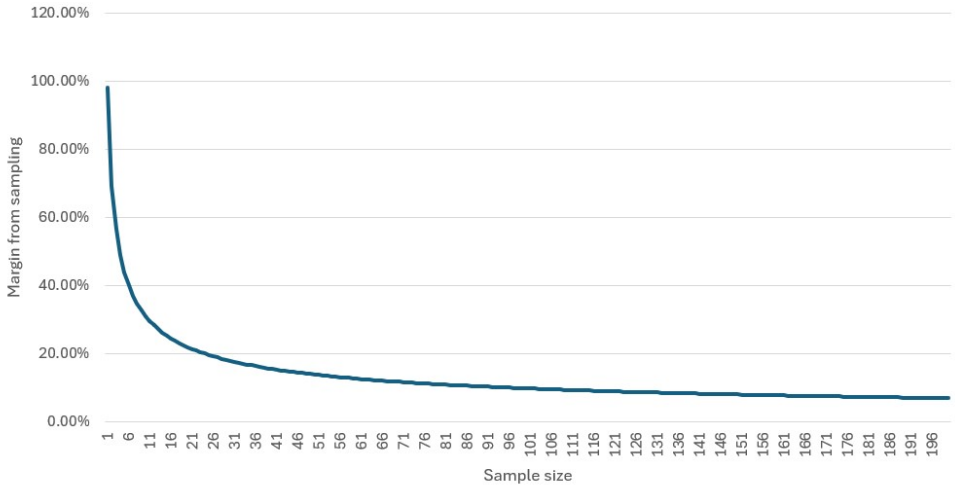

Figure 7.12: Sampling margin $M_{sampling}$ in function of the sample size, for an unlimited population and a confidence level of 95%

A too small sampling size would make the margin explode, which is also why a minimum of 30 samples is recommended. On the other hand, increasing the sampling size too much will not lead to a significant reduction of this margin. A good ratio between the reduction of $M_{sampling}$ and a fast measurement procedure would be between 30 and 100 samples.

7.5.4. Typical examples for annealed, heat-strengthened and fully toughened glass

This methodology is also tested for other cases. Typical characteristic pre-stress values for annealed, heat-strengthened and fully toughened glass are taken from the literature and synthesised in Table 7.8:

Table 7.8: Typical pre-stress levels for annealed, heat-strengthened and fully toughened glass

Glass type	Typical characteristic residual stress level
AN - Annealed	5.6 MPa
HS - Heat-strengthened	45 MPa
FT - Fully toughened	100 MPa

For comparison, the same 70 samples from the case study with the same margins will be used. Only the characteristic pre-stress level will be changed and M_V slightly adjusted for these three examples. The Monte Carlo simulation to optimise the margins is not carried out here and the safety levels are kept at 95%.

Typical annealed glass

Assuming the 70 glass panes have the same values as in the case study with a characteristic residual stress level of 5.6 MPa, the following classification would be obtained:

Table 7.9: Classification for typical annealed glass

	QL1	QL2	QL3	QL4	QL5	QL6
Characteristic strength	120 MPa	100 MPa	70 MPa	60 MPa	45 MPa	35 MPa
Maximaum linear flaw threshold $c_{l,threshold}$	-	-	-	-	68 µm	133 µm
Maximum spot flaw threshold $c_{s,threshold}$	-	-	-	-	193 µm	345 µm
Maximum linear flaw depth estimate $c_{l,class}$	-	-	-	-	18 µm	51 µm
Maximum spot flaw depth estimate $c_{s,class}$	-	-	-	-	75 µm	133 µm
Number of glass panes	0	0	0	0	30	36

In these conditions, 30 out of 70 glass panes could be reused as annealed glass, 36 could be reused with a reduced strength of 35 MPa and 4 would not qualify.

Typical heat-strengthened glass

Assuming the 70 glass panes have the same values as in the case study with a characteristic residual stress level of 45 MPa, the following classification would be obtained:

Table 7.10: Classification for typical heat-strengthened glass

	QL1	QL2	QL3	QL4	QL5	QL6
Characteristic strength	120 MPa	100 MPa	70 MPa	60 MPa	45 MPa	35 MPa
Maximum linear flaw threshold $c_{l,threshold}$	-	-	102 µm	182 µm	498 µm	813 µm
Maximum spot flaw threshold $c_{s,threshold}$	-	-	216 µm	341 µm	737 µm	1067 µm
Maximum linear flaw depth estimate $c_{l,class}$	-	-	39 µm	70 µm	192 µm	314 µm
Maximum spot flaw depth estimate $c_{s,class}$	-	-	83 µm	132 µm	285 µm	412 µm
Number of glass panes	0	0	54	14	2	0

In these conditions, 68 out of 70 glass panes could be reused as heat-strengthened glass and 2 as annealed glass.

Typical fully toughened glass

Assuming the 70 glass panes have the same values as in the case study with a characteristic residual stress level of 100 MPa, the following classification would be obtained:

Table 7.11: Classification for typical fully toughened glass

	QL1	QL2	QL3	QL4	QL5	QL6
Characteristic strength	120 MPa	100 MPa	70 MPa	60 MPa	45 MPa	35 MPa
Maximum linear flaw threshold $c_{l,threshold}$	83 µm	212 µm	632 µm	817 µm	1158 µm	1388 µm
Maximum spot flaw threshold $c_{s,threshold}$	165 µm	329 µm	758 µm	941 µm	1293 µm	1522 µm
Maximum linear flaw depth estimate $c_{l,class}$	30 µm	77 µm	229 µm	296 µm	420 µm	503 µm
Maximum spot flaw depth estimate $c_{s,class}$	60 µm	119 µm	275 µm	341 µm	468 µm	551 µm
Number of glass panes	50	18	2	0	0	0

In these conditions, 50 out of 70 glass panes could be reused as fully toughened glass and 20 as heat-strengthened glass.

7.6. Discussion

The residual pre-stress level can have a significant impact on the reuse potential of glass. As this value can vary considerably even for the same type of glass, manufacturer and batch, it should be measured

carefully.

The quality levels were defined here with fixed strength according to the regulations (QL1, QL3 and QL5) or at an intermediate level (QL2, QL4 and QL6). These intermediate levels cannot be used with the existing regulations, but show that these additional levels could improve the reuse potential of glass if they meet the design requirements. In addition, other quality level classes (QLx) could be defined with a specific strength level relevant to a particular project design and optimizing the number of panes to be reused. For example, if the design requirement is only of 20 MPa, a bespoke QL7 class could be added to include glass panes with greater flaw depths.

The safety margins have a variable, non-linear influence on the classification. For example, annealed glass will be more sensitive to the margins associated with Traceit® and the sample size, whereas tempered glass may be more sensitive to the margins associated with the SCALP-05 precision and the visual inspection. Annealed glass seems slightly more difficult to re-qualify globally, although it is still possible.

These tests could be completed with destructive tests to confirm the predicted glass strength. The results would have to be interpreted carefully, as large variations between samples and between theoretical and experimental results are to be expected.

8

Proposed methodology

8.1. Introduction

The methodology must be adaptable according to the precision level sought. If one is confident about the reuse potential of the glass, some parameters can be changed to make the methodology easier and faster to apply, in exchange for increased safety margins. Conversely, these parameters can be changed to increase precision.

This chapter will describe the general protocol for assessing the reuse potential of post-consumer glass. It will detail the improved protocol based on the experience of the case study.

8.2. Short impact study

8.2.1. Scope of the methodology

A short impact assessment is recommended to get an idea of the benefits of reuse compared to recycling and down-cycling. This study should be comparative (only focusing on the differences between the scenarios) and only on the modules shown in Figure 8.1.

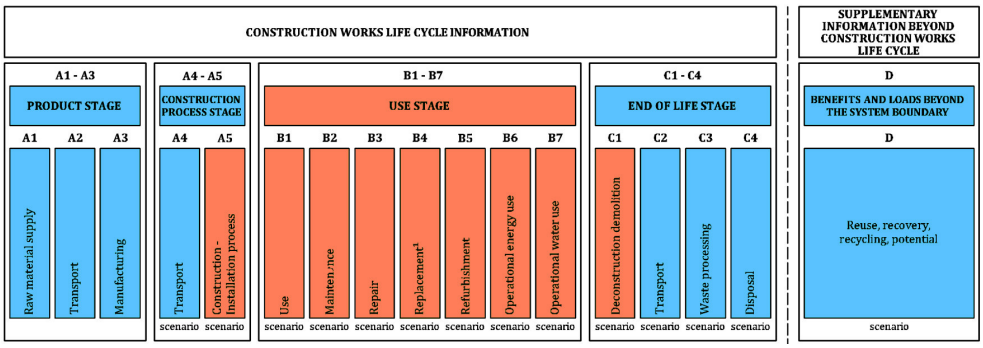

Figure 8.1: Modules to focus on (Adapted from EN 15804, 2019)

The three EoL scenarios are chosen:

- **Reuse:** 100% glass panels are reused on the same building.
- **Recycling:** 100% glass cullets are recycled to be used for flat glass or container glass.
- **Down-cycling:** 100% glass cullets are downcycled to be used for concrete rubbles or other mineral inert materials.

The landfill scenario is removed since it is very similar to down-cycling, and the latter is more relevant for this type of study.

The chosen indicators are the components for reuse (kg), materials for recycling (kg) and Global Warming Potential total (kg CO_2 eq.).

8.2.2. Absolute and relative results

The total avoided burden T is calculated based on the C and D modules as follows:

$$T = (C1 + C2 + C3 + C4 + D) \times mass \tag{8.1}$$

The first part of the results are the absolute differences between the different scenarios. The differences in Global Warming Potential total (kg CO_2 eq.) can be summarised in the form of the Table 8.1.

Module A1-A3 can be estimated in the same way as in the case study, based on the value from flat glass with 0% of secondary material of 1.29 kg CO_2/kg_{output} (Hartwell, Coult & Overend, 2023) summed with the estimated toughening contribution of 0.28 kg CO_2/kg_{output} as explained in Section 4.2, to obtain 1.57 kg CO_2/kg_{output}. This value may evolve and needs to be verified in the coming years.

All values from Table 4.2 have been converted to kg CO_2/kg_{output} and added to Table 8.1. These values should be replaced with those from updated EPDs specific to each project, but it can already provide an estimate of the GWP difference to be interpreted with caution. These values can be adjusted to a functional unit simply by multiplication. For example, for a functional unit of 25 kg, all these values should be multiplied by 25.

Table 8.1: Difference of kg CO_2/kg_{output} equivalent between reuse, recycling and down-cycling end-of-life scenarios

	A1-A3	A4	A5	B1-B7	C1	C2	C3	C4	D (estimate)	T (total avoided burden)
Reuse in situ	1.57	0.0244	-	-	0	0.00244	0	0.014	-1.5944	-1.57796
Recycling	1.57	0.0244	-	-	0	0.00244	0	0.014	-0.8	-0.78356
Down-cycling	1.57	0.0244	-	-	0	0.00244	0	0.014	0.0052	0.02164

The second part is optional but can provide complementary insights into the environmental impact of reuse. It consists of the same analysis as done in Table 8.1, but applied to the different façade components as well. This is made easier if a typical module can be taken from the façade.

The results can be summarised in the form of the Table 8.2, with values in percentage only.

Table 8.2: Difference of kg CO_2 equivalent between reuse, recycling and down-cycling relative to the façade

	Relative recycled mass	Relative reused mass	Relative GWP gains
Reuse	-	-	-
Recycling	-	-	-
Down-cycling	-	-	-

Both parts of this comparative study help to understand the magnitude of the environmental impact of reuse in kg CO_2 as well as relative to the whole façade system. The values in both parts should be relatively significant to make reuse relevant to the studies to be carried out in the following parts.

8.3. Probabilistic equivalence of the Heat-Soak Test

8.3.1. Aimed equivalent efficiency definition

Since the exact efficiency of the HST is not known and subject to discussions, one value must be chosen. The values in Table 8.3 are suggested. Although higher HST efficiencies could be considered, this is

based on the most widely accepted values and already reach a satisfactory efficiency level.

Table 8.3: Aimed equivalent efficiency of the HST

Tonnes of glass for one breakage, without HST	6
Tonnes of glass for one breakage, with HST	400
Aimed equivalent efficiency of the HST	98.50%

8.3.2. Probabilistic equivalence in function of time

The level of risk can be estimated solely in function of time. The largest and most conservative found dataset so far was the on described in Table 8.4.

Table 8.4: Chosen dataset of failure due to NiS inclusions over time (dataset 1)

Year	1	2	3	4	5	6	7	8	9	10	11	12	13	14
Number of failure	15	13	16	14	9	5	4	2	6	2	2	4	2	2
Cumulated number of failure	15	28	44	58	67	72	76	78	84	86	88	92	94	96

The CDF can then be fitted with a log-normal distribution using the Least Square Method. This distribution should have a mean μ = 1.3816 and a standard deviation σ = 1.1834. A list of the obtained equivalent efficiencies every decade is summarised in Table 8.5.

Table 8.5: Equivalent efficiency of the HST over time

Year	Probabilistic equivalence (Log-normal)
0	0%
10	78.18%
20	91.37%
30	95.60%
40	97.44%
50	98.38%
60	98.91%
70	99.23%
80	99.44%
90	99.58%
100	99.68%

Using these parameters, an equivalent efficiency of the HST can be justified from 50 years after fabrication. However, a satisfactory level of risk can already be reached from 30 years. In this case, the same approach should be applied to the dataset 2 from Section 5.3 with a log-normal distribution to provide complementary results. Below 30 years, a probabilistic equivalence of the HST can hardly be proven, but a certain level of risk reduction can be justified.

8.4. Structural assessment

8.4.1. Sampling

Samples should be selected to be as representative of the building as possible. It is recommended to use a systematic approach to randomly and approximately equally distribute the samples to the different

available locations in the building.

The theoretical sampling size can be calculated using Equation (8.2) and Equation (8.3):

$$n = \frac{z^2 \times \hat{p}(1-\hat{p})}{\epsilon^2} \tag{8.2}$$

$$n' = \frac{n}{1 + \frac{z^2 \times \hat{p}(1-\hat{p})}{\epsilon^2 \times N}} \tag{8.3}$$

where
n is the sample size for an unlimited population
n' is the sample size for a limited population
$z = 1.645$ is the z-score for a 95% confidence interval on one side (90% if both sides are considered)
$\hat{p} = 0.50$ is the population proportion
$\epsilon = 11.8\%$ is the margin of error estimated for the SCALP-05 device
N is the population size (number of glass panes to reuse)

The values of the z-score and ϵ can be adjusted depending on the aimed confidence and precision level.

There should be at least 30 samples to provide reliable results. The practical sample size should be greater or equal to the theoretical one. It can differ for practical reasons. For example if the building is divided into three equal parts, it makes more sense to have a sampling multiple of three.

8.4.2. Pre-stress measurements

The pre-stress measurements can be avoided if the manufacturer can provide the surface pre-stress distribution for the studied glass panes type, or at least a characteristic (5%-fractile) value. A typical value (e.g. 100 MPa for FT glass) should not be assumed since large variations can occur between panes, batches and manufacturers. If the glass type (AN, HS or FT) is well known, a very conservative value can be chosen (e.g. 60 MPa for FT glass or 30 MPa for HS glass). However, this conservative assumption leads to lower calculated strength and potentially less reused panes. It should only be applied to reuse glass panes in a lower strength type (e.g. FT glass reused as HS glass) where the margin between the calculated strength and the required strength is expected to be large.

The pre-stress level can be considered isotropic an identical on both sides of the panes. The variations over the pane surface are expected to be relatively small and often below the measuring device precision level, or above the value at the central point (such as in the corners). As the variations from one pane to another can be larger, it is preferred to make a minimal number of measurements on a maximal number of panes. The central point on the pane surface is chosen since it is considered to be representative and to be the most solicited location when the pane is exposed to uniform loads.

The measurement with a SCALP-05 device or equivalent should be carried out in a relatively dark environment. This can be achieved by placing a dark cloth around the window, a large dark sheet behind the glass or closing the blinds if possible. The protocol should be repeated consistently for each sample. The measurements shall meet the criteria detailed in Subsection 6.1.2.2.

8.4.3. Weathering measurements

The flaw depth should be found using a multi-scale approach:

- **Pane overview:** the glass pane is observed globally at a distance of approximately 1.5 metres in conditions approximating to diffuse daylight and opened blinds. If some flaws or more damaged areas are already noticeable, the observer can directly focus on these flaws or restricted areas. Otherwise, it moves on to the next stage for the whole pane.
- **Close observation:** the glass is examined at a distance of approximately 30 centimetres, from left to right following 'strips' of approximately 30 centimetres high from bottom to top. The largest visible flaw on the first 'strip' is marked. Then, only flaws looking larger than the previous one(s) are marked.

At the end, only the largest flaw is selected. If the largest flaw is a spot flaw, the largest linear flaw is also selected.

- **Depth measurement:** the largest flaw depth is measured with Traceit®. It should be carried out with an ambient light in the background, and avoiding direct sunlight coming in the device.

Each measurement with Traceit® should be made twice: once with the device at 0° (vertical) and once at 90° (horizontal). The measurements must meet the criteria described in Subsection 6.1.3.4. The largest flaw depth is taken from these two measurements.

Unlike for the pre-stress measurements, a reliability study of the flaw depth measurements should be carried out. Indeed, this margin is more variable and helps having a sense of the variability for this type of measurements. A minimum of 3 flaws should be examined. For each flaw, at least 5 measurements must be done at 0° (vertical) and 90° (horizontal).

If most of the flaws (and especially the largest flaws) appear to be linear, all the calculations can be done with the shape coefficient Y = 1.12 to make the process easier and faster.

Otherwise, each flaw can be classified as either spot or linear (one in-plane dimension being at least twice the size of the other). If there is any doubts, the flaw is classified as linear.

8.4.4. Safety margins

Margins greater or equal to the values in Table 8.6 must be applied. These margins are based on a safety level of 95% for the different variables. As detailed in Subsection 7.3.3, a Monte Carlo simulation can be carried out based on the experimental results to slightly increase the accepted risk level for each variable, and to slightly reduce the margins.

Table 8.6: Quality levels depending on the largest estimated flaws from visual inspection

Margin	Value	Notes
M_{SCALP}	2.3% (min 1 MPa)	Based on the reliability study of SCALP-05
$M_{Traceit}$	30% (min 20 µm)	Based on the reliability study of Traceit®
$M_{sampling}$	-	To define depending on the sampling size and margin of error
M_v	160% (min 60 µm)	Can be improved based on the differences between visual inspection and Traceit® measurements

8.5. Qualification of the glass panes

8.5.1. Classification process

Definition of $c_{threshold}$

A quality levels classification is proposed in Table 8.7. This classification can be modified to better fit the strength of the samples later on. The calculations from this chapter can be implemented in an Excel spreadsheet, for example.

Table 8.7: Quality levels classification with associated strengths

	QL1	QL2	QL3	QL4	QL5	QL6
Characteristic strength	120 MPa	100 MPa	70 MPa	60 Mpa	45 MPa	35 MPa
Qualification	FT	FT-	HS	HS-	AN	AN-

The characteristic strength is linked to the maximum flaw depth for each class according to the following formula:

$$\sigma_f(\sigma_{r,srf}, c_{max}) = \frac{K_{IC}}{Y\sqrt{\pi c_{max}}} + \sigma_{r,srf} \times (1 - 3 \times \frac{c_{max}}{d} + \frac{3}{2} \times (\frac{c_{max}}{d})^2) \tag{8.4}$$

with
$K_{IC} = 0.75$ is the material 'constant'
$Y = 1.12$ is the shape coefficient for scratches (linear flaws)
c_{max} is the maximum flaw depth
$\sigma_{r,srf}$ is the characteristic surface pre-stress level
d is the half of the pane thickness

The thermal pre-stress level is taken at the flaw tip, with a pre-stress profile following a parabola equation.

Based on Equation (8.4) and a characteristic strength to reach the maximum flaw depth $c_{threshold}$ can be defined for each class:

Table 8.8: Quality levels with associated maximum flaw depths

	QL1	QL2	QL3	QL4	QL5	QL6
Characteristic strength	120 MPa	100 MPa	70 MPa	60 MPa	45 MPa	35 MPa
Maximum flaw depth $c_{threshold}$	-	-	-	-	-	-

Definition of c_{class} and M_V

The visual impression margin can be taken directly from Table 8.6, or verified using the following procedure.

The measured panes are observed again, preferably on a separate day, after the Traceit® measurements but before data processing. Then, the observer should be able to link the visual inspection to the measured flaw depth, without knowing the exact answers. For each glass pane, the observer looks for the largest flaw using the same protocol as described in Subsection 8.4.3. The estimated flaw depth (multiple of 10µm) is then noted. Once completed, these results should be compared with the flaw depths measured using Traceit®.

The relative error between the estimated flaw depth $c_{estimate}$ and the adjusted Traceit® measurement c is calculated as follows:

$$\epsilon_{estimate} = |\frac{c - c_{estimate}}{c_{estimate}}| \tag{8.5}$$

The minimal margins related to visual inspection are then defined as follows:

Table 8.9: Visual inspection margins M_V applied

	Minimal value
Absolute margin $M_{V,abs}$	60 µm
Relative margin $M_{V,rel}$	$\geq$160% or 95%-fractile of the $\epsilon_{estimate}$ distribution, from all flaw depths above the absolute margin value

The maximum flaw depth estimate c_{class} is then calculated as follows:

$$c_{l,class} = MIN(c_{l,threshold} - M_{V,abs}; \frac{c_{l,threshold}}{1 + M_{V,rel}}) \tag{8.6}$$

Then, each glass pane can be classified in class i if the following requirement is satisfied:

$$c_{class,i-1} \leq c_{estimate} \leq c_{class,i} \tag{8.7}$$

Finally, the visual inspection margins must be verified, and increased if necessary to fulfill the following requirement for at least 95% of the samples:

$$c + M_T \leq c_{threshold} \tag{8.8}$$

In the end, a classification of the glass pane is obtained with characteristic strengths taking into account the different safety margins involved.

8.5.2. Global qualification process

For all the remaining glass panes to be evaluated, the maximum flaw depth per pane is estimated according to the classification previously described. This process should be carried out relatively quickly (less than one minute per pane) by the same observer as the one who did the flaw depth measurements. Based on this experience of observing at least 30 flaws at the naked eye and measuring their depth with Traceit®, the observer should be able to qualify the glass panes within the defined margins and safety levels.

The estimated depths can then be added to the Excel spreadsheet for example, where they can be automatically classified.

8.6. Verification protocol with destructive tests

These destructive tests were not carried out during the MSc thesis, but the approach is defined. As tempered glass cannot be cut, Coaxial Double Ring (CDR) tests cannot be conducted on these samples. The whole pane should then be tested, at least on 10 of the weakest samples. The glass panes are supported on all edges and loaded in bending with point loads until breakage. Examples of this type of test can be found in studies by Dalgliesh & Taylor (1990) or with more recent research from Ghent University, as shown in Figure 8.3.

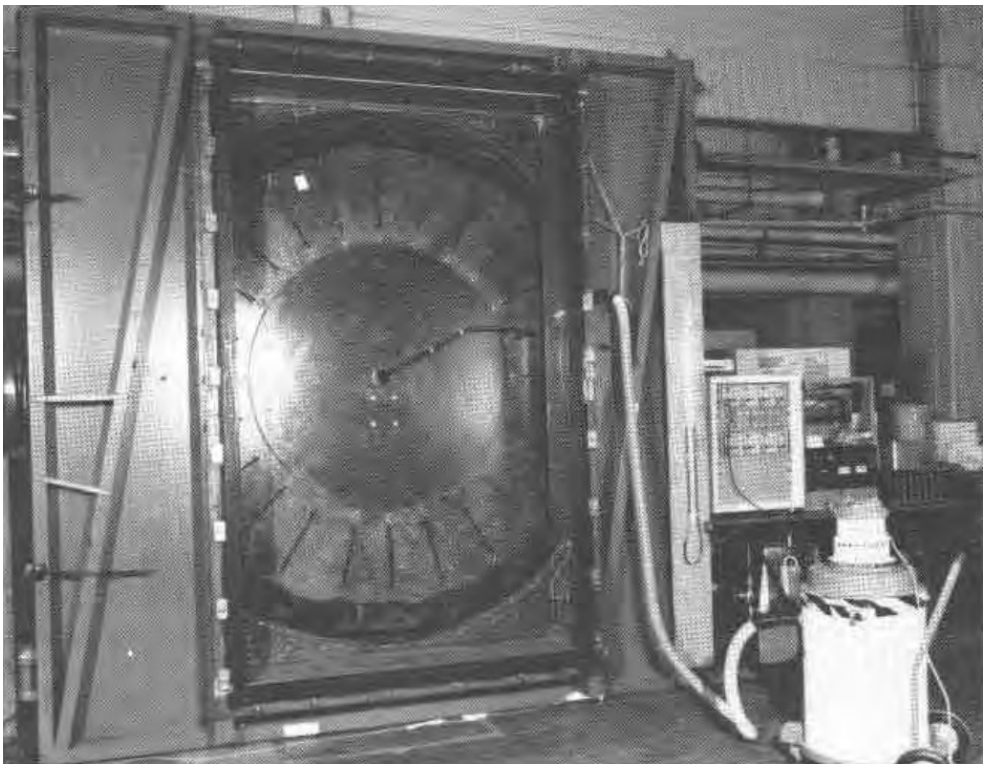

Figure 8.2: Dynamic glass testing rig (Dalgliesh & Taylor, 1990)

Figure 8.3: Example of a destructive test from Ghent University)

According to Annex B of NEN-EN 16612, the maximum tensile bending stress is:

$$\sigma_{max} = k_1 \frac{a^2}{h^2} F_d \tag{8.9}$$

with
k_1 the calculation coefficient defined in Table B.1 from NEN-EN 16612
a the shorter dimension of the pane
h the pane thickness F_d applied force

The coefficient k_1 depends on the non-dimensional load p^*:

$$p^* = (\frac{A}{4h^2})^2 \frac{F_d}{E} \tag{8.10}$$

with
A the pane surface area
h the pane thickness
F_d the applied force
E = 70 000 MPa the Young's modulus for glass

The coefficient k_1 is then defined as follows:

$\lambda = a/b$	p^*										
	0	**1**	**2**	**3**	**5**	**10**	**20**	**50**	**100**	**200**	**300**
1,0	0,268	0,261	0,244	0,223	0,190	0,152	0,135	0,130	0,129	0,128	0,128
0,9	0,319	0,309	0,286	0,260	0,218	0,172	0,152	0,145	0,144	0,144	0,144
0,8	0,380	0,369	0,341	0,309	0,257	0,199	0,173	0,164	0,162	0,162	0,162
0,7	0,449	0,437	0,408	0,372	0,311	0,236	0,199	0,186	0,184	0,184	0,184
0,6	0,524	0,515	0,490	0,457	0,391	0,294	0,238	0,215	0,212	0,211	0,211
0,5	0,600	0,595	0,580	0,559	0,506	0,395	0,302	0,255	0,247	0,245	0,245
0,4	0,671	0,669	0,664	0,655	0,631	0,551	0,429	0,322	0,297	0,290	0,289
0,3	0,724	0,723	0,722	0,721	0,716	0,694	0,629	0,471	0,388	0,356	0,349
0,2	0,747	0,747	0,747	0,747	0,747	0,745	0,738	0,699	0,613	0,502	0,457
0,1	0,750	0,750	0,750	0,750	0,750	0,750	0,750	0,749	0,748	0,740	0,729

For the purposes of calculation:

$$k_1 = \frac{1}{4\left[\frac{1}{z_2^2} + \frac{p^{*2}}{\left(z_3^2 + (z_4 p^*)^2\right)}\right]^{0.5}}$$

where $$z_2 = 24\left[0{,}044\,7 + 0{,}080\,3\left(1 - e^{\left(-1{,}17\left(\frac{1}{\lambda}-1\right)^{1{,}073}\right)}\right)\right]$$

$$z_3 = \frac{1}{\lambda}\left(4{,}5\left(\frac{1}{\lambda}-1\right)^2 + 4{,}5\right)$$

$$z_4 = \frac{1}{\lambda}\left(0{,}585 - 0{,}05\left(\frac{1}{\lambda}-1\right)\right)$$

Figure 8.4: Table B.1 from NEN-EN 16612 defining coefficient k_1

Non-negligible differences between the different panels are expected. However, the average results should be consistent between theory and experiment.

If the characteristic strength (P_f = 0.05) is higher than the requirement, the glass panels are verified.

8.7. Discussion

This protocol should be applied with a consistent approach, especially during the measurements. The results of the pre-stress and weathering measurements are always subject to a degree of uncertainty, and will be more reliable if the experiments are carried out in a consistent and systematic way.

Some aspects of the methodology have been simplified in this chapter to make the protocol easier and quicker to use. If the glass is aimed to be reused in the same type as it was originally designed (for example fully toughened glass to reuse as fully toughened glass only), or if there are unfavourable conditions (such as relatively low pre-stress level, annealed glass or large flaws), the methodology can be adapted to optimise the margins and facilitate the results. The following modifications may be considered:

- Increase sampling size
- Distinguish spot and linear flaws with Y = 0.713 or Y = 1.12 for spot and linear shapes respectively. The largest flaw depth can be a spot flaw only if there is no linear flaw of similar size. If there is any doubt, both flaw types should be noted and analyzed later on.
- Change the devices used or spend more time during measurements to reduce M_T, M_{SCALP} and M_V.

The intermediate strength levels are not applicable with the existing regulations. However, they would facilitate and increase the reuse potential of glass if it were implemented in the future. In addition, customised quality levels with a minimum strength corresponding precisely to the design requirements would be optimal.

9

Discussions

9.1. Impact of reusing glass

The first step of this methodology with a comparative LCA aims to provide a more accurate answer to the question: is it worth it?

Reusing glass is not yet a common practice, and this methodology, even in its simplified form, requires additional time and funding compared to sending the glass panes to the landfill and buying new ones. In this case study, 2464 glass panes with a total weight of 207 tonnes are considered for reuse. The project has a relatively large scale, and the absolute gain of CO_2 equivalent reaches 326 tonnes. By comparison, the average European citizen emits about 5.5 tons of CO2 equivalent per year (World Bank, 2023), although there are important variations between countries and debates about the exact figures. The 326 tonnes of CO_2 equivalent are about 59 times greater.

When compared relative to the façade, the estimated reuse gains reach 30%. If it were compared to the CO_2 emissions of the whole building, this ratio would obviously be even lower.

As discussed in Section 4.4, the benefits of reuse are also slightly reduced when considering mixed scenarios where 100% of the glass is not always reused, recycled or down-cycled.

This study takes into account a 0% rate of inputs of secondary material to be compatible with the avoided burden approach, and the contribution of toughening for fully toughened glass. However, it does not take into account the difference between reuse scenarios as fully toughened, heat-strengthened or annealed glass. These differences could be updated depending on the final reuse scenario to provide a more accurate GWP estimate, but are small enough to be simplified in this study.

Although there is no single answer to the minimum absolute and relative GWP gains to consider reusing glass, some considerations can be made. Firstly, the building with glass to be reused should be of relatively large scale, such as a small tower. Secondly, the building should have the majority of its façades composed with glass. Otherwise, the absolute or relative GWP for reusing glass may be too small, and it would be more relevant to focus the efforts elsewhere by reusing the main structure or optimising the new design for example.

9.2. Case study optimization

The results for this case study showed that all of the glass panes could be reused as heat-strengthened or annealed glass, and that the remaining glass panes are expected to have similar results. However, the glass panes surface condition, pre-stress level and various safety margins do not allow to demonstrate a strength level of fully toughened glass.

A question that arises is whether it is still possible to reuse it as fully toughened glass, for example by improving the methodology or the equipment used. Even with more time in a laboratory setting, this would be difficult to predict. The variations between different samples and between theoretical and experimental results are still expected to be high.

However, one can get an approximate idea of the 'real' strength distribution for the measured glass panes in Section 7.3. When removing all the margins to only combine the largest flaw depth, shape coefficient and pre-stress level measured on each of the 70 glass panes individually, the predicted distribution ranges from 105 MPa to 193 MPa. A majority of the glass panes could be above the 120 MPa threshold, but this cannot be demonstrated safely and some glass panes would still be below this threshold.

Another question is to what extent this methodology could be simplified in order to reuse the glass panes as heat-strengthened or annealed glass. The first thing that would make the methodology faster and simpler would be to consider all flaws to be linear. The shape coefficient Y would be equal to 1.12 everywhere and the absolute margin for visual inspection would be 60 µm. The impact on the final classification is shown in Table 9.1. For this case study of these 70 glass panes, the difference is not even visible if the panes are to be reused as heat-strengthened glass (QL3). However, if the important class were QL2 the reuse potential would be affected. Therefore, differentiating between spot and linear flaws is only useful if the chosen design strength is expected to be difficult to achieve, or if most of the largest flaws are of the spot type.

Table 9.1: Compared classifications obtained when differentiating spot and linear flaws or not

	QL1	QL2	QL3	QL4	QL5	QL6
Characteristic strength	120 MPa	100 MPa	70 MPa	60 MPa	45 MPa	35 MPa
Classification when differentiating spot and linear flaws	0	53	17	0	0	0
Classification when considering all flaws to be linear	0	47	23	0	0	0

The sampling could also have been reduced to 50 glass panes for example. Reducing more than that would cause $M_{sampling}$ to increase too quickly compared to the small gain of time, as shown in Figure 7.12. Sampling should not be reduced below 30 glass panes in order to obtain a representative sample and reliable statistical distributions.

In the scenario where the panes are reused as annealed glass, the methodology and the visual inspection could be carried out even faster, with larger safety margins. Only glass panes with very large flaws would not qualify for this requirement.

9.3. Importance of the pre-stress level

The pre-stress measurements could be avoided if the pre-stress level could be obtained from the manufacturer for example. However, this seems to be difficult to find in Europe for two reasons.

Firstly, the Eurocodes do not specify a minimum pre-stress level for heat-strengthened and fully toughened glass, but only on the final mechanical strength. This value is not limited and is not closely monitored, as long as the glass is strong enough in the end. Other regulations such as in the USA require a surface pre-stress level between 24 and 52 MPa for heat-strengthened glass, and over 69 MPa for fully toughened glass (ASTM C1048, 2012), but do not apply in Europe.

Secondly, the tempering process is not so easy to control precisely, and there can be relatively large variation even within the same batch from the same manufacturer. This has been observed in previous research grouped by Haldimann (2008) and in the experimental measurements of this study.

One should therefore be very careful when assuming a characteristic pre-stress level. Only very conservative assumptions could be made, such as approximately 50 MPa for fully toughened glass or 25 MPa for heat-strengthened glass. As these values are much lower than what could potentially be measured, they will significantly affect the final classification and reuse potential of the glass panes. These assumptions are only useful when the difference between the actual glass strength and the requirements is expected to be large, allowing the methodology to be simplified.

9.4. The case of annealed glass

While annealed glass is usually considered to have no residual surface stress, a small residual surface compression of the order of 5 MPa has been reported in previous research (Achintha, 2021 ; Aben et al.,

2010). Although this value seems small, its contribution can make a difference to reach the 45 MPa design requirement and increase the reuse potential of annealed glass.

Previously, it was shown that if the 70 glass panes had the same flaw depths and safety margins with a characteristic residual stress level of 5.6 MPa, 30 panes would qualify for reuse as annealed glass (QL5), 36 panes would have a reduced strength of 35 MPa (QL6) and 4 panes would not qualify for reuse. The margins optimization using a Monte Carlo simulation was not performed in this case.

In comparison, if the pre-stress contribution is set to 0 only 8 panes would qualify for reuse as annealed glass (QL5), 46 panes would have a reduced strength of 35 MPa (QL6) and 16 panes would not qualify for reuse.

Table 9.2: Compared classifications obtained for typical annealed glass with and without the residual stress contribution

	QL1	QL2	QL3	QL4	QL5	QL6
Characteristic strength	120 MPa	100 MPa	70 MPa	60 MPa	45 MPa	35 MPa
Classification with residual stress contribution	0	0	0	0	30	36
Classification without residual stress contribution	0	0	0	0	8	46

In this specific example, the reuse rate as annealed glass drops from 43% to 11%. This is an example of how a small contribution can have a large impact on the reuse potential. However, these differences could be less visible in other studies with smaller flaw depths or margins, or if an intermediate class is also accepted.

Annealed glass differs from heat-strengthened and fully toughened glass mainly by the fact that there is (almost) no residual surface compression. Not only does this allow larger flaw depth when subjected to an equivalent impact, but it also exposes the glass to stress corrosion without any healing phenomenon. Under certain loading conditions, existing flaws are more likely to continue to grow slowly over time. From a design perspective, this may only increase the measured flaw depth while the 45 MPa requirement remains the same.

An advantage of annealed glass for reuse is that there is no risk of spontaneous breakage due to NiS inclusion. There have been no reports of this type of breakage in annealed glass so far.

In conclusion, the reuse of annealed glass appears to more difficult to obtain than that of heat-strengthened and fully toughened glass, but it is still possible. Unless the glass is of excellent quality (estimated flaw depths $\leq$10 µm for scratches and $\leq$60 µm for digs), not taking into account the residual stress level makes it rather difficult to reuse the glass panes as QL5 with a good confidence level, but rather as QL6 or another customised class. If this residual stress level is taken into account, it becomes easier to reuse annealed glass as QL5 if it has a relatively good surface quality (estimated flaw depth $\leq$20 µm for scratches and $\leq$80 µm for digs). Allowing a lower strength, such as the 35 MPa of QL6 or from another bespoke class, could significantly increase the reuse potential of annealed glass, while still meeting design and safety requirements.

9.5. Possibility of a lower bound strength

The weathering measurements show consistent values when compared to other research. The range [4 µm ; 147 µm] of largest flaw depth is very similar to the one from Sofokleous (2022) of [19 µm ; 161 µm] measured on annealed glass samples exposed to weathering outside during 50 years as well. For approximately the same exposition duration, both samples seem to have similar ranges despite being exposed to different phenomena (interior vs exterior 'weathering').

Another research trying to find an equivalent weathering to 20 years of use with sand-abrasion (Datsiou & Overend, K. C. Datsiou & Overend 2017 also had a similar but slightly higher range of [72 µm ; 218 µm] for fully toughened glass, but a much higher one of [132 µm ; 1370 µm] for annealed glass. However, these values should be taken more carefully as the weathering was artificially done with sand-abrasion.

The possibility of a lower bound strength for aged glass was already mentioned in previous research (Ballarini, Pisano & Royer-Carfagni, 2016). It is possible that after a few years, the glass pane cannot get

much more damaged as flaw depths caused by an impact cannot become much larger without breaking the glass. This also rely on the assumption that the flaws do not overlap, which seems quite unlikely especially when the panes are inside the building. Based on the localisation (inside/outside), a conservative lower bound strength could be then investigated.

9.6. Intermediate strength levels and material factors

From a design perspective, another way to significantly increase the reuse potential of glass would be to tolerate 'reduced strength levels' or 'intermediate strength levels', such as the ones defined by QL2, QL4 and QL6. This, of course, has not been implemented in the existing regulations to date.

There are at least two arguments in favour of accepting these intermediate levels.

Firstly, the design strength for new glass panes does not necessarily have to be 120 MPa, 70 MPa or 45 MPa. A fully toughened glass proven to break into small pieces with an equivalent safety level as with a Heat-Soak Test and with a characteristic strength of 100 MPa may be safe enough in several design cases. An annealed glass window of small dimensions exposed to limited loads could also be safe enough with a characteristic strength of 35 MPa.

Secondly, the glass strength should not decrease linearly with time. As shown in Figure 2.15, the glass strength decreases more and more slowly as the flaw depth increases. In addition, other research suggests that weathering may reach an asymptote after some time, with a lower bound glass strength (Ballarini, Pisano & Royer-Carfagni, 2016). Although post-consumer glass may have a lower strength than new glass, it may be more stable over time, justifying a slightly lower strength requirement. This could allow reducing the material factor for aged glass. Previous research suggested a material factor $\gamma_{m;A}$ of 1.3-1.4 could be suitable for post-consumer glass (Stuurstraat, 2023), but this hypothesis still needs to be further investigated.

Due to their pre-stress, heat-strengthened and fully toughened glass are more suitable for these intermediate strength levels. Indeed, the surface residual compression protects the glass from stress corrosion most of the time, and may even induce 'healing' of some flaws. These phenomena still need to be further understood and demonstrated, but could significantly improve the reuse potential of glass.

A typical design strength for the case study can be calculated based on Equation (2.15), Equation (2.16) and Equation (2.17). The chosen coefficients between the French and Dutch norms have the same value in this case:

- λ_A = 1 for the surface effect
- λ_l = 1 for the dimension effect
- k_e = 1 for annealed and pre-stressed glass with polished joints
- k_{sp} = 1 for the surface quality
- k_{mod} = 1 for a short-term load duration
- $k_{e,p}$ = 1 for a load at the center
- $f_{g,k}$ = 45 N/mm² for the characteristic strength of annealed glass
- $f_{b,k}$ = 70 N/mm² for the characteristic strength of heat-strengthened glass and 120 N/mm² for fully toughened glass
- γ_M = 1.8 for the glass material factor classified in CC2
- γ_p = 1.2 for the glass pre-stress factor classified in CC2

As shown in Table 9.3, glass from intermediate classes designed with a reduced material factor γ_M (also called $\gamma_{m;A}$ in the Dutch norms) of 1.4 could have a design strength very close to new glass designed with a material factor γ_M of 1.8 in this case. For example, the design strength of tempered glass classified in QL2 would reach 79.17 MPa (vs 85 MPa for FT glass), the one from QL4 would reach 45.83 MPa (vs 43.33 MPa for HS glass) and the one from QL6 would reach 25 MPa (same as with AN glass).

Table 9.3: Design strength of intermediate classes QL2, QL4 and QL6 with reduced material factors, compared to design strength of AN, HS and FT glass

Glass type	FT	QL2	HS	QL4	AN	QL6
Characteristic strength (with pre-stress) $f_{b,k}$	120 MPa	100 MPa	70 MPa	60 MPa	-	-
Characteristic strength (without pre-stress) $f_{g,k}$	45 MPa	35 MPa	45 MPa	35 MPa	45 MPa	35 MPa
Glass material factor γ_M	1.8	1.4	1.8	1.4	1.8	1.4
Glass pre-stress factor γ_p	1.2	1.2	1.2	1.2	1.2	1.2
Design strength $f_{g,d}$	85 MPa	79.17 MPa	43.33 MPa	45.83 MPa	25 MPa	25 MPa

Therefore, not only could these intermediate strength levels be accepted, but they could even result in a design strength very similar to that of new glass.

10

Conclusions

10.1. Conclusions

The main research question of this MSc thesis is:
How can we assess the reuse potential of tempered glass in practice?

A new methodology to assess the reuse potential of post-consumer tempered glass on-site was developed in this study. This methodology was applied on a case study with about 2500 fully toughened glass panes to potentially reuse from a historical building in Paris built over 50 years ago.

As a first step, a comparative environmental impact assessment was defined. Through a simplified Life-Cycle Assessment, this step provides an idea of the environmental benefits of reuse compared to recycling and down-cycling, helping to understand if reusing glass is relevant. Reuse becomes much more relevant for relatively large scale buildings with a relatively high window-to-wall ratio.

A probabilistic equivalence of the Heat-Soak Test was discussed. Although available data is scarce, a reduced risk and an equivalent safety level to the HST can be justified for glass without HST after 50 years.

Finally, the methodology combines on-site measurements of the pre-stress level and flaw depths to estimate the glass strength. After calibrating the margins and visual inspection procedure, the reuse potential of the glass panes can be defined quickly without the need of special equipment on-site. Once trained, the observer should be able to qualify several glass panes relatively quickly with a characteristic strength (95% confidence level) defined with appropriate margins.

While the glass panes from the case study show a good potential for reuse as heat-strengthened glass, this methodology could be generalised to other projects. The influence of the residual pre-stress level was emphasised. Simulations of this methodology applied to typical annealed, heat-strengthened and fully toughened glass also show a great potential. These three types of glass could be reused with the same characteristic strength if their surface quality estimated by visual inspection has flaw depths smaller than approximately 20-40 µm. Qualification for reuse of these three types of glass with a reduced strength is also proposed. This could allow reusing glass panes with flaw depths of up to 500 µm for several design scenarios.

The sub-questions are:

How can we get a first estimate of the benefits of reusing glass compared to recycling and down-cycling?

To answer this question, three End-of-Life scenarios can be compared: reuse, recycling and down-cycling of the glass panes. It focuses only on the most relevant modules of the Life-Cycle Assessment. Three indicators are chosen: components for reuse (kg), materials for recycling (kg) and Global Warming Potential (kg CO_2 eq.). The study is then twofold.

Firstly, the benefits of reuse compared to recycling and down-cycling can be compared in relation to the studied glass panes only. The avoided burden approach is chosen to quantify the GWP differences in

Module D. At the end, a defined estimate of reused components, recycled materials and GWP gains is given.

Secondly, these values are compared in relation to the façade system. The focus can be on a typical module and then scaled to the whole façade system. Both parts of this assessment provide complementary insights into the impact of glass reuse.

How can the risk of spontaneous breakage due to NiS inclusion in aged glass be compared to that of new glass with HST?

The risk of spontaneous breakage due to NiS inclusion in aged glass can be estimated by fitting a log-normal distribution to the data sets of cumulative failures due to NiS inclusions over time. The scarcity of such data make this assessment a rational argumentation rather than a mathematical demonstration. However, it would be justified to consider glass without HST to have a similar risk reduction after 30 years to new glass with HST, and to have a very close (if not better) safety level after 50 years. In addition, as the risk reduction peaks in the first few years after installation and as the relevance of HST is sometimes questioned in relation to its cost, glass without HST could be considered to have a higher but reasonable enough risk after 30 years to qualify for reuse.

How can the strength of tempered glass be measured on-site?

A representative sample of appropriate size can be theoretically defined and applied by a systematic selection of glass panes. The strength can be estimated based on LEFM with two main variables: the surface pre-stress level $\sigma_{r,srf}$ and the flaw depth c.

The pre-stress level can be measured using the optical polariscope SCALP-05 or equivalent. It can be considered relatively homogeneous, isotropic and symmetrical on both sides of the glass. Relatively large variations can occur between glass panes, even if they are from the same batch and manufacturer. Therefore, a minimum number of mesurement points on a maximum number of different glass panes is recommended. The central point on the glass surface is the most relevant to obtain a representative value at the point of highest tensile stress under uniform loading.

The largest flaw depth can be estimated with a multi-scale approach to find the largest visible flaw and measure its depth using the optical profilometer Traceit® or equivalent. Although it is not realistic to find the exact critical flaw, it is possible to have a reasonable estimate of its size.

In the case study, the fully toughened glass pane had a relatively low (but still consistent) average surface pre-stress of 81.41 MPa. The standard deviation of 4.17 MPa is aligned with other values reported in the literature. The largest flaw depths ranged from 4 µm to 147 µm, also in agreement with other publications. The majority of these flaws were linear rather than punctual and were located on the lower half of the inner side of the panes, where they are most exposed during the life of the building.

What is the reuse potential for the aged glass of this case study, based on LEFM with appropriate margins?

When applied to the case study, the reuse in situ of the 2464 glass panes corresponds to 207 tonnes of glass and 326 tonnes of CO_2 eq. compared to a landfill scenario. Relative to the whole façade system, this is estimated to reach 29% of the mass and 30% of kg CO_2 eq. reduction. When considering mixed scenarios where only 95% of the glass panes are reused, these values are slightly reduced by 5%.

An equivalent safety level to the HST can be justified. Based on existing data of spontaneous breakage due to NiS inclusion over time, even conservative assumptions lead to a risk reduced by 98.5% after 50 years.

To comply with existing regulations, a characteristic strength must be estimated for each pane with a confidence level greater than or equal to 95%. In order to extend the strength estimation to the other glass panes in a more efficient and scalable way, a visual inspection procedure and appropriate margins have been defined.

The visual inspection must follow a defined procedure to quantify the difference between the estimated flaw depths made by a trained observer and the Traceit® measurements. A visual inspection margin is then calibrated together with the sampling margin and measurements margins from SCALP-05 and Traceit®. The glass panes are then classified following different 'Quality Levels' associated with a characteristic strength. The combination of these margins provides a classification verified on-site and scalable to the other glass panes.

The glass panes tested in this case study all qualify for reuse as heat-strengthened glass with a safety level greater than 95%, and these results could be extended to the other glass panes with a high confidence level. The characteristic pre-stress level and the surface quality with the margins do not allow reuse as fully toughened glass, but a characteristic pre-stress level of 100 MPa (more common for this type of glass) would allow reuse as fully toughened glass much more easily with the same methodology and margins. The design options considered heat-strengthened and annealed glass for the reused parts. Both of these options are possible following this methodology with a high confidence level.

How could this methodology be generalized?

This methodology can be summarised and eventually simplified to be applied in other projects for annealed, heat-strengthened and fully toughened glass. The comparative environmental impact assessment and the probabilistic equivalence of the Heat-Soak Test can be applied in a similar way. Guidelines for sampling, measurement protocols and minimum margins are provided. The pre-stress level can only be measured at the centre of the pane in order to measure as many different panes as possible within a defined time frame. Flaw depths should be measured at least twice with a 90° in-plane rotation to improve the reliability of the results. A classification with characteristic strengths corresponding to the Eurocodes requirements is given, together with equations for combining the measurements and safety margins.

Even for the same type of glass, variations in the level of pre-stressing can have a significant effect on the reuse potential of the panes. For example, a difference of 20 MPa in the characteristic pre-stress level of fully toughened glass can shift the final classification from mostly reusable as fully toughened glass to mostly reusable as heat-strengthened glass, with the same flaw depths and safety margins. This value should then be carefully assessed.

Although all three main types of glass (AN, HS and FT) are compatible with this methodology, annealed glass is expected to tolerate slightly smaller flaw depths than heat-strengthened or fully toughened glass. The absence of any significant pre-stress and the minimum margins make it somewhat more difficult to qualify annealed glass with a characteristic strength of 45 MPa. This stays however possible. Taking into account the residual surface pre-stress of approximately 5 MPa can significantly help in reaching the 45 MPa threshold, and should be considered in the methodology.

Intermediate strength levels are also considered. Although they are not yet implemented in the current regulations, these intermediate strength levels could greatly increase the potential for reuse of glass, while maintaining a sufficient safety level and even a similar design strength to that of new glass by justifying reduced material factors.

10.2. Recommendations

- **Improvements of the methodology precision:**

  The precision of the classification could be further improved. In contrast to SCALP-05, the Traceit® device is still rarely used with glass materials. Ways to improve the measurement procedure and the precision of the device could be further explored. Other measurement devices could be tried for pre-stress and flaw depth. Other parameters such as the shape coefficient Y and the material 'constant' K_{IC} are still the subject of theoretical and experimental research in order to define them more precisely.

- **Better understanding of the non-linear combination of the margins:**

  The non-linear combination of the margins between $\sigma_{r,srf}$ and c were evaluated with a Monte Carlo simulation. However, it was observed that this combination was not linear and could vary depending

on the statistical distributions of $\sigma_{r,srf}$ and c. While the case study allowed an uncertainty level of 10% for both variables separately, this value can be reduced to only 6% in the worst case. A more detailed study and a better understanding of the combination of these margins could be beneficial.

- **Visual inspection with different observers:**

  The visual inspection was carried out by a single observer in this study. The visual inspection safety margins directly depend on the observer's ability to estimate the glass surface quality. After an appropriate training, the observer should reach at least a certain level of accuracy with the associated margins detailed in Chapter 7. However, this methodology could be double-checked by a second observer, and if possible by a larger group of observers. This would allow to confirm the visual inspection safety margins, and potentially reduce it.

- **Simplifications of the methodology:**

  The pre-stress and flaw depth measurement procedure simplification could be investigated. The pre-stress measurements protocol could be improved. Indeed, positioning a dark curtain around the measurement location can become time-consuming if repeated several times. A faster protocol with dark plates that can be instantly positioned and removed (with succion cups for example) to replace the dark curtain could be explored. The pre-stress measurements could also be replaced by information from the manufacturer or conservative assumptions in cases where larger margins are tolerated. When the margins between actual glass strength and design requirements are very large (for example fully toughened glass reused as annealed glass), the approach could be even further simplified.

- **Evaluate the methodology with destructive testing:**

  The classified glass panes were not subjected to destructive testing. A study in which the failure stress of the classified glass panes is also tested experimentally would be useful to confirm the results. Even more than with other glass failure stress experiments, high variations between theoretical and experimental results can be expected for a single pane. However, this classification does not aim at predicting the exact failure stress, but rather to provide a characteristic strength with a confidence level greater than or equal to 95%.

- **Extend to other types of glass:**

  Other types of glass such as laminated glass were not considered in this study. The strength assessment of such a glass also depends on the quality of the interlayer and how it evolved over time. If the glass has any coatings or other treatments, additional parameters would need to be evaluated. It could potentially affect the measurement possibilities with the equipment chosen in this study, and lead to different choices for the measurement procedure.

- **Combine with float line scanners:**

  This methodology or part of it could be complementary to an analysis with optical scanners from float glass production lines tried in other studies (Rota, Zaccaria & Fiorito, 2023), and form a two-stage evaluation process. Some relationships could be explored between the 'Quality Levels' from the visual inspection based on flaw depth and the 'Quality Levels' from the optical quality of the glass based on the length and number of flaws.

References

Aben, H. et al. (2010). On non-destructive residual stress measurement in glass panels. *Estonian Journal of Engineering* 16 (2). 10.3176/eng.2010.2.04.

Achintha, M. (2021). A validated modelling technique for incorporating residual stresses in glass structural design. *Structures* 29, 446–457. 10.1016/j.istruc.2020.11.052.

ASTM-C1048-12 (2012). Standard specification for heat-strengthened and fully tempered flat glass.

Baker-Brown, D. (2021). The environmental impact of reuse in the construction sector: FutuREuse.

Ballarini, R., Pisano, G., & Royer-Carfagni, G. (2016). The Lower Bound for Glass Strength and Its Interpretation with Generalized Weibull Statistics for Structural Applications. *Journal of Engineering Mechanics* 142 (12). 10.1061/(ASCE)EM.1943-7889.0001151.

Belis, J., Louter, C., Nielsen, J. H., & Schneider, J. (2019). Architectural Glass. 10.1007/978-3-319-93728-1_52.

Bonati, A., Pisano, G., & Carfagni, G. R. (2019). A statistical model for the failure of glass plates due to nickel sulfide inclusions. *Journal of the American Ceramic Society* 102 (5). 10.1111/jace.16106.

Bos, F. P. (2009). Safety Concepts in Structural Glass Engineering - Towards an Integrated Approach.

Carmona, N., Kowal, A., Rincon, J. M., & Villegas, M. A. (2010). AFM assessment of the surface nano/microstructure on chemically damaged historical and model glasses. *Materials Chemistry and Physics* 119 (1-2). 10.1016/j.matchemphys.2009.08.052.

FD-CEN/TS-19100-1 (2022). Conception et calcul des structures en verre.

Dalgliesh, W. A. & Taylor, D. A. (1990). The strength and testing of window glass. *Canadian Journal of Civil Engineering* 17 (5), 752–762. 10.1139/l90-088.

Datsiou, K. & Overend, M. (2016). Evaluation of artificial ageing methods for glass. https://doi.org/10.7480/cgc.5.2431.

Datsiou, K. C. & Overend, M. (2017). The strength of aged glass. *Glass Structures and Engineering* 2 (2). 10.1007/s40940-017-0045-6.

DeBrincat, G. & Babic, E. (2019). Rethinking the life cycle of architectural glass. *Glass International* 42 (2).

EN12150-1+A1 (2019). Glass in building - Thermally toughened soda lime silicate safety glass - Part 1: Definition and description.

EN15804:2012+A2 (2019). Sustainability of construction works - environmental product declaration - core rules for the product category of construction product.

EN15978 (2011). Sustainability assessment of construction works – assessment of environmental performance of buildings – calculation method.

EN1863-1 (2011). Glass in building - Heat strengthened soda lime silicate glass - Part 1: Definition and description.

EN572-1+A1 (2016). Glass in building - Basic soda lime silicate glass products. Part 1: Definitions and general physical and mechanical properties.

EN572-8+A1 (2016). Glass in building - Basic soda lime silicate glass products. Part 8: Supplied and final cut sizes.

European-Commission (2024). Waste. Construction and demolition waste.

Gelowitz, M. & McArthur, J. (2016). Investigating the Effect of Environmental Product Declaration Adoption in LEED® on the Construction Industry: A Case Study. *Procedia Engineering* 145, 58–65. 10.1016/j.proeng.2016.04.014.

GlasStress-Ltd (2013). Scattered Light Polariscope SCALP Instruction manual.

Griffith, A. A. (1921). VI. The phenomena of rupture and flow in solids. *Philosophical Transactions of the Royal Society A* 221.

Haldimann, M., Luible, A., & Overend, M. (2008). Structural use of Glass. 10.2749/sed010.

Hammond, G. & Jones, C. (2011). Embodied Carbon: The Inventory of Carbon and Energy (ICE).

Hartwell, R., Coult, G., & Overend, M. (2023). Mapping the flat glass value-chain: a material flow analysis and energy balance of UK production. *Glass Structures & Engineering* 8 (2), 167–192. 10.1007/s40940-022-00195-9.

Hartwell, R. & Overend, M. (2019). Unlocking the re-use potential of glass Façade systems, 273–280.

Iglesias, A., Muniz-Calvente, M., Fernández-Canteli, A., Llavori, I., Martinez-Agirre, M., & Esnaola, J. A. (2022). Numerical-probabilistic assessment of tempered glass failure based on the generalised local model characterised by annealed plates. *Engineering Fracture Mechanics* 274. 10.1016/j.engfracmech.2022.108754.

Ingwersen, W. W. & Subramanian, V. (2014). Guidance for product category rule development: Process, outcome, and next steps. *International Journal of Life Cycle Assessment* 19 (3). 10.1007/s11367-013-0659-0.

Innowep-GmbH (2024). TRACEiT®.

ISO14040 (2006). Environmental Management – Life Cycle Assessment – Principles and Framework.

ISO14044 (2006). Environmental management - Life cycle assessment - Requirements and guidelines.

ISO4287 (2000). Geometrical product specification (GPS). Surface texture. Profile method. Terms, definitions and surface texture parameters.

Jacob, L. (2001). A Review of the Nickel Sulphide Induced Fracture in Tempered Glass.

Jacob, L. & Calderone, I. (2003). Nickel Sulphide Inclusions - Important Issues for the Designer. *Glass Processing Days*.

Karlsson, S. (2017). Spontaneous fracture in thermally strengthened glass - A review & outlook. *Ceramics - Silikaty* 61 (3). 10.13168/cs.2017.0016.

Kasper, A., Colvin, J., Rubbert, F., & Serruys, F. (2023). NiS in HS glass.

Kasper, A. (2019). Spontaneous cracking of thermally toughened safety glass part three: statistic evaluation of field breakage records and consequences for residual breakage probability. *Glass Structures and Engineering* 4 (3). 10.1007/s40940-018-00093-z.

Lasvaux, S., Leroy, Y., Briquet, C., & Chevalier, J. (2013). International Survey on Critical Review and Verification Practices in LCA with a Focus in the Construction Sector.

Lawn, B. (1993). Fracture of Brittle Solids. Cambridge University Press. 10.1017/CBO9780511623127.

Lindqvist, M. (2013). Structural glass strength prediction based on edge flaw characterization.

Matthews, H., Hendrickson, C., & Matthews, D. (2014). Life Cycle Assessment: Quantitative Approaches for Decisions that Matter. Vol. 13.

Modahl, I. S., Askham, C., Lyng, K. A., Skjerve-Nielssen, C., & Nereng, G. (2013). Comparison of two versions of an EPD, using generic and specific data for the foreground system, and some methodological implications. *International Journal of Life Cycle Assessment* 18 (1). 10.1007/s11367-012-0449-0.

Müller, H., Strubel, C., & Bange, K. (2001). Characterization and identification of local defects in glass. *Scanning* 23 (1). 10.1002/sca.4950230103.

NEN2608 (2014). Glass in building - requirements and determination method.

O'Regan, C. (2014). Structural use of glass in buildings. Second edn. London: Institution of Structural Engineers.

Orowan, E. (1934). Proc. Int. Conf. on Phys. *The Physical Society, London* 2 (81).

Overend, M. & Zammit, K. (2012). A computer algorithm for determining the tensile strength of float glass. *Engineering Structures* 45. 10.1016/j.engstruct.2012.05.039.

Papadopoulos, N. & Drosou, C. A. (2012). Influence of weather conditions on glass properties. *Journal of the University of Chemical Technology and Metallurgy* 47 (4).

Quéheille, E., Ventura, A., Saiyouri, N., & Taillandier, F. (2022). A Life Cycle Assessment model of End-of-life scenarios for building deconstruction and waste management. *Journal of Cleaner Production* 339. 10.1016/j.jclepro.2022.130694.

Quinn, G. D. (2020). NIST Recommended Practice Guide: Fractography of Ceramics and Glasses. 10.6028/NIST.SP.960-16e3.

Quinn, G. D. & Morrell, R. (1991). Design Data for Engineering Ceramics: A Review of the Flexure Test. *Journal of the American Ceramic Society* 74 (9), 2037–2066. 10.1111/j.1151-2916.1991.tb08259.x.

Ramesh, K. & Ramakrishnan, V. (2016). Digital photoelasticity of glass: A comprehensive review. *Optics and Lasers in Engineering* 87. 10.1016/j.optlaseng.2016.03.017.

Rota, A., Zaccaria, M., & Fiorito, F. (2023). Towards a quality protocol for enabling the reuse of post-consumer flat glass. *Glass Structures and Engineering* 8 (2). 10.1007/s40940-023-00233-0.

Saint-Gobain (1970). Les installations en glace trempée "SECURIT" en verre trempé "DURLUX". *Saint-Gobain Division Glaces*, 1–36.

Schneider, J., Schula, S., & Weinhold, W. P. (2012). Characterisation of the scratch resistance of annealed and tempered architectural glass. Vol. 520. 10.1016/j.tsf.2011.04.104.

Sofokleous, I. (2022). Methodology for the prediction of the strength of naturally aged glass based on surface flaw characterization.

Stuurstraat, N. (2023). Strength of naturally aged Insulated Glass Units determined by experimental testing.

Wang, Y. & Hadfield, M. (2004). Failure modes of ceramic rolling elements with surface crack defects. *Wear* 256 (1-2). 10.1016/S0043-1648(03)00409-5.

Weeks, R. M. (1933). The Making of a Sheet of Glass. *Royal Institution of Great Britain*, 20.

Weibull, W. (1951). A Statistical Distribution Function of Wide Applicability. *Journal of Applied Mechanics* 18 (3). 10.1115/1.4010337.

Weisstein, E. W. (2020). Log Normal Distribution. *mathworld.wolfram.com*.

Wurm, J. (2007). Glass Structures. DE GRUYTER. 10.1007/978-3-7643-8317-6.

Zammit, K. & Overend, M. (2009). Increasing the design strength of glass – fractography and stress testing. *Proceedings of the International Association for Shell and Spacial Structures (IASS) Symposium 2009* (October).

A

SCALP-05 reliability study

The reliability study for the SCALP-05 device is conducted by doing 10 measurements at the same location, with the same angle on 3 different glass panes.

The glass panes have been selected to be equally distributed in the sampling. They all are on different floors, with different solar exposition. The whole process (adding a drop of mineral oil, positionning the device, measuring and cleaning the glass) is repeated between every measurement. The largest difference between measurements at the same location reaches almost 5 MPa.

Table A.1: Reliability study results for 10 measurements on 3 samples

Point	Sample 1	Sample 2	Sample 3
1	81.77	84.79	86.83
2	81.55	86.69	87.18
3	82.10	87.56	87.46
4	79.79	85.85	83.88
5	82.61	86.49	86.64
6	77.62	86.54	88.34
7	82.40	87.35	86.93
8	81.69	87.08	86.74
9	79.61	87.13	86.98
10	81.45	87.22	87.57

Table A.2: Reliability study results analysis

Measurement	Sample 1	Sample 2	Sample 3	Samples average
Minimum	77.62	84.79	83.88	82.10
Maximum	82.61	87.56	88.34	86.17
Maximal difference	4.98	2.77	4.46	4.07
Average μ	81.06	86.67	86.86	84.86
Standard deviation	1.57	0.83	1.16	1.19
10%-fractile	79.05	85.61	85.37	83.34
δ 10% fractile-average	2.01	1.06	1.49	1.52
$M_{SCALP} = \delta/\mu$	2.48%	1.23%	1.71%	1.79%

B

Traceit® reliability study

The reliability study for the Traceit device is conducted by doing 10 measurements at the same location, on 3 different glass panes.

The first 5 measurements are done with an angle of 0° while the last 5 measurements have an angle of 90°. The 3 flaws were selected to be relatively different from each other in terms of depth, shape and location.

Table B.1: Reliability study results for 10 measurements on 3 samples

Point	Sample 1	Sample 2	Sample 3
1	20	85	47
2	37	87	64
3	26	120	50
4	39	90	65
5	26	99	57
6	42	80	64
7	27	79	43
8	38	112	64
9	22	81	43
10	28	84	49

Table B.2: Reliability study results analysis

Measurement	Sample 1	Sample 2	Sample 3	Samples average
Minimum	20	79	43	47
Maximum	42	120	65	76
Maximal difference	23	41	22	28
Average μ	30	92	55	59
Standard deviation	8	14	9	10
90%-fractile	40	110	66	72
δ 90% fractile-average	10	18	12	13
$M_T = \delta/\mu$	32.7%	19.7%	21.4%	22.5%

C

Pre-stress measurements

The surface pre-stress measurements are presented. Since most of the variations are still within the device's uncertainty, they must be interpreted with caution. The data included in the table are:

1. Local measurements following a 45-points grid on 7 selected glass panes
2. Difference between both faces on 7 selected glass panes
3. Difference between vertical (0°) and horizontal (90°) directions on 7 selected glass panes
4. Global measurements of 5 selected points on panes 1 to 35
5. Global measurements of 5 selected points on panes 36 to 70
6. Global measurements results statistics

Table C.1: Local surface pre-stress measurements (MPa) on 7 glass panes

Point	Pane 1	Pane 2	Pane 3	Pane 4	Pane 5	Pane 6	Pane 7	μ_l	σ_l
1	81.42	94.82	85.03	90.72	87.56	79.74	76.09	85.05	6.53
2	87.56	78.35	77.85	92.73	79.46	58.27	73.45	78.24	10.96
3	91.65	84.36	78.05	88.86	80.00	61.95	72.14	79.57	10.19
4	86.91	81.84	78.28	93.32	80.12	58.20	73.61	78.90	11.10
5	94.15	93.07	87.25	90.89	87.20	80.34	76.53	87.06	6.55
6	88.11	84.51	77.91	82.23	87.58	83.16	73.19	82.38	5.31
7	86.10	88.09	84.44	85.51	82.83	63.97	74.44	80.77	8.60
8	90.07	87.87	78.80	86.69	82.74	62.31	77.24	80.82	9.43
9	88.18	85.25	85.00	85.75	83.09	61.80	74.82	80.56	9.29
10	84.92	87.08	78.12	81.73	87.32	84.62	72.82	82.37	5.29
11	84.07	83.26	80.68	81.83	85.97	80.93	72.83	81.37	4.20
12	79.77	86.26	81.48	83.71	82.02	61.56	75.52	78.62	8.23
13	81.40	83.88	85.69	85.58	83.20	62.12	74.02	79.41	8.60
14	82.47	85.37	79.88	83.88	81.65	61.96	75.88	78.73	8.00
15	78.16	85.47	81.41	82.13	87.04	81.53	73.18	81.27	4.60
16	84.61	83.26	82.28	79.04	82.55	79.82	72.40	80.57	4.08
17	81.57	85.84	82.11	77.46	82.84	66.99	75.78	78.94	6.25
18	81.35	86.03	80.16	87.93	85.15	66.12	75.59	80.33	7.51
19	82.48	83.12	82.74	77.69	82.90	65.41	76.48	78.69	6.46
20	81.55	85.04	82.22	79.11	82.86	79.48	72.24	80.36	4.11
21	76.89	81.89	79.74	77.65	83.10	77.58	73.88	78.68	3.15
22	79.10	86.43	80.07	80.67	82.38	64.74	73.96	78.19	7.01
23	79.88	87.51	80.78	86.71	87.17	68.67	76.17	80.98	6.95
24	82.96	84.05	80.34	81.49	85.78	64.54	74.29	79.07	7.37
25	78.25	84.78	79.39	77.91	82.93	77.22	73.63	79.16	3.71
26	82.19	83.28	81.24	79.27	85.81	79.72	72.73	80.61	4.12
27	80.28	85.88	83.09	77.61	83.15	66.49	73.56	78.58	6.70
28	79.73	88.44	79.52	87.74	84.58	66.30	75.87	80.31	7.71
29	80.44	85.07	82.73	77.50	82.95	66.06	73.96	78.39	6.59
30	80.34	88.02	81.95	78.90	85.13	79.33	72.49	80.88	4.95
31	82.22	83.62	80.51	82.81	85.64	81.12	72.98	81.27	4.03
32	81.68	87.81	81.86	85.48	81.47	61.80	77.08	79.60	8.54
33	78.55	90.67	81.44	85.85	85.51	62.01	73.57	79.66	9.55
34	82.55	86.67	80.33	85.36	81.45	60.56	75.40	78.90	8.88
35	80.22	88.40	80.88	84.66	85.85	81.40	72.16	81.94	5.24
36	84.12	86.95	78.20	82.44	87.18	82.54	73.37	82.11	4.92
37	82.27	88.26	84.16	86.20	84.00	63.89	75.75	80.65	8.36
38	74.13	89.92	78.23	85.18	83.59	61.75	76.88	78.53	9.16
39	82.08	89.89	83.34	86.93	83.82	62.63	76.17	80.69	9.03
40	80.39	89.15	78.02	84.27	87.06	83.28	73.02	82.17	5.51
41	83.17	94.00	85.22	89.92	88.03	79.22	75.57	85.02	6.33
42	77.37	92.15	77.99	92.69	79.65	57.94	73.30	78.73	11.83
43	75.51	95.38	78.26	87.29	80.25	62.28	71.54	78.64	10.69
44	77.86	93.87	77.61	91.49	79.18	58.08	72.27	78.62	11.99
45	87.67	98.98	81.42	89.65	85.11	78.29	75.16	85.18	7.95

Table C.2: Pre-stress difference (MPa) between both faces of the glass pane

Point	Pane 1	Pane 2	Pane 3	Pane 4	Pane 5	Pane 6	Pane 7	μ_f	$\lvert\mu_f\rvert$	σ_f
1	1.23	1.31	3.10	-0.42	-0.06	-0.60	-9.09	-0.65	2.26	3.94
2	13.23	0.59	5.56	-0.10	-0.07	-0.22	-7.76	1.61	3.93	6.43
3	-4.40	-0.10	-0.42	-0.36	-0.38	-0.03	0.02	-0.81	0.82	1.59
4	-1.03	2.37	3.27	-0.35	-0.28	-1.73	-6.41	-0.59	2.21	3.14
5	4.59	-0.12	-0.56	-1.03	-2.47	-2.16	-6.45	-1.17	2.48	3.30

Table C.3: Pre-stress difference (MPa) between vertical (0°) and horizontal (90°) directions on the glass panes

Point	Pane 1	Pane 2	Pane 3	Pane 4	Pane 5	Pane 6	Pane 7	μ_i	$\lvert\mu_i\rvert$	σ_i
1	-2.68	1.68	3.27	-0.06	0.08	-3.63	-8.09	-1.35	2.79	3.80
2	0.33	-0.40	5.10	-0.43	-0.42	-1.23	-7.10	-0.59	2.14	3.56
3	0.82	0.65	0.09	-0.47	-0.72	-0.50	0.34	0.03	0.51	0.61
4	-9.63	3.62	3.06	0.57	-0.68	-3.37	-9.17	-2.23	4.30	5.43
5	-2.23	-0.33	-0.96	-1.37	-2.78	-5.21	-11.45	-3.48	3.48	3.86

Table C.4: Global surface pre-stress measurements (MPa) on panes 1 to 35

Pane	Point 1	Point 2	Point 3	Point 4	Point 5
1	78.42	78.61	79.64	74.67	82.45
2	80.93	81.81	82.07	75.23	78.26
3	72.01	72.26	72.74	80.25	92.59
4	85.23	84.76	84.59	86.00	86.59
5	79.60	80.18	78.37	75.09	82.60
6	80.03	80.57	80.52	80.86	92.60
7	84.58	84.90	84.25	75.97	83.46
8	78.11	78.28	78.93	75.39	82.27
9	85.91	86.74	80.48	79.81	94.47
10	79.82	80.86	81.79	81.66	95.51
11	82.28	79.70	78.93	78.73	97.03
12	77.85	79.38	79.62	75.04	83.85
13	77.59	83.13	84.16	84.71	83.59
14	85.93	86.17	86.72	88.68	97.41
15	78.96	79.34	79.87	79.25	92.65
16	79.83	83.44	82.99	76.54	82.84
17	86.71	87.68	87.04	90.29	89.72
18	85.22	84.16	84.80	84.66	83.95
19	83.94	84.50	84.19	86.23	90.45
20	83.34	82.91	82.15	75.94	83.38
21	86.56	86.80	86.47	79.65	93.31
22	87.66	87.88	88.83	86.98	96.47
23	85.03	84.64	85.07	85.91	82.87
24	86.64	86.23	86.01	86.91	88.31
25	82.75	85.24	84.92	75.85	83.05
26	79.01	79.34	79.20	78.61	93.10
27	76.57	75.99	75.42	78.04	88.07
28	84.79	85.11	85.68	85.15	80.07
29	83.63	83.90	85.70	75.40	83.74
30	78.01	79.11	79.40	80.74	87.34
31	79.30	79.39	78.94	79.60	93.18
32	84.78	82.76	82.94	82.64	78.51
33	90.42	91.43	90.93	92.21	87.41
34	74.39	73.96	77.84	74.90	82.26
35	82.72	81.85	82.11	75.12	83.42

Table C.5: Global surface pre-stress measurements (MPa) on panes 36 to 70

Pane	Point 1	Point 2	Point 3	Point 4	Point 5
36	79.74	78.85	79.33	76.78	93.10
37	83.41	84.89	83.27	80.89	87.87
38	81.20	82.49	82.22	82.91	82.38
39	74.51	82.23	82.44	83.31	83.58
40	75.33	75.22	75.72	77.47	81.06
41	79.23	78.06	79.34	77.98	91.16
42	75.17	78.47	78.87	80.29	83.45
43	83.11	82.93	84.00	83.24	83.65
44	78.97	78.22	78.30	77.92	80.21
45	88.11	83.82	87.19	86.86	92.62
46	78.65	79.00	78.76	81.41	91.28
47	83.53	83.43	83.06	84.45	83.25
48	78.43	78.33	78.04	77.69	81.10
49	80.58	81.41	80.42	80.84	83.60
50	82.26	83.56	83.90	84.16	88.87
51	84.21	84.42	84.67	85.78	84.29
52	81.21	80.61	80.81	83.06	90.91
53	77.60	78.21	78.13	77.77	81.74
54	80.57	80.82	79.47	81.35	90.96
55	84.96	86.56	88.00	87.11	93.09
56	84.09	85.30	84.50	83.96	83.64
57	78.00	77.82	76.17	80.83	80.62
58	87.30	87.66	86.65	85.98	90.09
59	80.89	80.27	80.78	85.94	91.19
60	77.89	78.45	77.64	78.55	80.93
61	83.53	84.28	83.70	82.12	87.61
62	82.18	82.26	83.50	82.75	78.90
63	78.66	79.69	80.29	79.93	94.10
64	79.88	81.57	80.44	78.25	87.67
65	87.51	85.84	85.07	84.78	98.98
66	80.78	82.11	82.73	79.39	81.42
67	86.71	77.46	77.50	77.91	89.65
68	87.17	82.84	82.95	82.93	85.11
69	68.67	66.99	66.06	77.22	78.29
70	76.17	75.78	73.96	73.63	75.16

Table C.6: Global surface pre-stress (MPa) statistics

Pane	Point 1	Point 2	Point 3	Point 4	Point 5
Minimum	66.99	66.06	68.67	73.63	75.16
Maximum	91.43	90.93	90.42	92.21	98.98
Average μ_g	81.61	81.59	81.41	80.97	86.69
Standard deviation σ_g	4.04	4.08	4.17	4.26	5.53
10%-fractile $\sigma_{char,function}$	76.43	76.36	76.07	75.52	79.61
10%-fractile σ_{char}	77.49	77.52	76.21	75.25	80.25

D

Weathering measurements

Table D.1: Flaw depth measurements on panes 1 to 35

Pane	Stamp	Flaw type	Innner/Outer side	Depth (µm)	Adjusted depth (µm)
1	S	L	O	22	22
2	P	S	O	19	30
3	S	L	O	20	20
4	S	L	O	12	10
5	P	L	O	40	40
6	S	L	O	12	12
7	S	L	O	0	10
8	S	L	I	50	50
9	S	L	O	35	35
10	P	L	O	11	11
11	P	L	O	0	10
12	P	L	O	0	10
13	P	L	O	12	12
14	P	L	O	0	10
15	P	L	O	18	18
16	P	L	O	6	10
17	S	L	O	0	10
18	P	L	O	0	10
19	P	S	O	55	55
20	P	L	O	49	49
21	P	S	O	146	146
22	P	L	O	42	42
23	P	L	I	10	10
24	P	L	O	0	10
25	S	L	O	40	40
26	P	L	O	119	119
27	P	L	O	123	123
28	S	S	O	34	34
29	S	L	O	7	10
30	P	L	O	0	10
31	S	L	O	0	10
32	S	L	O	0	10
33	P	L	O	79	79
34	P	L	O	0	10
35	P	L	O	0	10

Table D.2: Flaw depth measurements on panes 36 to 70

Pane	Stamp	Flaw type	Inner/Outer side	Depth (µm)	Adjusted depth (µm)
36	S	L	O	22	22
37	P	L	O	12	12
38	S	L	O	0	10
39	S	L	O	0	10
40	P	L	O	56	56
41	S	S	O	147	147
42	S	L	O	0	10
43	S	L	O	44	44
44	S	L	O	91	91
45	S	L	I	68	68
46	S	S	O	126	126
47	S	L	I	69	69
48	S	S	O	44	44
49	S	L	I	52	52
50	S	L	O	125	125
51	S	L	I	43	43
52	S	L	O	15	15
53	S	L	I	59	59
54	S	L	O	55	55
55	S	L	I	69	69
56	S	L	O	0	10
57	S	L	O	50	50
58	P	L	O	8	10
59	P	L	O	96	96
60	S	S	O	31	31
61	S	S	O	122	122
62	S	L	O	0	10
63	S	L	O	0	10
64	S	L	O	4	10
65	P	L	O	24	24
66	S	S	I	46	46
67	S	S	O	31	31
68	S	L	O	8	10
69	S	S	O	55	55
70	S	L	O	6	10

Table D.3: Quality level inspection on panes 1 to 35

Pane	Adjusted depth (µm)	Estimated depth (µm)	Difference (µm)	QL1	QL2	QL3	QL4	QL5	QL6
1	22	10	12		x				
2	30	30	0		x				
3	20	40	-20			x			
4	10	30	-20		x				
5	40	10	30		x				
6	12	50	-38			x			
7	10	10	0		x				
8	50	20	30		x				
9	35	30	5		x				
10	11	40	-29			x			
11	10	30	-20		x				
12	10	30	-20		x				
13	12	30	-18		x				
14	10	10	0		x				
15	18	40	-22			x			
16	10	10	0		x				
17	10	10	0		x				
18	10	30	-20		x				
19	55	40	15		x				
20	49	20	29		x				
21	146	60	86		x				
22	42	50	-8			x			
23	10	10	0		x				
24	10	10	0		x				
25	40	60	-20			x			
26	119	90	29			x			
27	123	60	63			x			
28	34	30	4		x				
29	10	40	-30			x			
30	10	10	0		x				
31	10	10	0		x				
32	10	30	-20		x				
33	79	30	49		x				
34	10	10	0		x				
35	10	10	0		x				

Table D.4: Quality level inspection on panes 36 to 70

Pane	Adjusted depth (µm)	Estimated depth (µm)	Difference (µm)	QL1	QL2	QL3	QL4	QL5	QL6
36	22	30	-8		x				
37	12	10	2		x				
38	10	10	0		x				
39	10	30	-20		x				
40	56	20	36		x				
41	147	80	67			x			
42	10	40	-30			x			
43	44	50	-6			x			
44	91	50	41			x			
45	68	30	38		x				
46	126	70	56		x				
47	69	40	29			x			
48	44	20	24		x				
49	52	20	32		x				
50	125	100	25			x			
51	43	40	3			x			
52	15	30	-15		x				
53	59	30	29		x				
54	55	20	35		x				
55	69	30	39		x				
56	10	30	-20		x				
57	50	30	20		x				
58	10	10	0		x				
59	96	50	46			x			
60	31	40	-9		x				
61	122	70	52		x				
62	10	10	0		x				
63	10	10	0		x				
64	10	30	-20		x				
65	24	30	-6		x				
66	46	30	16		x				
67	31	30	1		x				
68	10	10	0		x				
69	55	40	15		x				
70	10	10	0		x				